2022

Endogenous retroviral proteins as potential drug targets for merlin-deficient tumours

Agit, Bora

Copyright Statement

UNIVERSITY OF PLYMOUTH

ENDOGENOUS RETROVIRAL PROTEINS AS POTENTIAL DRUG TARGETS FOR MERLIN-DEFICIENT TUMOURS

by

Bora Agit

A thesis submitted to the University of Plymouth in partial fulfilment for the degree of

MASTER OF PHILOSOPHY

Peninsula Medical School

December 2021

Acknowledgement

Firstly, I would like to express my sincere gratitude to my supervisor Dr Sylwia Ammoun for the continuous support of my PhD study, for her patience, motivation, and knowledge; Prof Oliver Hanemann for all his support and advice; Dr Robert Belshaw for all his support and knowledge of endogenous retroviruses.

Thank you to the Parkinson laboratory group for collaborating and providing support. To the rest of the Hanemann laboratory group, old and new, for their continuous support and for becoming my family throughout my PhD. To all my friends in UK and Cyprus for being there when needed. I could not do it without you all.

Thank you to Action Medical Research and Action on Hearing Loss for funding my project, to Brain Tumour Research for helping to fund the laboratory and group, and to Plymouth University for sponsoring me to carry out my work.

Last but not the least, I would like to thank my parents for providing moral and financial support throughout my academic life.

Author's Declaration

At no time during the registration for the degree of Master of Philosophy has the author been registered for any other University award without the prior agreement of the Doctoral College Quality Sub-Committee.

Work submitted for this research degree at the University of Plymouth has not formed part of any other degree at the University of Plymouth or another establishment.

This research degree was financed with the aid of a studentship from the University of Plymouth with additional financial support for the research from the Action Medical Research (registered charity number: 208701), and the Action on Hearing Loss (registered charity number: 207720).

Publications linked to endogenous retroviruses:

Tatkiewicz W, Dickie J, Bedford F, Jones A, Atkin M, Kiernan M, Maze E.A, Agit B, Farnham G, Kanapin A, Belshaw R. (2020). Characterising a human endogenous retrovirus (HERV)-derived tumour-associated antigen: Enriched RNA-Seq analysis of the endogenous retrovirus HERV-K (HML-2) in Mantle Cell Lymphoma cell lines. Mobile DNA. Vol. 11, Article number: 9. https://doi.org/10.1186/s13100-020-0204-1

Maze E.A, Agit B, Reeves S, Hilton D, Parkinson D, Laraba L, Ercolano E, Kurian K.M, Hanemann CO, Belshaw R, Ammoun S. (2022). Human endogenous retrovirus type K promotes proliferation and confers sensitivity to anti-retroviral drugs in Merlin-negative schwannoma and meningioma. Cancer Research. Vol. 82, pp. 235-47. https://doi.org/10.1158/0008-5472.CAN-20-3857

Conferences attended where data was presented:

Annual Research Event for PUPSMD Postgraduate Students, Plymouth, 2017-2019

10th Brain Tumour Meeting, Berlin, Germany, May 2019

Word count of the main body of thesis: 33,938

Date: 8th December 2021

Data Gathering

The data presented in this thesis were generated by the author except as listed below:

Dr Emmanuel Atangana Maze generated the data on HERV-K Env protein expression in primary Schwann and schwannoma cells (Figure 12C).

Dr Sylwia Ammoun generated 5 repetitions of the HERV-K Env expression data in grade I meningioma (NF2-/-) biopsies (Figure 13A).

Dr Sylwia Ammoun generated 9 repetitions of the HERV-K Env expression data in grade I meningioma (NF2-/-) tissue lysates (Figure 14).

Dr Emmanuel Atangana Maze generated most of the data on HERV-K Env and Gag protein expression following Merlin re-introduction in primary schwannoma cells, and the blots shown in the figure are his repetitions (Figure 16). I contributed to one repetition for both HERV-K Env and Gag. The remaining repetitions were done by Dr Emmanuel Atangana Maze.

Dr Emmanuel Atangana Maze generated most of the data on HERV-K Env protein expression following the knockdown of $CRL4^{DCAF1}$ in primary schwannoma cells using shRNA1, and blot shown in the figure is his repetition (Figure 17). I contributed to two repetitions. The remaining repetitions were done by Dr Emmanuel Atangana Maze.

Dr Sylwia Ammoun generated the data on HERV-K Env protein expression following the knockdown of $CRL4^{DCAF1}$ in primary schwannoma cells using shRNA2, and the blot shown in the figure is her repetition (Figure 17).

Liyam Laraba, a PhD student at Plymouth University, has done the drug experiment (VT04153) on primary schwannoma cells shown in Figure 20, and he provided the samples for examining the effect on HERV-K Env protein expression. CTGF and its GAPDH control shown in Figure 20A are his western blotting results.

Dr Sylwia Ammoun generated one repetition of the HERV-K Env-FL expression following VT04153 treatment in primary schwannoma cells (Figure 20B).

Dr Sylwia Ammoun generated the comparison result between HERV-K (HML-2) and Homo sapiens chromosome 8 Clone RP11-26K8 (Figure S1)

Dr Emmanuel Atangana Maze generated the data on the presence of the TEAD binding motif on HERV-K (HML-2) LTR *in silico* (Figure S4).

Bora Agit

Title: Endogenous retroviral proteins as potential drug targets for merlin-deficient tumours

Merlin is a tumour suppressor, and its loss is the major cause of a hereditary disease Neurofibromatosis type 2 (NF2) characterised by the development of multiple tumours of the nervous system such as schwannomas, meningiomas and ependymomas. Current surgical treatments and radiotherapy for this group of tumours are not fully effective and there is an urgent need for new therapeutic options.

Human endogenous retroviruses (HERVs) are retroviruses that have been incorporated into the human genome during evolution, now comprising 5% of it. The majority of HERVs are defective except for a few groups, including type K (HERV-K) which kept full-intact open reading frames. HERV-K (HML-2) is transcriptionally active in many cancer tissues and tumour cell lines, and several studies have highlighted its role in cancer.

Preliminary data showed overall HERV-K upregulation in Merlin-deficient schwannoma, and thus this project aims to investigate the role of HERV-K (HML-2) in Merlin-deficient schwannoma and meningioma development and to investigate the potential of HERV-K as a novel therapeutic target as well as testing anti-retroviral drugs' efficacy for the treatment of these tumours.

I have demonstrated that HERV-K (HML-2) Env overexpression (Env o/e) in primary Schwann cells resulted in increased proliferation and elevated expression of the

transcription factor cJun. Env o/e also increased pERK1/2 activity and upregulated S phase cyclin A2. I have also revealed that HERV-K Env overexpression is regulated by TEAD-mediated transcription both in Merlin-deficient schwannoma and grade I meningioma.

Furthermore, I have successfully tested the FDA approved retroviral protease inhibitors Ritonavir, Atazanavir and Lopinavir which could be potentially repurposed for the treatment of Merlin-deficient schwannoma and grade I meningioma. Ritonavir and Lopinavir effectively decreased the proliferation of Merlin-deficient primary schwannoma cells at concentrations much lower than have already been achieved clinically. Atazanavir showed the same effect in primary schwannoma cells but at a higher concentration than the other two drugs.

In conclusion, HERV-K (HML-2) Env plays a contributory role in schwannoma tumorigenesis, and possibly meningioma tumourigenesis. The mechanism of HERV-K upregulation in Merlin-deficient tumours is partly driven by the TEAD transcription factors. Lastly, retroviral protease inhibitors Ritonavir and Lopinavir are suggested as potential treatments for NF2-associated tumours.

Table of Contents

1 List of Abbreviations 11
2 List of Illustrations and Tables 14
3 Introduction 16
3.1 Neurofibromatosis Type 2 and Associated Tumours 17
3.1.1 Schwannomas 18
3.1.2 Meningiomas 21
3.1.3 Ependymomas 24
3.2 *NF2* gene and Merlin 25
3.3 Merlin as a Tumour Suppressor 29
3.4 The Cell Cycle and Cancer 34
3.5 Retroviruses 37
3.5.1 Retrovirus Structure and Genome 37
3.5.2 Viral Cycle 41
3.5.3 Discovery and Classification 44
3.6 HERVs: Discovery and Classification 45
3.7 HERV-K (HML-2) 47
3.7.1 HERV-K (HML-2) Genome Structure and Transcripts 47
3.7.2 HERV-K (HML-2) Proteins 51
3.7.3 HERV-K (HML-2) and Cancer 52
3.8 Retroviral Protease Inhibitors in Cancer Therapy 56
3.9 HERV-K (HML-2) and Schwannoma: What We Know So Far 58
3.10 Aims and Objectives 60
4 Materials and Methods 62
4.1 Cell Culture 62
4.1.1 Clinical Sample Collection and Ethics 62
4.1.2 Schwann Cell Culture 62
4.1.3 Schwannoma Cell Culture 63
4.1.4 Meningioma Cell Culture 64
4.1.5 Cell line culture 64
4.2 Chemicals, Compounds and Kits 66
4.3 Antibodies 69
4.4 Viral Infections 71
4.4.1 Adenoviral (AdV) Re-Introduction of Merlin into Schwannoma Cells 71
4.4.2 Lentiviral Transduction 71
4.5 Drug Treatments 76

4.5.1 Verteporfin 76
4.5.2 VT04153 76
4.5.3 Anti-Retrovirals 76
4.6 Immunohistochemistry (IHC) 77
4.7 Immunocytochemistry (ICC) 78
4.8 Western Blotting 79
4.8.1 Sample Lysis 79
4.8.2 SDS-PAGE and Transfer to PVDF membrane 80
4.8.3 Immunoblotting 80
4.9 RNA Quantification 81
4.9.1 RNA Preparation 81
4.9.2 Primers 81
4.9.3 qRT-PCR 82
4.10 Data Analysis 83
5 Results 84
5.1 Potential Role of HERV-K in Schwannoma Development 84
5.1.1 Attempts to Knockdown HERV-K in HEI193 cells 84
5.1.2 HERV-K Env Protein Contributes to Schwannoma Development 87
5.2 HERV-K Proteins are Overexpressed in Merlin-Deficient Meningioma 93
5.3 Mechanisms of HERV-K Upregulation in Merlin-Deficient Tumours 98
5.3.1 HERV-K Overexpression in Schwannoma is Partially Merlin-Dependent 98
5.3.2 $CRL4^{DCAF1}$/YAP/TEAD/Hippo Pathway is Involved in HERV-K Env Upregulation 100
5.4 Repurposing Anti-Retroviral Drugs to Treat Merlin-Deficient Tumours 109
5.4.1 Retroviral Protease Inhibitors Ritonavir, Atazanavir and Lopinavir Reduce Schwannoma Cell Proliferation 110
5.4.2 Ritonavir and Atazanavir Reduce BenMen Cell Proliferation 113
6 Discussion 115
6.1 HERV-K Env Signalling Pathway in Merlin-Deficient Schwannoma 116
6.2 HERV-K Env Upregulation in Merlin-Deficient Schwannoma and Grade I Meningioma 118
6.3 Potential Therapeutics for Schwannomas and Meningiomas 122
7 Conclusion 125
8 Future Work 125
9 References 126
10 Supplementary Information 150

1 List of Abbreviations

AKT1: *Protein kinase B*
ALV: *Avian leukosis virus*
AP-1: *Activator protein 1*
AR: *Androgen receptor*
ARID1A: *AT-rich interaction domain 1A*
ARID1B: *AT-rich interaction domain 1B*
ATM: *Ataxia telangiectasia mutated gene*
BAP1: *Ubiquitin carboxyl-terminal hydrolase*
BenMen: *Ben-Men-1*
CA: *Capsid*
cAMP/PKA: *c-AMP dependent protein kinase A*
CAR: *Chimeric Antigen Receptor*
Casp3: *Cleaved Caspase-3*
CDC27: *Cell division cycle 27*
CDH4: *Cadherin 4*
CDK: *Cyclin-dependent kinase*
CDKN2A: *Cyclin-dependent kinase inhibitor 2A*
CHOP: *C/EBP homologous protein*
CNS: *Central nervous system*
c-RAF: *RAF protooncogene serine/threonine protein kinase*
CRL4^{DCAF1}: *Cullin 4A-RING E3 ubiquitin ligase/DDB1 and CUL4 associated factor 1*
CTT: *C-terminal domain*
CTGF: *Connective tissue growth factor*
CUL4: *Cullin 4*
DDB1: *DNA damage-binding protein 1*
DDR1: *Discoidin domain receptor family, member 1*
DMEM: *Dulbecco's modified eagle medium*
DNA: *Deoxyribonucleic acid*
dsDNA: *Double-stranded DNA*
dUTPase: *dUTP diphosphatase*
EED: *Embryonic ectoderm development*
EGFR: *Epidermal growth factor receptor*
EMT: *Epithelial to mesenchymal transition*
Env: *Viral envelope glycoprotein*
ER: *Endoplasmic reticulum*
ErbB: *Epidermal growth factor family B*
ERK: *Extracellular signal-regulated kinases*
ERM: *Ezrin-radixin-like*
ERp44: *Endoplasmic reticulum protein 44*
ERV: *Endogenous retrovirus*
ESR: *ER stress response*
FAK: *Focal adhesion kinases*
FAT1: *FAT atypical cadherin 1*
FBS: *Foetal bovine serum*
GAPDH: *Glyceraldehyde-3-phosphate dehydrogenase*

GCSF: *Granulocyte colony stimulating factor*
GFM: *Growth factor medium*
GKS: *Gamma Knife Surgery*
Grb: *Growth factor receptor-bound protein*
GRP78: *Glucose regulated protein 78*
HERV: *Human endogenous retroviruses*
HERV-K: *Human endogenous retrovirus type K*
Hh: *Hedgehog*
HIV: *Human immunodeficiency virus*
HMC: *Human meningeal cells*
HML-2: *Human endogenous MMTV-like 2*
hSGT: *Human small glutamine-rich tetratricoprotein repeat peptide*
HTLV-1: *Human T-cell lymphotropic virus 1*
IAP: *Hamster intracisternal A particle*
IBMX: *3-isobutyl-1-methylxanthine*
IC50: *Half maximal inhibitory concentration*
IGF1R: *Insulin-like growth factor receptor 1*
IGF2R: *Insulin-like growth factor receptor 2*
IL-6: *Interleukin 6*
IL-8: *Interleukin 8*
IL-10: *Interleukin 10*
IN: *Integrase*
JNK: *cJun N-terminal kinase*
KLF4: *Krüppel-like factor 4*
KMT2D: Lysine Methyltransferase 2D
Lats 1/2: *Large tumour suppressor kinase 1/2*
LNX: *Ligand of NUMB protein X*
LRP6: *Low density lipoprotein receptor related protein 6*
LTR: *Long terminal repeat*
LZTR1: *Leucine zipper-like transcriptional regulator 1*
MA: *Matrix*
MCP-1: *Monocyte chemoattractant protein 1*
MED2: Mediator of RNA polymerase II transcription subunit 2
MEK1: *Mitogen-activated protein kinase kinase*
Merlin: *Moesin ezrin radixin-like protein*
MIP-1α: *Macrophage inflammatory protein-1 alpha*
MIP-1β: *Macrophage inflammatory protein-1 beta*
MITF-M: Melanocyte inducing transcription factor, isoform M
MLV: *Murine leukaemia virus*
MMTV: *Murine mammary tumour virus*
MN-GI-NF2-/-: *Merlin-deficient grade I meningioma*
MN-GI-NF2+/+: *Merlin-positive grade I meningioma*
mRNA: *Messenger RNA*
Mst 1/2: *Mammalian STE20-like protein kinase 1/2*
mTOR: *Mammalian target of rapamycin*
MTORC1: *Mammalian target of rapamycin complex 1*
NC: *Nucleocapsid*

NF1: *Neurofibromatosis type 1*
NF2: *Neurofibromatosis type 2*
NFAT: *Nuclear factor of activated T-cells*
NFkB: *Nuclear factor-kappa B*
NMT-NF2+/+: *Normal meninges*
Oct4: *Octamer-binding transcription factor 4*
ORF: *Open reading frame*
P70S6 kinase: *Ribosomal protein S6 kinase*
PAK: *p21-activated kinase*
PBS: *Primer binding site*
PDGFR: *Platelet-derived growth factor receptor*
Pen/Strep: *Penicillin/Streptomycin*
PI: *Protease inhibitor*
PI3K: *Phosphatidylinositol-3 kinase*
PIC: *Pre-integration complex*
PIK3CA: *Phosphatidylinositol-4, 5-biphosphate 3-kinase catalytic subunit alpha*
PIKE-L: *PI3-kinase enhancer*
PLZF: *Promyelocytic leukaemia zinc finger protein*
POLR2A: *RNA polymerase II*
PPT: *Polypurine tract*
PR: *Protease*
PRC2: *Polycomb repressive complex 2*
PRKAR1A: *Protein kinase A cAMP-dependent regulatory subunit 1*
R: *Repeat sequence*
Rac1: *Ras-related C3 botulinum toxin substrate 1*
Ras: *Rat sarcoma family*
Rb: *Retinoblastoma*
Rich1: *Rho-GTPase-activating protein 17*
RNA: *Ribonucleic acid*
RSV: *Rous sarcoma virus*
RTK: *Receptor tyrosine kinase*
RT: *Reverse transcriptase*
Sch-NF2-/-: *Merlin-deficient schwannoma*
Sch-NF2+/+: *Normal Schwann*
SCID: *Severe combined immunodeficient*
Scr: *Scramble*
SMARCB1: *SW1/SBF-related matrix associated actin-dependent regulator of chromatin, subfamily B, member 1*
SMO: *Smoothened*
SOS: *Son of sevenless protein*
SP: *Signal peptide*
STNFRII: *Soluble tumour necrosis factor receptor type II*
SU: *Surface unit*
SUFU: *Suppressor of fused homolog*
SUZ12: *Polycomb repressive complex 2 subunit*
SWNTS: *Schwannomatosis*
TERT/hTERT: *Telomerase reverse transcriptase*
TM: *Transmembrane unit*

TP53: *Tumour protein 53*
TRAF7: *Tumour necrosis factor (TNF) receptor associated factor 7*
tRNA: *Transfer RNA*
TSS: *Transcription start site*
TTS: *Transcription termination site*
YAP: *Yes-associated protein*
U: *Unique sequence*
uPAR: *Urokinase-type plasminogen activator receptor*
USP8: *Ubiquitin specific peptidase 8*
VS: *Vestibular Schwannoma*

2 List of Illustrations and Tables

Figure 1. Scanning electron microscopic pictures showing the differences in cell phenotype between schwannoma (NF2-/-) and normal Schwann cells (NF2+/+). 19
Figure 2. Schematic diagram demonstrating the regulation of Merlin's activity. 28
Figure 3. Merlin loss leads to overactivation of the mitogenic signalling pathways and oncogenic gene expression. 33
Figure 4. Schematic representation of a retrovirus virion. 39
Figure 5. Structure of retroviral RNA genome in virion and DNA provirus in host. 40
Figure 6. Replication cycle of retroviruses 43
Figure 7. Proviral organisation of HERV-K and mRNA transcripts. 49
Figure 8. HERV-K Env and Pol mRNA levels after attempting to knockdown HERV-K in HEI193 cells using constructs from AMSBIO and Li et al. [9] 85
Figure 9. Published shRNA constructs from Li et al. [9] reduced HERV-K Env-Full Length (FL) protein expression but increased HERV-K Env-Transmembrane (TM) protein expression in HEI193 cells. 87
Figure 10. Overexpressing HERV-K Env in HEK293T cells activated ERK1/2. 88
Figure 11. Overexpression of HERV-K Env in primary Sch-NF2+/+ cells significantly increased cell proliferation and expression of the transcription factor cJun. 90
Figure 12. Overexpression of HERV-K Env in primary Sch-NF2+/+ cells increased ERK activity and cyclin A2 expression but decreased the expression of cyclin D1. 92
Figure 13. Immunohistochemical analysis showed increased HERV-K Env and Gag expression in grade I meningioma compared to normal meninges. 94
Figure 14. HERV-K Env is overexpressed in MN-GI-NF2-/- tissue lysates compared to normal meningeal tissue lysates. 95
Figure 15. HERV-K Env is overexpressed in primary MN-GI-NF2-/- cells and BenMen cells compared to control HMC 97
Figure 16. HERV-K upregulation in schwannoma is partially Merlin-dependent. 99

Figure 17. HERV-K Env upregulation in Sch-NF2-/- is partially regulated by $CRL4^{DCAF1}$ whereas HERV-K Gag is not. 101
Figure 18. Verteporfin decreased the expression of HERV-K Env in Sch-NF2-/-. 103
Figure 19. Verteporfin decreased Sch-NF2-/- proliferation and induced apoptosis. 105
Figure 20. Pan-TEAD inhibitor VT04153 decreased the expression of HERV-K Env in Sch-NF2-/-. 106
Figure 21. Pan-TEAD inhibitor VT04153 decreased the expression of HERV-K Env in MN-GI-NF2-/-. 107
Figure 22. Pan-TEAD inhibitor VT04153 significantly decreased MN-GI-NF2-/- proliferation. 108
Figure 23. Ritonavir significantly decreased primary Sch-NF2-/- cell proliferation but had no effect on primary Sch-NF2+/+ cells. 111
Figure 24. Lopinavir and Atazanavir decreased Sch-NF2-/- proliferation. 112
Figure 25. Atazanavir and Ritonavir decreased BenMen cell proliferation. 113
Figure 26. Mechanism of HERV-K upregulation. 121

Table 1. Mutated genes identified in meningiomas from different locations. Table adapted from [90]. 24
Table 2. Human specific HERV-K (HML-2) proviruses that have ORFs. Table adapted from [245]. 50
Table 3. Table of chemicals, compounds and kits used in the experiments. 66
Table 4. Table of antibodies used in the experiments. 69
Table 5. shRNAs used for the knockdown of HERV-K. 73
Table 6. Primers. 81

Table S 1. The scoring of immunohistochemistry analysis shown in Figure 13. 151

Figure S 1. Homo sapiens chromosome 8, clone RP11-26K8 showed 99% similarity with HERV-K sequence. 150
Figure S 2. Specificity of anti-HERV-K Env antibody for HERV-K Env-FL and Env TM was confirmed by overexpressing HERV-K Env in Sch-NF2+/+ cells. 152
Figure S 3. Alignment of 19 HERV-K (HML-2) proviruses confirms the presence of shRNA target sequence in multiple proviruses. 153
Figure S 4. The presence of TEAD binding site on HERV-K (HML-2) LTR in silico. 154
Figure S 5. Proliferation index for anti-retroviral drug treatment experiments with primary Sch-NF2-/- and Sch-NF2+/+ cells in basal conditions (media). 155

3 Introduction

Merlin (also known as schwannomin) is a tumour suppressor encoded by the *NF2* gene [1, 2]. Genetic alterations in both copies of the *NF2* gene result in loss of function or deletion of Merlin leading to the formation of tumours of the nervous system such as schwannomas, meningiomas, and ependymomas. These tumours may occur spontaneously or as part of the hereditary disease Neurofibromatosis type 2 (NF2). NF2 is caused by biallelic mutations of the *NF2* gene which then results in associated tumours. However, NF2-associated tumours can also occur as a result of spontaneous Merlin loss leading to sporadic development of these tumours [1-4].

Current treatments for Merlin-deficient tumours are surgery and single target radiosurgery that are partially effective. Complete resection difficulty, nerve damage, tumour accessibility, tumour reoccurrence, and risk of additional mutations are common problems faced while performing surgery and radiosurgery for these patients [5]. Therefore, new effective drug-based treatments are urgently needed, which have been recently addressed in an international meeting of researchers, clinicians, representatives of the biotechnology industry, and patient advocates [6].

The human endogenous retrovirus type K (HERV-K) superfamily is the most biologically active member of the HERVs. Especially, the HERV-K subgroup HML-2 is transcriptionally active in several cancerous tissues and tumour cell lines [7-11]. In addition, recent studies have shown the tumourigenic potential of HERV-K (HML-2) [9, 12-18]. Likewise, our preliminary group data showed the presence of HERV-K (HML-2) in Merlin-deficient schwannoma. Therefore, my project aims to investigate

the tumourigenic potential of HERV-K (HML-2) in Merlin-deficient tumours and whether it could be used as a target for the treatment of NF2-related tumours.

3.1 Neurofibromatosis Type 2 and Associated Tumours

Neurofibromatosis type 2 (NF2; MIM #101000) is an autosomal dominantly inherited tumour predisposition syndrome caused by mutations in the *NF2* gene on chromosome 22. The *NF2* gene codes for the tumour suppressor protein Merlin and mutations in both copies of the *NF2* gene lead to the formation of tumours such as schwannoma, meningioma, and ependymoma. These tumours may occur sporadically or as part of NF2. NF2 patients are born with a monoallelic mutation of the *NF2* gene, and the second genetic hit occurs during their lifetime. Spontaneous Merlin loss occurs as a result of biallelic mutations during the life of the patients resulting in the sporadic development of NF2 associated tumours [1-3]. *NF2* gene mutation may also be acquired early in embryogenesis, creating two cell populations (mosaicism) [19]. The latest study by Evans *et al.* predicted a higher rate of mosaicism in *de novo* cases (59.7%) compared to the previous reports (25-33%), showing that NF2 has by far the highest proportion of *de novo* mosaicism among other tumour predisposition syndromes [20-22]. NF2 has a prevalence of 1 in 33000 [23], and the clinical diagnostic criteria from the National Institute of Health includes bilateral vestibular schwannoma, a family history of NF2, and any two of the following; schwannoma, meningioma, ependymoma, glioma, neurofibroma or posterior subscapular lenticular opacities (reviewed in [24]).

3.1.1 Schwannomas

Schwannomas can be found in two types: benign and malignant. Benign schwannomas mostly occur sporadically; however, some are associated with NF2, schwannomatosis (SWNTS) or Carney's complex (reviewed in [25]). Malignant schwannomas, also known as malignant peripheral nerve sheath tumours (MPNST), are associated with Neurofibromatosis type 1 (NF1; MIM #162200) [26]. NF1 is caused by a germline mutation in Neurofibromin 1 (*NF1*) gene and has an incidence of 1:2500 [27]. NF1 patients are born with a monoallelic mutation of the *NF1* gene, and the second genetic hit occurs during their lifetime leading to loss of Neurofibromin 1 protein in cells and tumour development [28]. Neurofibromin 1 protein is a Ras GTPase tumour suppressor that suppresses RAF/MEK/ERK signalling and therefore inhibits cell growth [29]. Half of MPNSTs have *NF1* gene mutations, and the remaining majority of cases have mutations in *TP53*, *CDKN2A/p16*, *SUZ12*, *EED*, and *PRC2* (Polycomb repressive complex 2) [30-34]. MPNSTs only occur in irradiated NF2 patients but it is extremely rare, suggesting that the *NF2* gene mutation is not sufficient by itself [35]. The project does not focus on MPNSTs and thus, all future reference to 'schwannoma' refers to benign schwannoma.

Schwannomas are slow-growing tumours developing from the Schwann cells that wrap around nerve fibres. Compared with normal human Schwann cells, Merlin-deficient human schwannoma cells show slightly increased proliferation and cell spreading [36, 37], increased adhesion to the extracellular matrix [38], altered cytoskeleton [36, 39, 40], and slightly decreased apoptosis [41] (Figure 1). Schwannomas can form in different locations: peripheral, spinal, and intracranial. Patients suffer from varying

symptoms depending on the location including hearing loss, tinnitus, balance dysfunction, headache, and numbness [42]. Vestibular schwannoma is the most common intracranial schwannoma that forms at the 8th cranial nerve. Bilateral development of vestibular schwannomas has been accepted as the hallmark feature of NF2. Spinal schwannomas are also very common, and they constitute 30% of all spinal tumours. 70% of sporadic and 100% of NF2-related schwannomas have the *NF2* gene mutations resulting in Merlin-deficiency [24, 43-48].

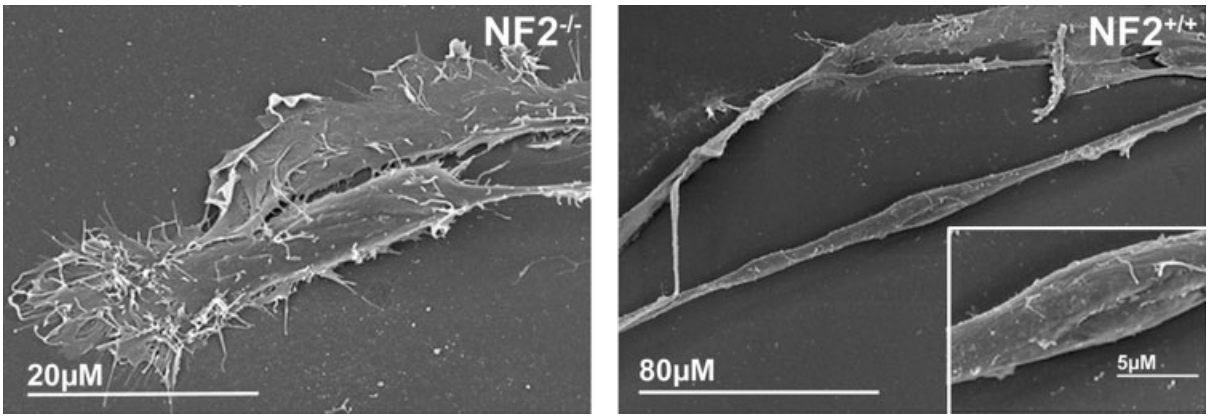

Figure 1. Scanning electron microscopic pictures showing the differences in cell phenotype between schwannoma (NF2-/-) and normal Schwann cells (NF2+/+).

Schwannoma cells (NF2-/-) demonstrate more cell spreading along with multiple membrane extensions and loss of contact inhibition. Normal Schwann cells (NF2+/+) show less spreading along with a few membrane extensions; and they have thin, elongated, bipolar structure. The image is taken from Hanemann 2008 [46].

As well as being part of NF2, schwannomas can also result from SWNTS which is characterised by multiple peripheral nerve and spinal nerve root non-intradermal schwannomas. Furthermore, patients do not have bilateral vestibular schwannomas which are only characteristic of NF2 [43, 49]. SWNTS appears to be a genetically heterogeneous disease, in contradiction to genetically homogenous NF2 [3, 50]. Two major clinical/molecular forms of SWNTS have been described so far. SWNTS1 (MIM

#162091) has been the first to be described as a distinct form of neurofibromatosis in 2007, and it is caused by constitutional inactivating mutations of the *SMARCB1* gene (SW1/SBF-related matrix-associated actin-dependent regulator of chromatin, subfamily B, member 1) [50]. SWNST2 (MIM #601607) is the second and most recently characterised form of SWNST, and it is caused by constitutional/germline inactivating mutations of the *LZTR1* gene (leucine zipper-like transcriptional regulator 1) [51-53]. SWNTS shows considerable overlap with sporadic and NF2 related schwannomas. However, the diagnostic differences are usually clear [54-58].

NF2 gene mutations remain the most characteristic genetic risk factor for schwannoma [1, 2, 59-62]. Piotrowski *et al.* identified *LZTR1* as a gene predisposing to an autosomal dominant inherited disorder of multiple schwannomas in ~80% of 22q-related schwannomatosis cases lacking mutation in *SMARCB1* [52]. *SMARCB1* gene mutations were identified in 45% of familial and 7% of sporadic schwannomatosis cases [63], and these mutations were shown to be involved in the development of some sporadic spinal schwannomas [64]. Pathmanaban *et al.* determined the frequency of these predisposing mutations in solitary schwannomas by screening 135 schwannoma cases using Sanger sequencing or next-generation sequencing, and the results demonstrated that *NF2*, *LZTR1,* or *SMARCB1* mutations were found in 54.5% of them [61]. Agnihotri *et al*. identified recurrent mutations in *NF2*, *ARID1A*, *ARID1B*, and *DDR1* by performing whole exome sequencing on vestibular schwannomas [65]. Additionally, Havik *et al.* identified *NF2*, *CDC27*, and *USP8* as the most common tumour-specific mutations in vestibular schwannomas [66]. Finally, Gao *et al*. performed whole genome sequencing on nine spinal schwannomas and paired blood samples, and the results showed that

ATM, *CHD4*, *FAT1*, *KMT2D*, *MED12*, *NF2*, and *SUFU* were the most frequently mutated tumour-specific genes in the spinal schwannomas [67].

3.1.2 Meningiomas

Meningiomas are tumours arising from arachnoidal cap cells of the leptomeninges, tissue layers that surround and protect the brain and spinal cord. The incidence rate of meningiomas is 8.03 per 100,000 population, and it rises sharply over the age of 65 [68]. Meningiomas constitute over a third of primary central nervous system (CNS) tumours, making them the most common primary intracranial tumour [68]. They can occur throughout the craniospinal axis, and the symptoms depend entirely on the location. Common locations are the convexity, olfactory groove, tuberculum sellae, parasagittal, parafalcine, sphenoid wing, petroclival, posterior fossa, or spinal. Headaches and potential seizures are the most frequent symptoms of all intracranial meningiomas [69, 70]. According to the 2016 World Health Organization (WHO) classification, meningiomas have 3 grades and 15 histopathological subtypes. WHO grade I, II, and III meningiomas are benign, atypical, and malignant, respectively [71]. Accurate diagnosis of meningiomas is often difficult because of their vast diversity and going into the various subtypes and their properties are beyond the scope of this thesis.

Overall, meningiomas are relatively heterogeneous and their genetics are far more complex than any other tumour associated with NF2. Therefore, the mutational landscape for meningiomas can be divided into two main groups: *NF2* and non-*NF2* mutations. The majority being sporadic, only a small portion of meningiomas is associated with NF2 (~15%). Approximately, 50-60% of sporadic and 100% of NF2-

related meningiomas have the *NF2* gene mutations resulting in Merlin-deficiency [72-74]. Merlin-deficiency leads to dysregulation of multiple important downstream pathways causing *NF2* mutant meningiomas to have a higher proliferative index and larger tumour size compared to other genotypic variants [75].

NF2 gene mutations are found in only half of all meningiomas. The recent advances in next-generation sequencing technologies have played a significant role in finding several additional genes that were recurrently mutated: *TRAF7*, *AKT1*, *KLF4*, *PI3KCA*, *SMO*, *SUFU*, *PRKAR1A* and *POLR2A*. It is important to mention that these genes are mutated mostly mutually exclusive of the *NF2* mutation [76]. *TRAF7* (tumour necrosis factor [TNF] receptor associated factor 7) has been linked to activation of cellular stress pathways, induction of apoptosis, ubiquitination of multiple cellular targets, and modulation of the nuclear factor-kappaB (NFκB) transcription factor [77]. Approximately, 20% of meningiomas have *TRAF7* gene mutations [76]. *AKT1* (also referred to as protein kinase B) is a known oncogene controlled by phosphatidylinositol-3 kinase (*PI3K*). 10% of sporadic meningiomas harbour *AKT1* gene mutations. All *AKT1* gene mutations (c.49G>A, $AKT1^{E17K}$) identified in meningioma result in constitutive *AKT1* activation independent of *PI3K* signalling and promotes tumour growth [76, 78, 79]. *KLF4* (Krüppel-like factor 4) is crucial for regulating cellular proliferation, differentiation, migration, inflammation and pluripotency [80, 81]. *KLF4* gene mutations (c.1225A>C, $KLF4^{K409Q}$) are specific for meningioma, resulting in tumour cell growth [82]. *PIK3CA* (phosphatidylinositol-4, 5-bisphosphate 3-kinase catalytic subunit alpha) represents the catalytic subunit of *PI3K*. Mutations in *PIK3CA* leads to *PI3K* activation, and they are found in 4-7% of meningiomas [76, 83-85].

AKT1, *KLF4* and *PIK3CA* mutations in meningioma can all concomitantly occur with *TRAF7*, but they are mutually exclusive of each other [76, 84]. *SMO* (smoothened) is a G-protein coupled-like receptor and key component of the hedgehog (hh) signalling pathway. *SMO* mutations are mutually exclusive with *NF2* and other non-*NF2* mutations, and they occur in 3-6% of meningiomas [76, 84]. *SUFU* is a tumour suppressor gene that functions downstream of *SMO* to inhibit the hh signalling pathway. Aavikko *et al.* have previously reported a family with multiple meningiomas which resulted from germline *SUFU* mutations (p.Arg123Cys) with a somatic loss of the wild-type allele [86]. *PRKAR1A* (protein kinase A cAMP-dependent regulatory subunit 1) mutations have recently been reported in meningioma [87]. *POLR2A* (RNA polymerase II) is the protein that mediates transcription of all protein-coding genes in eukaryotes. 6% of grade I meningiomas harbour *POLR2A* mutations [87]. Further to gene mutations that affect single factor dysregulation; *SMARCB1*, *BAP1*, and *TERT* gene mutations found in meningiomas are also important to mention (reviewed in [88]).

The genomic profile of meningiomas is associated with their location, and it has an impact on the aggressive nature of the tumour and the chance of recurrence [89, 90]. Mutated genes identified in meningiomas from different locations are summarised in Table 1.

Table 1. Mutated genes identified in meningiomas from different locations. Table adapted from [90].

Gene	WHO Grade	Meningioma Tumour Location
NF2	I-III	Parafalcine Posterior Fossa Spine
TRAF7	I-III	Anterior Skull Base Middle Cranial Fossa Sphenoid Wing
PIK3CA	I-III	Anterior & Middle Skull Base
SMARCB1	I-III	Parafalcine Spine
SMO	I	Anterior Skull Base
KLF4	I	Central Skull Base
AKT1	I	Anterior & Central Skull Base Posterior Fossa
POLR2A	I	Parasellar

3.1.3 Ependymomas

Ependymomas are rare tumours that were previously thought to arise from ependymal cells lining the cerebral ventricles, choroid plexus and the central canal of the spinal cord but have more recently been suggested to be of glial origin [91-94]. They constitute 3-5% of all adult intracranial tumours, 8-10% of childhood tumours of CNS, and 15% of all spinal cord tumours [91, 95-99]. Approximately, 33% of ependymomas have the *NF2* gene mutations resulting in Merlin deficiency, and Merlin loss most commonly occurs in adult spinal ependymomas [46, 100]. Intracranial ependymomas are associated with increased intracranial pressure, impaired balance, hearing, speech, and swallowing. Spinal ependymomas cause back pain and extremity weakness [4, 100, 101]. Diagnosis of ependymomas are often difficult, and 30% of cases are misdiagnosed

as they show similarities with other CNS tumours such as oligodendroglioma, pilocytic astrocytoma and papillary glioneuronal tumours [102, 103], which can lead to complications related to genetic analysis and cell culture of ependymomas. Additionally, Derriford Hospital does not have access to ependymoma tumour tissue. For these reasons, the project only focussed on schwannoma and meningioma.

3.2 *NF2* gene and Merlin

The *NF2* gene was discovered by positional cloning and loss of heterozygosity studies, and it was localised on chromosome 22, band 22q12.2, with a length of 110 kb [1, 2, 104, 105]. It consists of 17 coding exons alternatively spliced into two major isoforms, and only the first 15 exons have been found to harbour pathological mutations [106]. So far, there are eight alternatively spliced isoforms of the *NF2* gene reported which are all initiated from several transcription start points. Two of the isoforms are predominantly expressed; isoform I which lacks exon 16, and isoform II which encompasses exons 1 to 16 [107].

In total there are 450 mutations of the *NF2* gene reported by the Human Gene Mutation Database [108], consisting of splice site mutations, frameshifts, small deletions, small insertions, gross deletions, gross insertions/duplications, complex rearrangements, nonsense and missense mutations [109-111]. Position and the type of *NF2* gene mutations determine the severity of resultant tumours. For instance, truncating nonsense mutations or frameshift mutations that are diagnosed at a younger age lead to a higher number of schwannomas with severe clinical phenotype [112, 113]. Conversely, frameshifts, large deletions and missense mutations result in a much milder disease in

NF2 patients [113]. Additionally, NF2 patients harbouring splice site mutations in exons 1-5 of the *NF2* gene suffer from a more severe disease than those harbouring splice site mutations in exons 11-15 [73].

The protein product of the *NF2* gene is Moesin Ezrin Radixin-like (ERM) protein (Merlin), a tumour suppressor protein that belongs to the superfamily of band 4.1 proteins [1, 114]. The ERM family proteins link the cytoskeleton to the cell membrane via integral membrane proteins or indirectly via membrane-associated proteins [115]. Merlin consists of a C-terminal tail domain (CTT) that lacks the canonical actin-binding motif of other ERM proteins, an α-helical domain, and an N-terminal FERM domain that contains an actin-binding domain through which Merlin can interact with the cytoskeleton [116]. Merlin can form a CTT-FERM (head-to-tail) interaction like other ERM proteins, and switch between open and closed conformation depending on its phosphorylation status. p21-activated kinases (PAKs) and c-AMP-dependent protein kinase A (cAMP/PKA) independently phosphorylate CTT of Merlin at serine 518 (Ser518), thereby disrupting head-to-tail interaction and rendering the protein in open conformation [117, 118]. Furthermore, phosphorylation of Merlin decreases its association with the actin cytoskeleton [118-121]. Merlin and PAK1 have a dynamic interaction that is facilitated upon increased cell density. Merlin inhibits the activation of PAK1 via binding to the PAK1 protein binding domain, thus interfering with the binding of active Rac to the PAK1 protein binding domain. Loss of Merlin has been shown to result in hyperactivation of PAK1 [122]. De-phosphorylation of Merlin at Ser518 occurs via myosin phosphatase MYPT1-PP1δ, which activates its tumour suppressor role [123]. In its open conformation, Merlin has an active scaffolding role

linking F-actin, transmembrane receptors and intracellular effectors to modulate receptor-mediated signalling pathways controlling cell proliferation and survival [42]. For example, Merlin promotes downstream Hippo signalling by directly binding and recruiting the effector kinase Lats1 to the plasma membrane [124]. However, Merlin's tumour suppressor roles are activated when it has a semi-open conformation [125, 126]. Merlin's tumour suppressor activities are regulated by cell density. At low cell density, Merlin is phosphorylated by PAK at Ser518, and the signalling cascade is initiated by activated Rac and activated Cdc42 [119]. The Rac/Cdc42 mediated phosphorylation of Merlin at Ser518 can increase cAMP and promote myelination [127]. cAMP has been shown to increase the expression of myelin genes and proteins *in vitro* [128]. Furthermore, cAMP-dependent phosphorylation of the transcription factor nuclear factor-κB is essential for the myelin formation [129]. cAMP-dependent PKA can also phosphorylate Merlin at Ser518 when the PAK activity is suppressed, indicating that PKA and PAK function independently [118]. Activation of the cAMP/PKA pathway promotes Schwann cell growth and cell cycle progression [130], and it is crucial for the myelin formation [131]. Although there is no direct functional relationship between PAK and PKA, they both put Merlin in a growth permissive state where it inhibits the binding of Merlin to CD44, a transmembrane hyaluronate receptor. At high cell density, Merlin is de-phosphorylated and inhibits cell growth. Morrison *et al.* have shown that Merlin binds to the ERM-binding motif in the CD44 cytoplasmic tail at high cell density causing Merlin de-phosphorylation and activation of its tumour suppressor activities [118, 132, 133]. Finally, the regulation of Merlin's activity is summarised in Figure 2.

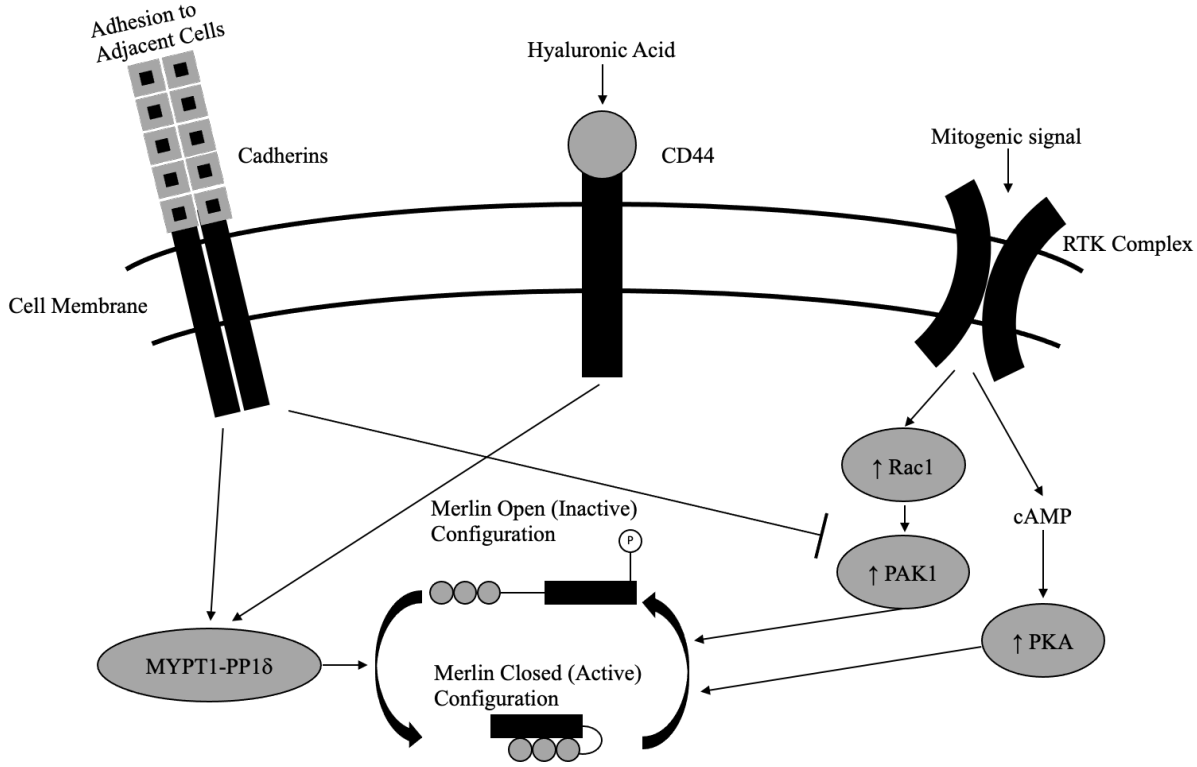

Figure 2. Schematic diagram demonstrating the regulation of Merlin's activity.

Merlin can form a CTT-FERM (head-to-tail) interaction like other ERM proteins, and switch between open and closed conformation depending on its phosphorylation status. Merlin's tumour suppressor activities are regulated by cell density. At low cell density, Merlin is phosphorylated by p21-activated kinase 1 (PAK1) at Ser518, and the signalling cascade is initiated by activated Rac1 and activated Cdc42. cAMP-dependent protein kinase A (PKA) can also phosphorylate Merlin at Ser518 independently of PAK1. Both PAK1 and PKA put Merlin in a growth permissive (inactive) state where it inhibits the binding of Merlin to CD44, a transmembrane hyaluronate receptor. At high cell density, myosin phosphatase MYPT1-PP1δ de-phosphorylates Merlin at Ser518. Additionally, Merlin binds to the ERM-binding motif in the CD44 cytoplasmic tail at high cell density causing Merlin de-phosphorylation by myosin phosphatase MYPT1-PP1δ at Ser518. De-phosphorylation of Merlin at Ser518 activates its tumour suppressor activities including the inhibition of PAK1. The figure is adapted from [134].

Merlin acts as a tumour suppressor in several key pathways via receptor tyrosine kinases, small GTPases, mammalian target of rapamycin (mTOR), phosphatidylinositol 3-kinase (PI3K)/AKT pathway, and the Hippo Pathway; thereby controlling cell proliferation and survival [135]. Merlin prevents the activation of Ras/Raf/MEK,

PI3K/AKT and Rac/PAK pathways, regulating cell-cell contact at adherens junctions, regulating growth factor receptors, CD44 and integrin expression. Loss of Merlin leads to dysregulation/activation of these pathways which then cause altered cell adhesion properties, increased cell proliferation and survival (reviewed in [46]).

3.3 Merlin as a Tumour Suppressor

Merlin is a tumour suppressor protein that functions at the membrane as an inhibitor of CD44, integrins and receptor tyrosine kinases (RTKs) mediated mitogenic/survival signalling, and in the nucleus as a suppressor of the E3 ubiquitin ligase $CRL4^{DCAF1}$ (Figure 3).

Merlin inhibits growth by interacting with many cellular proteins and regulating their function. Receptor tyrosine kinases (RTKs), including PDGFR (platelet-derived growth factor receptor), ErbB family (epidermal growth factor family B; EGFR, ErbB2 and ErbB3), VEGFR (vascular endothelial growth factor receptor) and IGF1-R (insulin-like growth factor receptor) are among these proteins. PDGFR is overexpressed in human schwannoma tumours, and overexpression of Merlin accelerates the degradation rate of PDGFR in HEI193 cells. As a result, PDGF-mediated Erk1/2 and Akt activation is downregulated leading to decreased cell proliferation in HEI193 cells [136]. Lallemand *et al*. showed that Merlin overexpression in mouse Schwann cells inhibits the delivery of RTKs such as ErbB2, ErbB3, IGF1Rβ and PDGFRβ, to the plasma membrane via secretory vesicles leading to their degradation [137]. Lallemand *et al*. also demonstrated elevated levels of ErbB2, ErbB3, IGF1Rβ and PDGFRβ in Merlin-deficient human schwannoma samples [137]. Accordingly, Merlin knockdown increased EGFR, ErbB2,

and ErbB3 protein expression in the human Schwann cells [138]. PDGFR and ErbB family receptors were also shown to be overexpressed and activated in vestibular schwannoma. Specifically, EGFR was strongly phosphorylated as well as ErbB2, ErbB3, and ErbB4. Additionally, other RTKs including PDGFRβ, AXL, SKY, MER and RON were phosphorylated and activated in vestibular schwannoma samples [139]. Ammoun *et al*. also demonstrated that IGF1R and IGF2R are highly overexpressed in human schwannoma cells, leading to increased proliferation, adhesion and survival via activation of ERK1/2, cJun N-terminal kinase (JNK), and AKT pathways [140]. These data show that a wide range of RTKs are upregulated and hyperactivated in the absence of Merlin, thereby causing downstream mitogenic pathway activation.

Merlin also acts as a negative regulator/inhibitor of several signalling pathways that are involved in cell growth. Merlin regulates Rac/PAK pathway via multiple mechanisms. As explained in the previous section, Merlin and PAK1 have a negative feedback loop between each other. Merlin directly binds to PAK1 and inhibits its binding to Rac1, thus blocking PAK1 recruitment to focal adhesions [122]. Merlin also inhibits Rac activation by mediating contact inhibition of growth via binding to CD44 and suppressing membrane recruitment of Rac1 [132, 141]. Additionally, Merlin binds to Angiomotin through competitive binding and releases Rich1 from the Angiomotin-inhibitory complex, allowing Rich1 to inactivate Rac1 [142]. Therefore, Rac1 inactivation blocks the activation of its downstream effector PAK1 which is required for the phosphorylation of c-Raf and MEK1, leading to reduced Raf/MEK/ERK signalling [122, 142, 143]. Kaempchen *et al.* showed highly elevated Rac activity in human schwannoma cells compared to normal Schwann cells, and they analysed it by

measuring the amount of active Rac-GTP bound to its downstream effector PAK. In addition, they demonstrated increased levels of phosphorylated JNK in the nuclei of human schwannoma cells [144]. Utermark *et al*. also demonstrated upregulated integrin chains β1 and β4 in Merlin-deficient human schwannoma cells resulting in enhanced cell-matrix adhesion and loss of polarity [38]. Furthermore, there are studies showing evidence that increased cell-matrix adhesion due to integrin upregulation is possibly both a consequence and cause of activation of Rac/PAK/JNK and Raf/MEK/ERK pathways [36, 145-147]. Flaiz *et al*. linked increased focal adhesions in Merlin-deficient human schwannoma cells to Rac1 activation [148]. Accordingly, Merlin has been shown to directly bind the components of focal adhesions such as β1 integrin, paxillin and FAK [149, 150]. FAK is also hyperactivated in human schwannoma cells, and its phosphorylated form (phospho-FAK^{Y397}) colocalises with phospho-ERK1/2 in focal adhesions, suggesting that FAK hyperactivation can further increase Raf/MEK/ERK signalling [151]. Finally, Merlin can inhibit Ras activation independent of Rac1 inhibition by displacing ERM proteins and Ras from the Grb-SOS complex, thereby preventing downstream Raf/MEK/ERK signalling [152].

PI3K/Akt/mTOR pathway is a central regulator of cell growth, protein translation, survival, and metabolism. It is also one of the most frequently altered pathways in cancer [153]. Integrin-mediated adhesion has been shown to promote mTORC1 activation in the absence of Merlin [154]. Merlin suppresses PI3K activation through binding to its enhancer PIKE-L, causing decreased Akt activation and reduced cell growth [155]. James *et al*. demonstrated enhanced mTORC1 activity and increased cyclin D1 expression in Merlin-deficient human meningioma and vestibular

schwannoma. More importantly, mTORC1 activation was independent of PI3K/Akt and Raf/MEK/ERK signalling; and cyclin D1 upregulation in Merlin-deficient human meningioma cells was partially mTORC1 dependent [156].

Merlin also interacts with LRP6 and inhibits its phosphorylation, which in turn blocks the activation of Wnt/β-catenin signalling and prevents β-catenin dependent transcription of genes such as *c-myc* and *cyclin D1* [157]. Zhou *et al*. demonstrated higher levels of active nuclear β-catenin, *c-myc* and *cyclin D1* in Merlin-deficient primary human schwannoma cells compared to normal Schwann cells, indicating enhanced Wnt/β-catenin signalling in Merlin-deficient schwannoma. Moreover, the activation of Wnt/β-catenin signalling was Src/PDGFR and PAK2 dependent [158].

Hippo pathway is known to regulate organ development through restraining cell proliferation and promoting apoptosis [159]. Several studies demonstrated Merlin's regulatory roles along the Hippo pathway. Firstly, active Merlin translocates to the nucleus and inhibits nuclear E3 ubiquitin ligase $CRL4^{DCAF1}$ via binding to its DCAF1 and DDB1 components [160]. Secondly, it promotes downstream Hippo signalling by recruiting Lats1/2 to the plasma membrane where it is phosphorylated by Mst1/2 facilitated by Sav [124]. Lats1/2 acts as a tumour suppressor in downstream Hippo signalling by phosphorylating the transcription coactivator YAP, thereby suppressing oncogenic gene expression [161, 162]. On the other hand, $CRL4^{DCAF1}$ targets Lats1 for proteasomal-dependent degradation and also inhibits the kinase activity of Lats2 in the nucleus [161]. In the absence of Merlin, $CRL4^{DCAF1}$ promotes cell cycle progression and anchorage-independent growth, leading to tumourigenesis [160, 163, 164]. Li *et al*.

demonstrated significantly lower levels of phosphorylated YAP in Merlin-deficient human meningioma and vestibular schwannoma samples. Li *et al*. also showed increased expression of YAP target genes in Merlin-deficient mesothelioma cells, indicating that $CRL4^{DCAF1}$ is required for YAP activation in Merlin-deficient mesotheliomas [161].

Ultimately, Merlin loss results in hyperactivation of mitogenic signalling, and thus lead to tumourigenesis (Summarised in Figure 3).

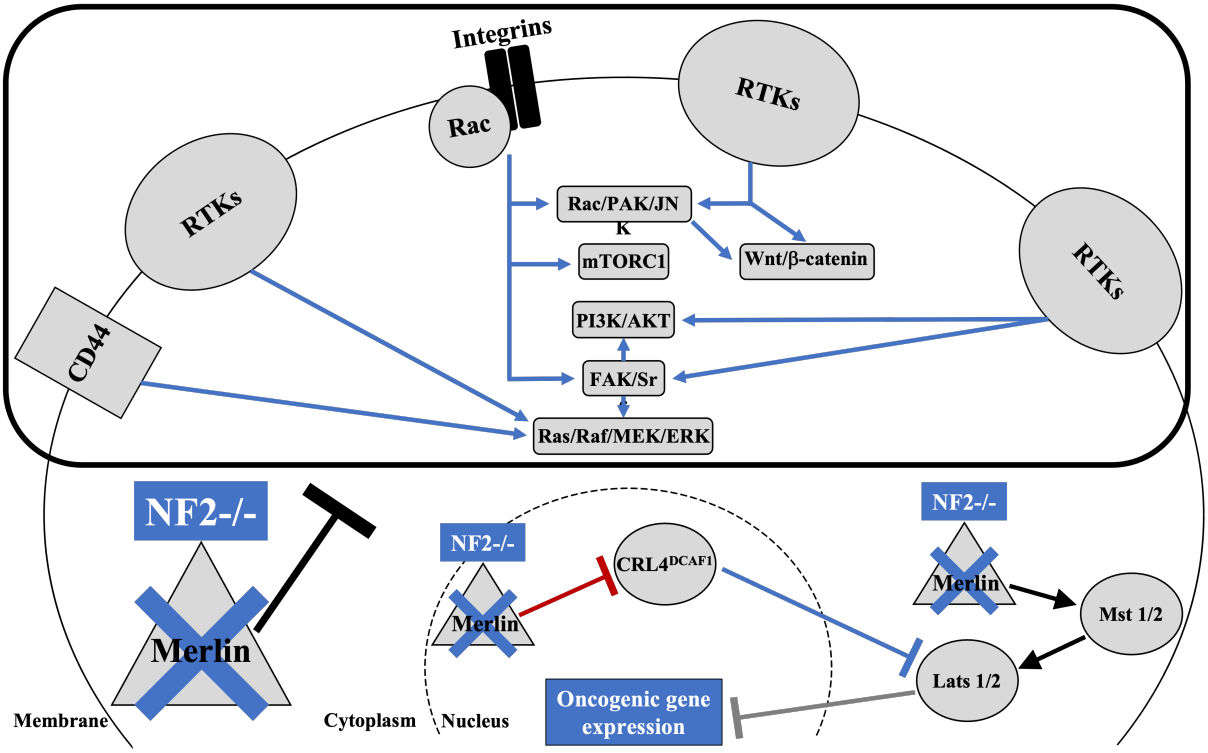

Figure 3. Merlin loss leads to overactivation of the mitogenic signalling pathways and oncogenic gene expression.

Merlin is a tumour suppressor protein that functions at the membrane as an inhibitor of CD44, integrins, and receptor tyrosine kinases (RTKs) mediated mitogenic signalling (indicated by black T-bar and square), and in the nucleus as a suppressor of the E3 ubiquitin ligase $CRL4^{DCAF1}$ (Red T-bar indicates the inhibition of $CRL4^{DCAF1}$ by Merlin; black arrows indicate the translocation of Lats1/2 to the plasma membrane by Merlin, where it is phosphorylated by Mst1/2; gray T-bar indicates the inhibition of oncogenic gene expression by Lats1/2 in the

presence of Merlin). Lack of tumour suppressive Merlin (NF2-/-) dysregulates several signalling pathways mediated by CD44, integrins and RTKs; and causes elevated oncogenic expression (Blue crosses indicate the absence of Merlin; blue arrows indicate the overactivation of the mitogenic signalling pathways in the absence of Merlin; blue T-bar indicates the inhibition of Lats1/2 by $CRL4^{DCAF1}$ in the absence of Merlin). Overall, Merlin deficiency cause altered cell adhesion properties, increased proliferation, and survival. The figure is adapted from Zhou and Hanemann 2012 [165].

3.4 The Cell Cycle and Cancer

The cell cycle is the process through which cells replicate and make two new identical cells. The cell cycle has four sequential phases: G1 (gap phase 1), S (DNA synthesis), G2 (gap phase 2), and M (mitosis/meiosis) [166]. The cell increases in size during the G1 phase, and it initiates the transcription of cell cycle control genes such as the cyclins and begins protein synthesis while performing a series of checks before DNA synthesis. Once the cell enters the S phase, its entire genome is replicated. At the G2 phase, the cell prepares for division and checks for size and DNA replication errors. Finally, the cell divides into two identical daughter cells during the M phase. Following the completion of cell division, the cells either renter the G1 phase or remain quiescent in the G0 phase [166]. Progression through the cell cycle is tightly regulated by the cyclin dependent-kinase (CDK) family of serine/threonine kinases and their regulatory partners the cyclins. Cyclin D-CDK4, cyclin D-CDK6 and cyclin E-CDK2 complexes drive the G1 phase progression through the restriction point at the end of the mid G1 phase which commits the cells to complete the remaining phases of the growth cycle [167, 168]. Cyclin E-CDK2 induces DNA synthesis, whereas cyclin A-CDK2 promotes the completion of DNA synthesis and entry into the G2 phase. Lastly, Cyclin B-CDK1 regulates progression through the G2 phase and promotes M phase entry [168].

Progression through each cell cycle phase and transition from one phase to the next is induced by mitogenic signals and monitored by checkpoints, which detect aberrant or incomplete cell cycle events (DNA damage). In response to DNA damage, checkpoint pathways carry the detected signal to the effectors that can trigger cell cycle arrest until the error is corrected. The effectors consist of CDK inhibitors (CDKIs), which can reversibly halt cell cycle progression [169, 170].

Stimulation by mitogenic factors activate cascades of intracellular signalling pathways that impinge CDK4 and CDK6 to drive cell cycle progression from the G0 or G1 phase into the S phase. These pathways eventually activate transcription factors such as β-catenin, MYC or activator protein 1 (AP-1) and induce the synthesis of several cell cycle proteins, including cyclin D [171]. Cyclin D-CDK4/6 complexes phosphorylate and inactivate the retinoblastoma protein Rb, and the closely related proteins p107 and p130, thereby activating E2F transcription factors. The E2F transcription factors induce transcription of genes involved in cell cycle progression from G1 into S phase, including cyclin E [172]. The CDK4/6-Rb pathway is commonly mutated in human cancers, including glioblastoma, melanoma, and lymphoma. Especially, the cyclin D1 gene is the second most frequently amplified locus among all human cancer types [173-176].

Cyclin E-CDK2 complexes phosphorylate many proteins required for cell cycle progression, DNA replication and centrosome duplication [177, 178]. During the S phase, cyclin E is degraded via F-box/WD repeat-containing protein 7 (FBXW7)-mediated ubiquitylation [179, 180]. Subsequently, CDK2 form a complex with newly synthesised cyclin A2 to form active cyclin A-CDK2 complexes [181]. CDK2

mutations are rare among human cancers. However, the catalytic activity of the cyclin E-CDK2 complex is hyperactivated by cyclin E overexpression resulting from either genomic amplification, loss of function mutations in FBXW7 or expression of a hyperactive, truncated form of cyclin E1 [182-186]. Cyclin A is also frequently overexpressed in human cancers because of genomic amplification which was observed in hepatocellular carcinomas [187], and colorectal [188] and breast cancers [189]. CDK2 activity itself is important in MYC-overexpressing tumours where CDK2-mediated phosphorylation of MYC is required to suppress senescence [190, 191]. Furthermore, CDK2 depletion suppressed growth and cell cycle progression in melanoma [192].

CDK1 is the most crucial CDK for the cell cycle progression [193], where it binds to and becomes activated by cyclin A2 and cyclin B during the G2 phase. Mitotic entry results in cyclin A2 degradation, whereas CDK1 activity is maintained in complexes with B-type cyclins. Therefore, CDK1 kinase activity is necessary for mitotic entry and several mitotic events [193-195]. Current research has shown that dysregulation of CDK1 in melanoma leads to rapid tumour growth and spontaneous proliferation of cancer cells [196]. CDK1 was also shown to be involved in the progression of colorectal, liver, and lung cancers. Furthermore, overexpression of CDK1 is associated with reduced survival time [197-199]. Cyclin B1 is the regulatory subunit of CDK1, and its deregulation has been shown to play a role in chromosomal instability in human cancers [200-204]. Cyclin B1 is overexpressed in various carcinomas including oesophageal squamous cell carcinoma, laryngeal squamous cell carcinoma and colorectal carcinoma [205-207]. Furthermore, cyclin B1 overexpression is correlated

with poor prognosis and resistance to radiotherapy in head and neck squamous cell carcinoma [205, 206].

3.5 Retroviruses

Retroviruses are a large and diverse family of enveloped RNA viruses that are characterised by two main features: (1) the ability to reverse transcribe viral RNA into DNA and (2) integrate the viral DNA into the host genome. The fact that retroviruses can become part of the host genome through infection makes them unique among other virus families.

3.5.1 Retrovirus Structure and Genome

Members of the retrovirus family share common structural features. Retrovirus virions are enveloped viral particles with a diameter of 80-100 nm. Virion core contains the retroviral genome, which is genetically diploid, consisting of two linear, positive-sense, single-stranded RNA molecules. The RNA strands are held together by hydrogen bonds near the 5' ends, and each RNA strand has a specific host transfer RNA (tRNA) base-paired to the primer binding site (PBS) near the 5' end. The RNA strands are complex with the nucleocapsid (NC) proteins in a helical structure. The virion core is enclosed within a polymer of capsid (CA) proteins. Matrix (MA) proteins surround the layer outside the virion core and interact with the host-derived lipid envelope [208-210] (Figure 4). Viral envelope protein is synthesised and glycosylated in the rough endoplasmic reticulum as a precursor glycoprotein, which oligomerises predominantly into trimers. Oligomerised Env glycoprotein is transported to the Golgi and *trans*-Golgi

network and proteolytically cleaved by cellular furin or furin-like proteases [211] to yield the mature surface (SU) glycoprotein and the transmembrane (TM) glycoprotein. Following cleavage, SU and TM glycoproteins remain associated with non-covalent interactions. Then, complexes of SU-TM glycoproteins are transported to the plasma membrane through the secretory pathway and are incorporated as trimeric spikes into virus particles [212]. SU is responsible for receptor binding. TM functions as a membrane-spanning anchor that mediates virus and host cell membrane fusion during virus entry [208-210, 213] (Figure 4).

The RNA genome in a virion (8-10 kb in length) has a cap structure at the 5' end and a poly (A) tail at the 3' end. Four ORFs (open reading frames) that encode the virion structural and replication proteins (5'-*gag-pro-pol-env*-3') are in the middle. Non-coding regions at both ends are composed of *cis*-acting elements (5'-R-U5-PBS and PPT-U3-R-3') that regulate the structural transformations of the RNA genome during the viral cycle. R (repeat sequence) elements that are positioned at both ends of the RNA genome contains transcription start and termination sites.

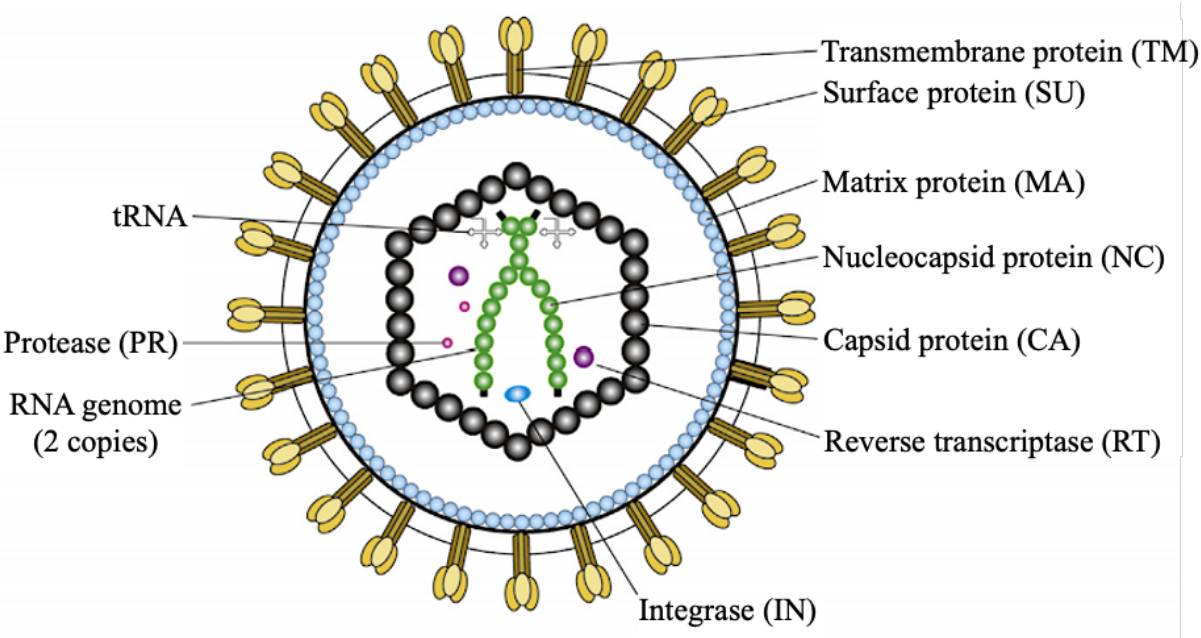

Figure 4. Schematic representation of a retrovirus virion.

Virion core is surrounded by capsid protein (CA), and it contains two RNA strands dimerised through hydrogen bonds near the 5' ends, complexed with nucleocapsid protein (NC). Each RNA strand has a host transfer RNA (tRNA) attached near the 5' end. Two envelope glycoproteins (SU and TM) form the viral envelope, and they interact with the virion core through matrix protein (MA). Three viral enzymes (PR, IN, and RT) are indicated. The figure is taken from Molecular Virology of Human Pathogenic Viruses, p.229 (Ryu, 2017) [209].

Sequence elements U5 (unique sequence 5) and U3 (unique sequence 3) are located next to the R elements at 5' end and 3' end, respectively. U5 in some viruses contains responsive elements to transcription factors. U3 contains the poly (A) signal (polyadenylation signal), as well as promoters, enhancers, and responsive elements to transcription factors. PBS (primer binding site) is located downstream of the U5 element. PBS is base paired with a specific host tRNA that acts as an RNA primer for the first strand DNA synthesis during viral reverse transcription. PPT (polypurine tract) element is located upstream of the U3 element, and it acts as an RNA primer for the second strand DNA synthesis during viral reverse transcription. Lastly, the sequence

for encapsidation signal (Ψ) is located between the U5 element and the first ORF [209, 210] (Figure 5).

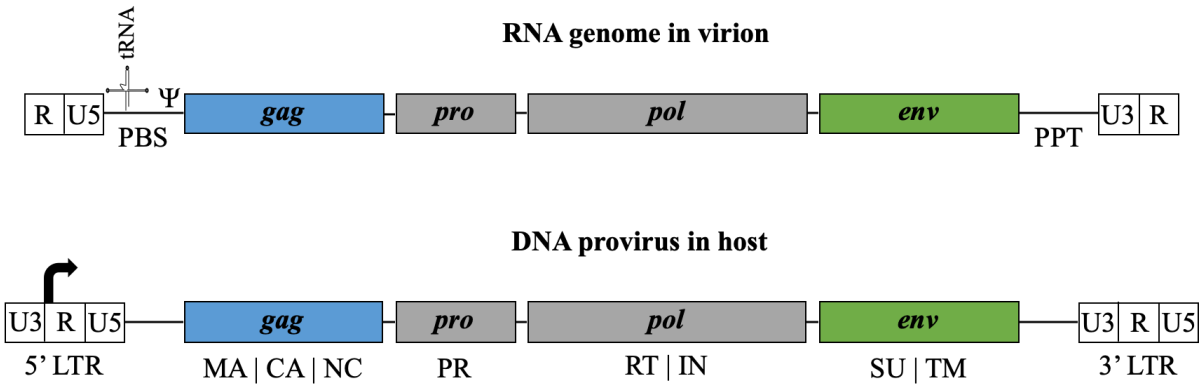

Figure 5. Structure of retroviral RNA genome in virion and DNA provirus in host.

In the virion, the RNA genome is arranged as follows: R (repeat sequence) at each end; U5 (unique sequence 5) after R at the 5' end; PBS (primer binding site) base-paired to host transfer RNA (tRNA), located downstream of U5; Y is the sequence for encapsidation signal, located between U5 and the beginning of *gag* ORF (open reading frame); followed by *gag*, *pro-pol*, and *env* ORFs; PPT (polypurine tract) located after *env* ORF; and U3 (unique 3 sequence) located downstream of PTT, before R at the 3' end. In the host, DNA provirus has the same arrangement as RNA genome with additional LTRs (long terminal repeats) consisting of U3, R, and U5. The figure is adapted from Molecular Virology of Human Pathogenic Viruses, p.229 (Ryu, 2017) [209] and Johnson 2019 [214].

Following viral entry, the RNA genome in virion is reverse transcribed into dsDNA. Additionally, U3 and U5 elements are duplicated to generate two identical LTRs (long terminal repeats) at both ends of the DNA strands. The LTRs contain the primary promoter and regulatory elements for provirus expression, as well as *cis*-acting elements required for integration. Between the LTRs are ORFs for the major structural and replication proteins of the virion (Figure 4). The *gag* ORF encodes for the Gag polyprotein which is made of matrix (MA), capsid (CA), and nucleocapsid (NC) proteins. The *pro-pol* ORFs encode for the viral enzymes required for structural and

replication proteins: protease (PR) which cleaves Gag polyprotein into separate structural components (MA, CA, NC); reverse transcriptase (RT) which reverse transcribes RNA genome into dsDNA; and integrase (IN) which integrates the viral dsDNA into the chromosomal DNA of the host cell, where it forms the DNA provirus [209, 210, 214] (Figure 4 and 5).

3.5.2 Viral Cycle

As with other virus families, retroviruses need host cell transcription machinery for the replication process. The viral cycle of retroviruses is divided into two main stages. The first stage consists of events involved in viral entry and integration of the provirus. During the second stage, all virus components are produced and packed for the release of progeny virions (Figure 6).

Viral entry is initiated by the attachment of the viral envelope SU to the host cell-surface ligand. Virus attachment subsequently exposes and activates the fusion peptide embedded in TM, and thus triggering the fusion of two lipid membranes and insertion of the viral core into the cell cytoplasm. Following entry, the viral core is transported near the nucleus via intracellular trafficking. During the transit, viral DNA is synthesised by the viral reverse transcription process, and the capsid surrounding the viral core is uncoated. The resulting viral DNA with additional LTRs (explained in the previous section) is then complexed with the viral integrase, where it forms a complex termed the pre-integration complex (PIC). PIC serves as a precursor for chromosomal integration, and it enters the nucleus either during nuclear membrane breakdown in dividing cells (M phase) or via nuclear pores in nondividing cells, which is a process

that entirely depends on the type of retrovirus. Following nuclear entry, the DNA provirus becomes integrated into the chromosomal DNA. Integration tends to occur in regions where the chromosome is undergoing active transcription [208, 209, 213].

The integrated provirus is transcribed by cellular RNA polymerase II into full-length viral RNA molecules (viral genome) and mRNA molecules that have been spliced into smaller RNAs by the host cell spliceosome to provide a template for the Gag, Pro, Pol, Env, and the accessory viral proteins. U3 element at the 5' LTR acts as the promoter for transcription. Transcription is initiated from the 5' R and it proceeds to the end of 3' R. U5 element at the 3' LTR signals cleavage and polyadenylation of the RNA where it forms the poly (A) tail at the 3' end. After the transcription process is complete, viral mRNA molecules are transported into the cytoplasm to be translated into viral proteins by host cell ribosomes. Following their translation, the Env glycoproteins SU and TM are glycosylated in the cytoplasmic Golgi apparatus and subsequently trafficked to the plasma membrane [208, 209, 213].

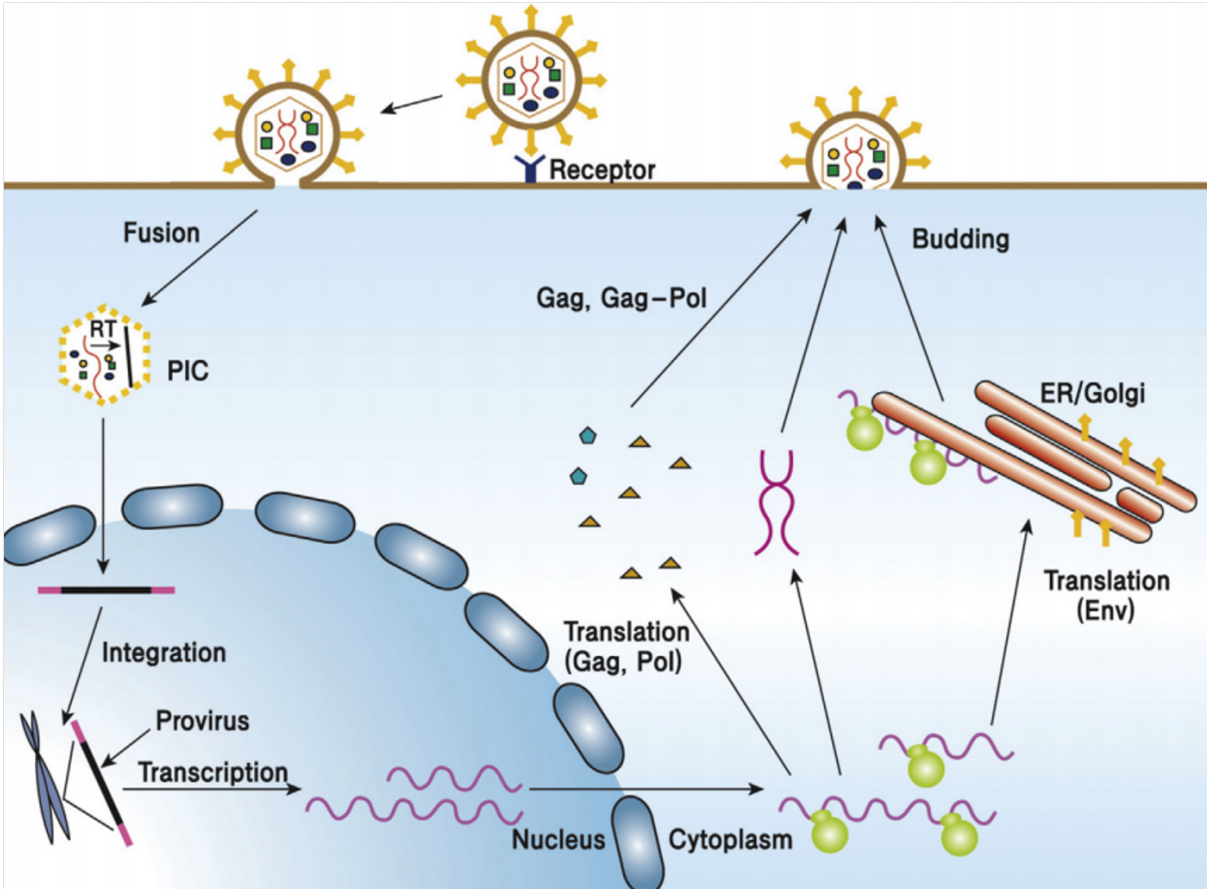

Figure 6. Replication cycle of retroviruses.

The retroviral cycle starts with the interaction between the viral SU and a cellular receptor. The interaction leads to a fusion between the viral and cellular lipid membranes and thus causing the viral core to enter the cell cytoplasm. The viral core is subsequently uncoated, and the viral RNA is reverse transcribed by RT into DNA. The viral DNA complexes with IN to form the PIC that serves as a precursor for chromosomal integration. Following the nuclear entry of PIC, DNA provirus is integrated into host chromosomal DNA. The integrated provirus is transcribed by cellular transcription machinery into mRNA molecules that are later transported into the cytoplasm to be translated into viral proteins by host cell ribosomes. After translation, the Env glycoproteins are glycosylated in the cytoplasmic Golgi apparatus, and they are transported to the plasma membrane. The immature core is linked to the Env glycoproteins by the MA. Finally, the progeny virions bud from the plasma membrane. The figure is taken from [209].

After translation, the Gag polyprotein binds to the viral genome in the cytoplasm and initiates viral assembly. As a result, the Gag/RNA complex is recruited to the plasma

membrane for the capsid assembly. Viral capsid assembly is then coupled with the packaging of the viral RNA genome. NC domain of Gag recognises the packaging signal (Ψ) and triggers packaging. Afterwards, the MA domain of Gag links the Gag/RNA complex with the Env glycoproteins at the plasma membrane. Finally, the progeny virions bud from the plasma membrane which provides them a lipid bilayer membrane after budding. Budding is followed by the cleavage of Gag polyprotein by the protease into NC, CA, and MA proteins that are crucial for the maturation and infectivity of progeny virions [208, 209, 213].

3.5.3 Discovery and Classification

Avian leukosis viruses (ALVs) and Rous sarcoma virus (RSV) were the very first traces of retroviruses, discovered by Ellernan & Bang (1908) and Peyton Rous (1911), respectively. After 25 years, John Bittner identified the first mammalian retrovirus and demonstrated the importance of these discoveries. Human T-cell lymphotropic virus type 1 (HTLV-1) was the first human retrovirus to be described in 1980 which was later followed by the discovery of human immunodeficiency virus type-1 (HIV-1) in 1983 [208].

The newest classification divides the family *Retroviridae* (retroviruses) into two subfamilies (*Orthoretrovirinae* and *Spumaretrovirinae*) and seven genera, and the classification is based upon their genomic sequence. The subfamily *Orthoretrovirinae* is further subdivided into six genera: *Alpharetrovirus, Betaretrovirus, Gammaretrovirus, Deltaretrovirus, Epsilonretrovirus,* and *Lentivirus.* On the other hand, the subfamily *Spumaretrovirinae* is formed by a single genus, *Spumavirus*. Five

of these genera includes potentially oncogenic retroviruses (formerly known as oncoviruses) such as RSV, ALVs, and HTLV-1. However, the genera *Spumavirus* and *Lentivirus* (which includes HIV-1) are not tumourigenic [213].

3.6 HERVs: Discovery and Classification

Howard M. Temin was the first scientist ever to propose the DNA provirus hypothesis which stated that RSV viral RNA is converted to genetically stable DNA in infected cells. In that way, cells transformed by the oncogenic RSV infection maintained their phenotype through many mitoses, even in the absence of viral replication [215]. Eventually, Temin and David Baltimore discovered the viral enzyme reverse transcriptase in 1970 and led to the acceptance of the DNA provirus hypothesis [216, 217]. Interestingly, the initial evidence for endogenous retroviruses (ERVs) was gathered in the same period in the late 1960s. Virology and genetics studies in chickens (ALV and RSV), mice (murine leukaemia virus and murine mammary tumour virus), and cats (feline leukaemia virus) revealed the presence of proviral sequence in the genome of these species (reviewed in [218]). As most of these ERVs had a tumourigenic outcome, it was important to screen humans for any presence. Martin *et al*. (1981), Callahan *et al*. (1982) and Ono (1986) established the first evidence of human endogenous retroviruses (HERVs) by hybridising human DNA using probes derived from murine leukaemia virus (MLV), murine mammary tumour virus (MMTV) and Hamster Intracisternal A (IAP), respectively [219-221]. In addition, Horn *et al*. demonstrated the presence of endogenous proviral genomes in human chromosomes and suggested that HERVs could contribute to tumourigenesis through insertional

mutagenesis and proto-oncogene capture [222]. Eventually, all these studies opened new doors to study HERVs further to investigate their role in human diseases.

Retroviruses generally infect somatic tissues but the fact that they can spread in a host population raises the possibility of integration in germline cells or in the precursor of germline cells. Such cells can result in the production of host gametes that carry proviral genomes or in other words endogenous retroviruses which can be inherited by successive generations according to Mendel's first law. Over the course of millions of years, the genomes of vertebrates have accumulated hundreds of thousands of ERV loci that originate from ancient, extinct exogenous retroviruses. However, the majority became defective as a consequence of mutations, deletions, and termination signals accumulated within coding sequences across thousands to millions of years of vertebrate evolution (reviewed in [214]).

HERVs have integrated themselves into the human genome across evolution and now they form 5% of it [223]. Over 20 HERV families have been identified so far, and they are distributed among classes I, II and III of ERVs that are related to the *Gammaretrovirus*, *Betaretrovirus* and *Spumaretrovirus*, respectively. HERVs are classified into different groups based on the similarity of their PBSs to host tRNAs. HERV-K for instance was named after the tRNA that corresponds to lysine [224, 225]. Over time, HERVs became defective and lost their infectious ability. However, a limited number of them have the potential to produce structurally intact retrovirus particles. Several studies revealed the presence of retrovirus particles in germ cell tumours [226-230] and melanomas [231] that were coded by HERV-K. Additionally,

Boller *et al*. reported the provirus HERV-K113 as the candidate for producing intact retrovirus particles resembling those that were observed in germ cell tumours [232]. Although there are studies showing the presence of retrovirus particles, no infectious human endogenous retrovirus has ever been identified.

3.7 HERV-K (HML-2)

HERV-K is a family of HERV that phylogenetically belongs to the class II of ERVs, and it is the most recently integrated and best-preserved HERV family that are still transcriptionally active [10, 233-237]. HML-2 (human endogenous MMTV-like 2) is the youngest and most active subgroup of HERV-K family, and many HML-2 proviruses possess intact ORFs encoding for all retroviral genes. In addition, HML-2 transcripts and proteins have been identified in healthy tissues [238], embryonic cells [239], and malignancies [7, 8, 10, 11, 240-244]. Since the project only aims to investigate the HML-2 subgroup of the HERV-K, all future reference for HML-2 will only be addressed as "HERV-K".

3.7.1 HERV-K (HML-2) Genome Structure and Transcripts

The human genome accommodates more than 1000 reported HERV-K (HML-2) loci whose insertional elements possess 85 reference (hg19) provirus insertions, 946 reference (hg19) solo-LTR insertions, 5 non-reference (not present in the human reference genome) provirus insertions, and 27 non-reference solo-LTR insertions [245-248]. Subramanian *et al*. reported 91 HERV-K (HML-2) related full-length and near full-length proviruses in the human genome [245], classifying them into two subtypes: type I that constitutes ~26% of all proviruses and possess a 292-bp deletion in the *pol*-

env junction; type II that constitutes ~74% of all proviruses and lacks the 292-bp deletion [227, 245]. Proviral organisation of HERV-K is similar to present-day exogenous retroviruses such as HIV-1 and HTLV-1, consisting of four ORFs (*gag*, *pro*, *pol*, and *env*) flanked by a 5' and 3' LTR [249] (Figure 6). Both LTRs consist of U3, R, and U5 regions, and they possess promoter and enhancer elements, multiple transcription binding sites, and a polyadenylation signal [250]. Additionally, there are two splice donor (SD) and two splice acceptor (SA) sites that are involved in the splicing events following transcription of the provirus. HERV-K produces four mRNAs [249] (Figure 7). mRNA 1 is an unspliced transcript that has three ORFs that encode for Gag, Gag-Pro and Gag-Pro-Pol polyproteins. Within mRNA 1, only *gag* ORF has a start codon (AUG); *pro* and *pol* translation is initiated by two ribosomal frameshifts (Figure 7). Gag possesses the sequences to form the structural proteins MA, CA, and NC. Pol has the sequence for RT, which contains Rnase H and polymerase domains, and IN. The *pro* ORF encodes for the protease and dUTPase. All the functional and structural proteins are formed by proteolysis of all three polyproteins (Figure 7). mRNA 2 is a spliced transcript that results from mRNA 1. mRNA 2 encodes for Env, which has three domains: the signal peptide (SP), SU and TM (Figure 7). mRNA 3 results from alternative splicing of the *env* ORF and encodes the accessory protein Rec. mRNA 3 is only produced by type II HERV-K proviruses that lack the 292-bp deletion at the *pol-env* junction. Lastly, mRNA 4 also results from alternative splicing of the *env* ORF. However, it encodes for Np9, which is only produced by type I HERV-K proviruses that possess the 292-bp deletion at the *pol-env* junction. SD_2 is lost due to the deletion and an alternative SD is used for the splicing event (Figure 7). In addition, Rec shares

87 amino acids with Env, corresponding to its first exon; and Np9 shares the first 14 amino acids of it with Env and Rec (Figure 7) [251-253].

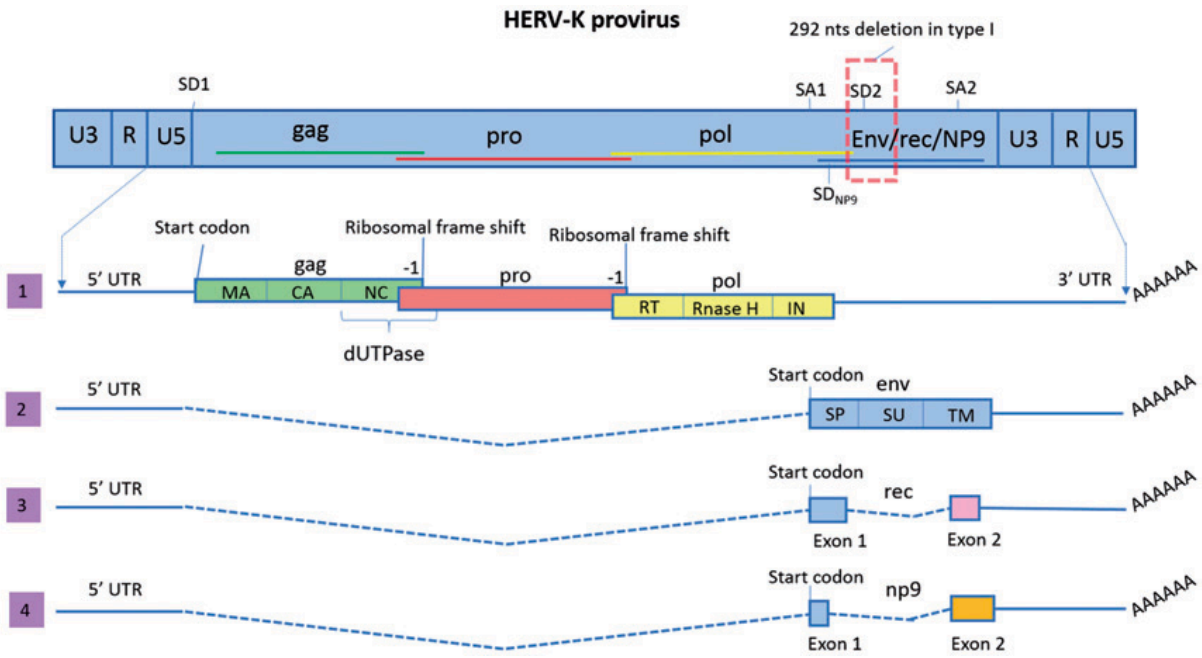

Figure 7. Proviral organisation of HERV-K and mRNA transcripts.

The HERV-K provirus possesses four ORFs (*gag*, *pro*, *pol* and *env* sequences overlapping). Splice donor (SD) and splice acceptor (SA) sites are shown. LTRs on both sites consist of the U3, R and U5 regions. HERV-K transcription starts after the R, and it forms four main mRNA. mRNA 1 is an unspliced transcript that harbour *gag-pro-pol* ORFs, where only *gag* possesses a start codon (AUG). *pro* and *pol* translation is initiated by two ribosomal frameshifts (-1). *gag* produces matrix (MA), capsid (CA) and nucleocapsid (NC); *gag-pro* junction produces dUTPase; and *pol* produces reverse transcriptase (RT), Rnase H and integrase (IN). The polyproteins Gag, Gag-Pro and Gag-Pro-Pol go through proteolysis to form the functional proteins. mRNA 2 transcript results from the splicing of mRNA 1 and it encodes for Env, which has three domains: the signal peptide (SP), surface (SU) and transmembrane (TM). The *env* ORF also goes through alternative splicing to result in either Rec (mRNA 3) or Np9 (mRNA 4) depending on the type of HERV-K. The figure is taken from Garcia-Montojo *et al*. [253].

A recent investigation of the HERV-K (HML-2) proviruses found up to 23 transcriptionally active HERV-K (HML-2) proviruses in the human genome [254],

which possess ORFs for the retroviral genes. Human-specific HERV-K proviruses containing *gag*, *env*, and *pol* ORFs are summarised in Table 2.

Table 2. Human specific HERV-K (HML-2) proviruses that have ORFs. Table adapted from [245].

Locus	Alias	ORFs	References
1p31.1	K4, K116, ERVK-1	*gag*	[255]
3q13.2	K106, K(C3), K68, ERVK-3	*gag*	[234]
3q24	ERVK-13	*gag*	[245]
3q27.2	K50b, K117, ERVK-11	*gag, pol*	[256]
5q33.3	K107/K10, K(C5), ERVK-10	*gag, pol*	[257]
6q.14.1	K109, K(C6), ERVK-9	*gag, env*	[234]
7p22.1a	K108L, K (HML.2-HOM), K(C7), ERVK-6	*pol, env*	[234]
7p22.1b	K108R, ERVK-6	*pol, env*	[234]
7q22.2	ERVK-14	*gag*	[245]
8p23.1a	K115, ERVK-8	*gag, pol, env*	[235]
10p12.1	K103, K(C10)	*gag, pol*	[234]
10q24.2	ERVK-17, c10_B	*gag*	[258]
11q22.1	K(C11c), K36, K118, ERVK-25	*pol*	[259]
12q13.2	-	*gag, pol*	[260]
12q14.1	K(C12), K41, K119, ERVK-21	*gag, pol, env*	[259]
19p12b	K113	*gag, pol, env*	[235]
19q11	K(C19), ERVK-19	*gag, env*	[261]

3.7.2 HERV-K (HML-2) Proteins

HERV-K Gag polyprotein (74 kDa) is cleaved by protease into MA (15.3 kDa), SP1 (spacer peptide of 14 amino acids, 1.5 kDa), p15 (15 kDa), CA (27.7 kDa), NC (10 kDa), and two C-terminally encoded glutamine- and proline-rich peptides, QPI (2.5 kDa) and QP2 (2.1 kDa), that forms the virion core structure [262]. HERV-K protease (334 amino-acid in length) is encoded by *pro* and it processes Gag polyprotein, as described previously [263]. The *pol* ORF encodes for RT with a Rnase H domain (209 amino-acid in length), which is responsible for the reverse transcription of the retroviral RNA into DNA; and IN (180 amino-acid in length), which integrates the retroviral DNA into the host genome [264-266]. The *env* ORF encodes a 70 kDa polyprotein that consists of three domains: signal peptide (SP, 13 kDa), surface (SU, 44 kDa) and TM (26 kDa). The signal peptide directs the Env polyprotein to ER for glycosylation. Considering glycosylation, the size of Env-FL (full length) ranges from 70-95 kDa, with SU ranging from 42-55 kDa and TM from 26-38 kDa [267, 268]. Finally, Rec and Np9 are 14.5 kDa and ~9 kDa protein, respectively. Rec is an accessory protein that helps the viral transcripts with their nucleocytoplasmic transport and facilitates the incorporation of the viral genome into particles in the cytoplasm [269]. In comparison, Np9 has no known function in HERV-K viral replication cycle.

3.7.3 HERV-K (HML-2) and Cancer

The tumorigenic potential of HERV-K is widely investigated on a variety of tumours found in different parts of the human body, and current findings suggest that HERV-K has the potential to facilitate the tumourigenesis process. Recent studies suggested four potential mechanisms of HERV-K induced tumourigenesis: chromosomal rearrangements, LTR activation of oncogenes, immunosuppression and HERV-K derived tumourigenic proteins (reviewed in [253]).

HERV LTRs show sequence similarities which make homologous recombination possible between two different LTRs, leading to internal proviral sequence loss, in other words, solo LTRs [245]. More importantly, homologous recombinations can occur between distant LTRs existing in different chromosomes, which can result in chromosomal rearrangements [256]. Some HERV-K loci have been shown to contribute to human genome evolution through chromosomal rearrangements [256]. However, there is also a small possibility that HERV-K may contribute to tumourigenesis through homologous recombination resulting in chromosomal rearrangements [253, 256].

LTR induced tumourigenesis is another possible mechanism of HERV-K associated tumourigenesis. As explained in Section 3.7.1, HERV-K possesses LTRs that act as a promoter of the provirus. Therefore, derepressed HERV-K LTRs could recruit transcription factors and act as an alternative promoter of adjacent host genes involved in cell proliferation [270-272]. In addition, Tomlins *et al*. showed that chromosomal rearrangements in prostate cancer lead to fusion of HERV-K LTR (22q11.23) with transcription factor ETV1, causing overexpression of truncated ETV1 [273]. A similar

outcome has also been observed in the 8p12 stem cell myeloproliferative disorder, where the FGFR1 gene is fused with HERV-K LTR on chromosome 19 [274]. However, there is no supporting evidence for HERV-K LTR contributing to aberrant overexpression of FGFR1 in the 8p12 stem cell myeloproliferative disorder. Overall, studies have demonstrated the binding of transcription factors Oct4 [275], NFκB and NFAT [276], MITF-M [272], Sp1 and Sp3 [271], YY1 [277] to HERV-K LTR using chromatin immunoprecipitation (ChIP) and electrophoretic mobility shift assay (EMSA). All the addressed transcription factors contribute to tumourigenesis in several types of cancer [278-283], but it is still unknown whether HERV-K LTR contributes to the tumourigenesis process via binding to these transcription factors.

Finally, HERV-K derived proteins have been shown to contribute tumourigenesis and aid the tumourigenesis process by immunosuppression. Through its immunosuppressive domain, HERV-K TM protein can inhibit human immune cell proliferation by overexpressing immunosuppressive cytokines including IL-10, IL-6, IL8, MCP-1, MIP-1α, MIP-1β, uPAR, sTNFRII and GCSF [284, 285]. Additionally, HERV-K Np9 protein promotes the growth of myeloid and lymphoblastic leukaemia cells by activating the Wnt/ β-catenin signalling pathway [286]. Multiple tumours have been shown to activate β-catenin signalling in dendritic cells, suppressing their ability to prime CD8+ T cell responses following antigen cross-presentation [287].

The overall aim of my project is to investigate HERV-K derived tumourigenic proteins; as such, the following sections will focus on the expression and roles of these proteins in various cancers.

3.7.3.1 HERV-K (HML-2) Expression in Cancer

Recent studies have shown HERV-K protein expression in four types of cancer with a significant frequency in patients. Approximately, 85.7% of breast cancer tissues from patients showed HERV-K Env expression. Whereas, HERV-K Env was only expressed in 7.14% of normal breast tissues from healthy donors [10]. In addition, several different loci of HERV-K are overexpressed in the basal subclass of breast cancer, where 70% of basal breast cancer patients showed high expression of HERV-K compared with 50% or less for the other subtypes. Johanning *et al*. also provided evidence that HERV-K expression is higher in basal breast tumours that have wild-type H-Ras [16]. 45% of metastatic melanoma biopsies and 44% of melanoma cell lines were positive for spliced Env and Rec expression. Furthermore, 70% of metastatic melanoma biopsies showed HERV-K Gag expression [241]. 84% of ovarian tissues were positive for HERV-K Env staining, whereas all normal ovarian tissues were negative [11]. Seminoma samples from patients were positive for HERV-K but tissues from healthy testes were stated as negative [243]. HERV-K Env overexpression was also detected in pancreatic cancer biopsies (80%) and seven pancreatic cancer cell lines [9]. Finally, Conteras-Galindo *et al*. demonstrated the presence of HERV-K viral particles in the plasma of lymphoma patients [242].

HERV-K transcripts are also present in many organs. Rec and Np9 transcripts were observed in the brain, the colon, the lung, the liver, the placenta, the spleen, the thymus, the prostate, the testis, the pancreas, the kidney, the heart, the small intestine and leukocytes [288]. However, upregulation of HERV-K transcripts was only observed in

a few types of cancer including breast cancer [10], prostate cancer [7, 8], pancreatic cancer [9] and some ovarian cancers [11].

3.7.3.2 Role of HERV-K (HML-2) in Cancer

The presence of HERV-K in cancer brought interest to study its tumourigenic potential. Zhou *et al*. demonstrated the importance of HERV-K Env protein activation for the tumourigenesis and metastasis of breast cancer cells *in vitro* and in immunodeficient mice xenografted with human breast cancer cell lines by knocking down HERV-K Env [18]. Additionally, Lemaitre *et al*. overexpressed HERV-K Env in a non-tumourigenic human breast epithelial cell line leading to epithelial to mesenchymal transition (EMT), and increased expression of transcription factors involved in breast cancer metastasis. Lemaitre *et al*. also overexpressed HERV-K Env in HEK293T, which led to ERK1/2 activation [17]. Lastly, Johanning *et al*. indicated that high levels of cyclin-dependent kinase 6 (CDK6) in basal breast cancer is positively correlated with HERV-K expression and this might promote the phosphorylation of tumour suppressor protein Retinoblastoma (Rb), which could result in uncontrolled cell cycle progression [16]. Li *et al*. also showed decreased cell proliferation and tumour growth in pancreatic cancer cell lines *in vitro* and in mice xenotransplantation models by knocking down HERV-K Env. As well as reducing proliferation and tumourigenesis, knocking down HERV-K Env in pancreatic cancer cell line xenografted mice nearly eliminated the metastasis of pancreatic cancer cells to lung tissues. Furthermore, Li *et al*. demonstrated that HERV-K Env may facilitate pancreatic cancer cell proliferation by upregulating K-Ras through the RAS/MEK/ERK pathway and by upregulating p70S6 Kinase/JNK/c-Jun signalling [9]. In addition to HERV-K Env, its splice variants Rec and Np9 are also potentially

tumourigenic which was demonstrated in transgenic mice [13, 14]. Transient coexpression of Rec or Np9 with the promyelocytic leukaemia zinc finger protein (PLZF) restrict the transcriptional repression of the c-myc proto-oncogene, leading to increased cell proliferation and survival [13]. Rec can bind to human small glutamine-rich tetratricopeptide repeat protein (hSGT), restricts its role as a negative regulator of androgen receptor (AR) and cause tumourigenesis due to hyperactivation of the AR [15]. Finally, Np9 has been shown to facilitate tumourigenesis through the LNX/Numb/Notch pathway [12].

3.8 Retroviral Protease Inhibitors in Cancer Therapy

Several studies are demonstrating the anti-tumour effects of retroviral protease inhibitors (PI). Furthermore, HIV patients using PIs are showing decreased incidence of Kaposi sarcoma and non-Hodgkin lymphoma [289]. Ritonavir was shown to inhibit the proliferation of primary endothelial cells and induce apoptosis in Kaposi's sarcoma cell lines through inhibition of cytokine production and inhibition of transcriptional activation of NFκB [290]. Ritonavir also inhibited NFκB activation and its target gene expression and induced apoptosis in primary adult T-cell leukaemia cells [291]. In a study, Ritonavir induced G1 arrest, reduced expression of cyclin-dependent kinases 2, 4, and 6 and cyclin D1, reduced the chaperone function Hsp90 and inhibited AKT phosphorylation in breast carcinoma cell lines [292]. Similarly, Ritonavir induced apoptosis and reduced proliferation in glioma cells [293]. Ritonavir also prevented HEP2 head and neck carcinoma progression in mice and it was even more effective when combined with radiation [294]. Additionally, Ritonavir blocked AKT signalling, induced apoptosis, and inhibited migration and invasion in ovarian cancer cells [295].

Similar results were observed in pancreatic cancer cells [296]. Finally, Ritonavir prevented the growth of K-ras mutant and K-ras wild type lung adenocarcinoma cells by causing G0/G1 arrest and apoptosis [297].

In contrast to Ritonavir, there are not as many studies showing the anti-tumour effects of Lopinavir and Atazanavir. Hampson *et al*. showed increased levels of nuclear wild-type p53 in cervical cancer cell lines following Lopinavir treatment which subsequently induced selective apoptosis of HPV-transformed cervical carcinoma cells [298]. Atazanavir was shown to induce endoplasmic reticulum (ER) stress response in malignant glioma cells causing misfolded proteins and resultant cell death. ER stress response (ESR) was measured by increased expression of two ESR markers, GRP78 and CHOP, and activation of ESR-associated caspase-4 [299]. Interestingly, the combination of Lopinavir and Ritonavir inhibited the growth of both renal and bladder cancer cells by inducing ER stress synergistically. ESR was measured by increased expression of ESR markers GRP78 and ERp44 [300]. Ritonavir has also been shown to have additive effects on non-PI anti-tumour drugs. Combining docetaxel with Ritonavir increased its anti-proliferative and proapoptotic effects in androgen-independent prostate cancer cell lines in vitro and in vivo [301]. Ritonavir has also been shown to increase the efficacy of 1,25-dihydroxyvitamin D_3 [$1,25(OH)_2D_3$)] by downregulating cytochrome P450 24A which deactivates $1,25(OH)_2D_3$, causing growth arrest and differentiation of human myeloid leukaemia cells [302]. Finally, Ritonavir prevented the functional activity of the multidrug resistance-associated protein 1 (MRP1) [303], suggesting that cytotoxic chemotherapy might be combined with Ritonavir clinically to reduce drug resistance.

3.9 HERV-K (HML-2) and Schwannoma: What We Know So Far

Halum *et al*. synthesised a double-stranded cDNA library from Poly (A)+ mRNA isolated from a vestibular schwannoma. cDNA inserts were sequenced and analysed using BLAST software with GenBank, EMBL, DDJB, and PDB databases. Consequently, BLAST multi-database comparison of the sequence data obtained from 50 randomly selected clones resulted in the identification of 13 known human genes and 17 sequences with unknown functions [304]. Dr Sylwia Ammoun submitted those sequences with unknown function to BLAST. As a result, Homo sapiens chromosome 8 Clone RP11-26K8 (1 of the 17 unknown sequences) showed 99% similarity to HERV-K (HML-2) sequence inciting us to study the role of HERV-K in schwannoma (Figure S1). Additionally, Homo sapiens 12q BAC RP11-421H10 (1 of the 17 unknown sequences) showed 73% similarity to HERV-K (HML-2) sequence (data not shown). HERV-K (HML-2) is the only HERV that was shown to have tumourigenic potential (Explained in Section 3.7.3.2). For that reason, other HERV families were not investigated.

Using immunohistochemistry (IHC), our group showed that HERV-K Env and Gag are strongly overexpressed in schwannoma (Sch-NF2-/-) biopsies compared to normal nerve control biopsies. This finding was further supported by demonstrating overexpressed HERV-K Env and Gag in primary Sch-NF2-/- cells compared to normal Schwann (Sch-NF2+/+) cells, using immunocytochemistry (ICC) and immunoblotting. Additionally, increased expression of HERV-K Env accessory proteins Rec and Np9 were observed in primary Sch-NF2-/- cells compared to Sch-NF2+/+ cells, examined

by ICC. Overall, preliminary data demonstrate HERV-K upregulation in Merlin-deficient schwannoma.

Consequently, our group started investigating the tumorigenic potential of HERV-K and whether it contributes to schwannoma development. Preliminary data show that treatment with anti-HERV-K Env and Gag antibodies significantly reduced proliferation (ICC/Ki67 staining) of primary Sch-NF2-/- cells but had no effect on primary Sch-NF2+/+ cell proliferation. Furthermore, both antibodies decreased the expression of cyclin D1 and the activation of pERK1/2, pFAK397, and pAKT in primary Sch-NF2-/- cells. The effects of anti-HERV-K Env antibody may indicate HERV-K Env mediated auto/paracrine signalling [305]. Furthermore, previous studies reported the release of HERV-W Env (Synctin-1 and Synctin-2) via exosomes [306-308]. Based on these findings, our group investigated whether HERV-K Env is released in similarly. Exosome isolation experiments revealed the release of HERV-K Env-TM protein from primary Sch-NF2-/- cells via exosomes, which was further supported by demonstrating the co-localisation of HERV-K Env and the late endosome/exosome markers CD9 and CD63 in the cytoplasm. Based on the evidence in literature [306-308], it can be concluded that HERV-K Env may facilitate the uptake of exosomes potentially produced by Sch-NF2-/- cells, and that could be a way of aiding tumourigenesis, as exosomes are involved in tumourigenesis (reviewed in [309]).

3.10 Aims and Objectives

Aim 1: To investigate the potential role of HERV-K in schwannoma development.

Objective 1: *Knockdown HERV-K in Merlin-deficient schwannoma cells and measure the effects on cell proliferation and key oncogenic pathways.*

Objective 2: *Overexpress HERV-K Env in Schwann cells and measure the effects on cell proliferation and key oncogenic pathways.*

Aim 2: To investigate whether HERV-K shows a similar pattern in Merlin-deficient meningioma.

Objective 1: *Measure the expression of HERV-K Env and Gag in Merlin-deficient grade I meningioma biopsies compared to normal meninges, by immunohistochemistry.*

Objective 2: *Measure the expression of HERV-K Env in Merlin-deficient grade I meningioma tissue lysates compared to normal meninges tissue lysates.*

Objective 3: *Measure the expression of HERV-K Env in Merlin-deficient grade I meningioma cells and Benmen compared to HMC.*

Aim 3: To look for mechanisms regulating HERV-K expression in Merlin-deficient tumours.

Objective 1: *Re-introduce Merlin into Merlin-deficient schwannoma cells and measure the effect on HERV-K expression.*

Objective 2: *Knockdown $CRL4^{DCAF1}$ in Merlin-deficient schwannoma cells and measure the effect on HERV-K expression.*

Objective 3: *Treat Merlin-deficient schwannoma with the Yap inhibitor Verteporfin and measure the effect on HERV-K expression.*

Objective 4: *Treat Merlin-deficient schwannoma and grade I meningioma cells with Pan-TEAD inhibitor VT04153 and measure the effect on HERV-K expression.*

Aim 4: Repurposing Anti-Retroviral drugs for Merlin-deficient tumours.

Objective 1: *Treat Merlin-deficient schwannoma with anti-retroviral drugs Ritonavir, Atazanavir and Lopinavir; and measure the effect on cell proliferation.*

Objective 2: *Treat BenMen cells with anti-retroviral drugs Ritonavir, Atazanavir and Lopinavir; and measure the effect on cell proliferation.*

The findings of this study should provide evidence for the role of HERV-K in Merlin-deficient schwannoma and meningioma development and examine the potential of HERV-K as a novel therapeutic target as well as testing anti-retroviral drugs' efficacy for the treatment of these tumours.

4 Materials and Methods

4.1 Cell Culture

4.1.1 Clinical Sample Collection and Ethics

Primary human tumour samples and primary human healthy donor samples were used for most of the experiments in this project to bridge the gap between the bench and the bedside, allowing the work done within this project to be more clinically translatable. Schwann cells were isolated from post-mortem donors at Derriford Hospital with informed consent from next of kin and after ethical approval under the Research Ethics Committee (REC) number REC6/Q2103/123. Schwannoma samples were collected after informed consent from patients at both Derriford Hospital and Bristol Southmead Hospital under local R&D approval Plymouth Hospitals NHS Trust: R&D No: 14/P/056 and North Bristol NHS Trust: R&D No: 3458. A subset of schwannomas and all the meningiomas used were collected under the Molecular Targets (MOT) project that involves both Derriford and Southmead Hospitals. The project was granted full ethics approval by the South West research ethics committee (REC number 14/SW/0119). All tumours used in this project were classified as WHO grade I.

4.1.2 Schwann Cell Culture

Human nerve samples were isolated from the sural nerve in the lower leg. Upon arrival, samples were dissected, and the fascicles were removed from the nerve sheaths. Individual fascicles were placed in culture dishes containing Dulbecco's modified Eagle medium (DMEM, Thermofisher Scientific, MA, USA); 10% foetal bovine serum (FBS, Sigma, MO, USA), and 100 U/ml penicillin/streptomycin (pen/strep, Thermofisher

Scientific), and pre-incubated in a humidified atmosphere with 10% CO_2 at 37°C for 1-2 days. Pre-incubated fascicles were then digested with a mixture of 160 U/ml type IA collagenase (Sigma) and 0.8 U/ml dispase grade I (Sigma) in conjunction with mechanical digestion by pipetting. After digestion, Schwann cells were cultured in a growth factor medium (GFM): DMEM; 10% FBS; 100 U/ml pen/strep; 2.5 µg/ml insulin (Thermofisher Scientific); 0.5 µM forskolin (Tocris, Bristol, UK); 2.5 µg/ml Amphotericin (Sigma); 10 nM ß1-heregulin (Bio-Techne, MN, USA); 0.5 mM 3-isobutyl-1-methylxanthine (IBMX, Bio-Techne), maintained in a humidified atmosphere with 10% CO_2 at 37°C on plates coated with poly-L lysine (Sigma) and laminin (Thermofisher Scientific). Finally, a set of cultured cells were stained with immunofluorescent S100 marker (Sigma) to ensure a pure Schwann cell population devoid of fibroblasts as previously described [37, 310].

4.1.3 Schwannoma Cell Culture

Schwannoma samples were pre-incubated upon arrival for 1-2 days in DMEM with 10% FBS and 100 U/ml pen/strep in a humidified atmosphere with 10% CO_2 at 37°C. Pre-incubated samples were then digested with a mixture of 160 U/ml type IA collagenase and 1.25 U/ml dispase grade I in conjunction with mechanical digestion by pipetting. After digestion, schwannoma cells were cultured in GFM: DMEM; 10% FBS; 100 U/ml pen/strep; 2.5 µg/ml insulin; 0.5 µM forskolin; 2.5 µg/ml amphotericin; 10 nM ß1-heregulin; 0.5 mM IBMX, maintained in a humidified atmosphere with 10% CO_2 at 37°C on plates coated with poly-L lysine and laminin.

4.1.4 Meningioma Cell Culture

Meningioma samples were preincubated upon arrival for 1-2 days in DMEM with 10% FBS and 100 U/ml pen/strep in a humidified atmosphere with 10% CO_2 at 37°C. Pre-incubated samples were then digested with a mixture of 20 U/ml type III collagenase and with mechanical digestion by pipetting. Once digested cells were cultured in GFM: DMEM; 15% FBS; 100 U/ml pen/strep; 1% glucose (Thermofisher Scientific); 1% glutamine (Thermofisher Scientific), maintained in a humidified atmosphere with 10% CO_2 at 37°C.

4.1.5 Cell line culture

4.1.5.1 Human Meningeal Cell (HMC) Culture

Foetal-derived, human meningeal cells from ScienCell™ (CA, USA) were maintained in the manufacturer's recommended media (meningeal cell media, ScienCell™) in a humidified atmosphere with 5% CO_2 at 37°C.

4.1.5.2 Ben-Men-1 Benign Meningioma Cell Culture

Ben-Men-1 (abbreviated to BenMen in this report) is a benign Merlin-deficient meningioma cell line created by transducing Merlin deficient primary meningioma cells with the hTERT gene, resulting in increased telomerase activity, elongated telomere length and extension of life span [311]. Cells were cultured in DMEM with 10% FBS; 100 U/ml pen/strep; 1% glucose; 1% glutamine, maintained in a humidified atmosphere with 5% CO_2 at 37°C. BenMen cells were used in this project as a preliminary study model for primary Merlin-deficient grade I meningioma cells.

4.1.5.3 HEK293T Cell Culture

Human Embryonic Kidney HEK293T cells (Thermofisher Scientific) were cultured in DMEM; 10% FBS; 100 U/ml pen/strep, maintained in a humidified atmosphere with 5% CO_2 at 37°C. HEK293T cells were used to produce lentiviral particles, see section 4.4.2.1 for further information.

4.1.5.4 HEI-193 Cell Culture

HEI-193 cell line was derived from an NF2 patient with spontaneous bilateral vestibular schwannomas [312]. HEI-193 cells express Merlin isoform 3 that was reported to have a mild tumour suppressor activity [313]. HEI-193 cells were cultured in GFM: DMEM; 15% FBS; 100 U/ml pen/strep; 1% glucose; 1% glutamine, maintained in a humidified atmosphere with 5% CO_2 at 37°C. The cells were used in HERV-K shRNA knockdown experiments, see chapter 4.4.2.3 for further information.

4.2 Chemicals, Compounds and Kits

Table 3. Table of chemicals, compounds and kits used in the experiments.

Chemical/Compound/Kit	Company	Catalogue Number
Acrylamide Solution 40%	BioRad, Watford, UK	1610140
Atazanavir	BioVision, CA, USA	B1901
Bovine Serum Albumin	Fisher Scientific, Loughborough, UK	BP9703
Bromophenol Blue	Sigma-Aldrich, Gillingham, UK	B0126
CytoTox-Glo™ Cytotoxicity Assay Kit	Promega, Southampton, UK	G9290
DAPI	Sigma-Aldrich, Gillingham, UK	D9542
3,3′-Diaminobenzidine (DAB)	Sigma-Aldrich, Gillingham, UK	D12384
Dimethyl sulfoxide (DMSO)	Sigma-Aldrich, Gillingham, UK	276855
DTT	Sigma-Aldrich, Gillingham, UK	10197777001
Ethylenediaminetetraacetic acid (EDTA)	Sigma-Aldrich, Gillingham, UK	ED-100G
Glycerol	Sigma-Aldrich, Gillingham, UK	G5516
Glycine	Sigma-Aldrich, Gillingham, UK	G8898
Goat Anti-Mouse IgG (H+L)-HRP Conjugate	BioRad, Watford, UK	1721011

Goat Anti-Rabbit IgG (H + L)-HRP Conjugate	BioRad, Watford, UK	1706515
Halt™ Protease Inhibitor Cocktail, EDTA-Free (100X)	Thermofisher Scientific, Paisley, UK	87785
Hygromycin B	Thermofisher Scientific, Paisley, UK	10687010
Immun-Blot® PVDF Membrane	BioRad, Watford, UK	1620177
Lopinavir	Sigma-Aldrich, Gillingham, UK	SML1222
NaCl	Sigma-Aldrich, Gillingham, UK	S7653
Nonidet P40 substitute	Sigma-Aldrich, Gillingham, UK	11332473001
Pierce™ BCA Protein Assay Kit	Thermofisher Scientific, Paisley, UK	23225
Pierce™ ECL Plus Western Blotting Substrate	Thermofisher Scientific, Paisley, UK	32132
Pierce™ ECL Western Blotting Substrate	Thermofisher Scientific, Paisley, UK	32209
Phosphotase Inhibitor Cocktail B	Insight Biotechnology, Wembley, UK	SC-45045
Phosphotase Inhibitor Cocktail C	Insight Biotechnology, Wembley, UK	SC-45065
Power SYBR™ Green RNA-to-CT™ 1-Step Kit	Applied Biosystems, CA, USA	4389986
Precision Plus Protein™ Dual Colour Standards	BioRad, Watford, UK	1610374
Protamine sulphate salt from salmon	Sigma-Aldrich, Gillingham, UK	P4020

Puromycin	Sigma-Aldrich, Gillingham, UK	P9620
Ritonavir	Sigma-Aldrich, Gillingham, UK	SML0491
Skim Milk Powder	Sigma-Aldrich, Gillingham, UK	70166
Sodium Deoxycholate	Sigma-Aldrich, Gillingham, UK	D6750
TURBO DNA-free™ Kit	Ambion, TX, USA	AM1907
Tween™ 20 Detergent Solution	Thermofisher Scientific, Paisley, UK	85115
VECTASTAIN® Elite® ABC-HRP Kit	Vector Laboratories LTD., Peterborough, UK	PK-6100
Verteporfin	Tocris, Bio-Techne Ltd, Abingdon, UK	5305

4.3 Antibodies

Table 4. Table of antibodies used in the experiments.

Antibody	Type	Company	Cat. Number	Dilution
Anti-HERV-K Env	Mouse Monoclonal Antibody	Austral Biologicals, CA, USA	HERM-1811-5	1:500 (WB) 1:100 (ICC)
Anti-HERV-K Gag	Mouse Monoclonal Antibody	Austral Biologicals, CA, USA	HERM-1841-5	1:500 (WB)
c-jun	Rabbit Polyclonal Antibody	Merck Millipore, Feltham, UK	PC06L	1:100 (ICC)
Cleaved Caspase-3 (Asp175)	Rabbit Monoclonal Antibody	New England Biolabs, Hitchin, UK	#9661	1:50 (ICC)
CTGF	Rabbit Polyclonal Antibody	Abcam Cambridge, UK	ab6992	1:1000 (WB)
Cyclin A2 (BF683)	Mouse Polyclonal Antibody	New England Biolabs, Hitchin, UK	#4656	1:500 (WB)
Cyclin D1	Rabbit Polyclonal Antibody	New England Biolabs, Hitchin, UK	#2922	1:500 (WB)
GAPDH	Mouse Monoclonal Antibody	Merck Millipore, Feltham, UK	MAB374	1:10000 (WB)
Ki67 (MIB-1)	Mouse Monoclonal Antibody	Agilent Technologies Ltd., Stockport, UK	M7240	1:100 (ICC)
Merlin D1D8	Rabbit Monoclonal Antibody	New England Biolabs, Hitchin, UK	#6995	1:1000 (WB)
Pan-TEAD (D3F7L)	Rabbit Monoclonal Antibody	New England Biolabs, Hitchin, UK	#13295	1:1000 (WB)
Phospho AKT^{S473}	Rabbit Monoclonal Antibody	New England Biolabs, Hitchin, UK	#9271	1:500 (WB)
Phospho-p44/42 MAPK$^{T202/Y204}$ (pErk1/2)	Rabbit Monoclonal Antibody	New England Biolabs, Hitchin, UK	#9101	1:1000 (WB)

Phospho FAK^{Y397}	Rabbit Polyclonal Antibody	New England Biolabs, Hitchin, UK	#3283	1:500 (WB)
Phospho Merlin^{S518}	Rabbit Polyclonal Antibody	New England Biolabs, Hitchin, UK	#9163	1:500 (WB)
Pan AKT (C67E7)	Rabbit Polyclonal Antibody	New England Biolabs, Hitchin, UK	#4691	1:500 (WB)
p44/42 MAPK (137F5) (Erk1/2)	Rabbit Monoclonal Antibody	New England Biolabs, Hitchin, UK	#4695	1:1000 (WB)
Total FAK	Rabbit Monoclonal Antibody	New England Biolabs, Hitchin, UK	#3285	1:500 (WB)
α-Tubulin	Rabbit Polyclonal Antibody	Abcam Cambridge, UK	ab4074	1:20000 (WB)
VPRBP (CRL4^{DCAF1})	Rabbit Polyclonal Antibody	Proteintech, Manchester, UK	11612-1-AP	1:1000 (WB)
YAP (D8H1X)	Rabbit Monoclonal Antibody	New England Biolabs, Hitchin, UK	#14074	1:1000 (WB)

4.4 Viral Infections

4.4.1 Adenoviral (AdV) Re-Introduction of Merlin into Schwannoma Cells

Merlin wild type and control GFP-containing vector adenoviruses (AdV-NF2 and AdV-GFP, respectively) obtained from J. Testa (Xiao et al. 2005) were amplified in 293T. For AdV infection, schwannoma cells were plated and cultured in 6-well plates to 70-80% confluency [314]. Then, AdVs were introduced to the culture medium. Cells were kept with viruses for 72 hours. Then, the cells were lysed and stored at -20°C for further analysis.

4.4.2 Lentiviral Transduction

4.4.2.1 Production of Lentiviral Particles

On day 1, HEK293T cells were seeded in a 60 mm cell culture dish (2 x 10^6 cells). On day 2, DNA plasmids and transfection reagent were mixed in Opti-MEM™ (Thermofisher). DNA plasmids contained a mix of packaging plasmids (Origene, RKV, USA) that contains pCMV-DR8.2 plasmid encoding for lentiviral core and pVSV-G plasmid encoding for lentiviral Env, and the target DNA plasmid. The mixture was incubated at room temperature for 15-25 minutes, and it was added drop by drop into the cell culture dish. Cells were then incubated for 72 hours at 37°C. Finally, the medium was collected and centrifuged to remove cellular debris. The supernatant containing the viral particles was stored as 2 ml aliquot in cryotubes at -80°C.

4.4.2.2 Knockdown of $CRL4^{DCAF1}$ in Schwannoma Cells

Schwannoma cells were seeded in 6-well plates at high density (minimum 70% confluency). The cells were then incubated with fresh GFM containing $CRL4^{DCAF1}$ or scramble control (scr) shRNA lentiviral particles (both produced and kindly provided by J. L. Rimmer) and protamine sulphate (8 µg/ml, Sigma) at 37°C for 72 hours. Protamine sulphate was added to serve as a source of positively charged polycations to increase the efficiency of lentiviral infection by reducing repulsion between the cell surface and the viral particles. Infected cells were selected with puromycin (4 µg/ml, Sigma) for 3-6 days before being lysed and subjected to Western blotting.

4.4.2.3 Knockdown of HERV-K in HEI193 Cells

HEI193 cells were seeded in 6-well plates at high density (minimum 70% confluency). The cells were then incubated with fresh GFM containing target or scr shRNA lentiviral particles and protamine sulphate (8 µg/ml, Sigma) at 37°C for 48-72 hours. Protamine sulphate was added to increase the efficiency of lentiviral infection (see 4.4.2.2). Infected cells were selected with puromycin (4 µg/ml, Sigma) for 3-6 days before being lysed and subjected to Western blotting and qRT-PCR.

HERV-K knockdown experiments were done using two sets of custom shRNA lentiviral particles purchased from two different companies: AMSBio (Abingdon, UK) and System Biosciences (CA, USA). For shRNA 1-20 (see Table 5), HERV-K113 *gag* ORF, HERV-K113 LTR, and HERV-K108 *env* ORF were used as query sequences submitted to RNA interference online tool (siDirect version 2.0) which was used to predict the best candidates of siRNA, based on the algorithms designed by Ui-Tei *et al*.

[315], Reynolds *et al*. [316], and Amarzguioui *et al*. [317]. Dr Emmanuel A. Maze picked 10 sequences (shRNAs ID#: 1-10, see table 5) that target HERV-K LTR within HERV-K113 provirus (5 downstream of the transcription start site at position nt 793, and 5 before upstream of transcription termination site at position nt 876) [271], 5 sequences (shRNAs ID#: 11-15, see table 5) that target HERV-K *gag* ORF within HERV-K113 provirus, 5 sequences (shRNAs ID#: 16-20, see table 5) that target HERV-K *env* ORF within HERV-K108 provirus, and 1 scr control (shRNA ID#: scr, see table 5). Each target sequence was synthesised as an shRNA and inserted in lentiviral-expressing vectors (pGFP-C-shLenti) by AMSBio. shRNA lentiviral particles purchased from System Biosciences consisted of shRNAc (scr control, see table 5) and shRNAenv (targeting *env* ORF within HERV-K10 provirus, see table 5) sequences that were from [9]. Both sequences were inserted in pGreenPuro (CMV) shRNA cloning and expression lentivector by System Biosciences.

Table 5. shRNAs used for the knockdown of HERV-K.

Target position (nt)	Target sequence	ID #	HERV-K (HML2) ORF Location	Origin (Company)	Provirus
Negative control	GTCTCCACGCGCAGTACATTT	scr	-	AMSBio	-
65-87	GACTCCATTTTGTTATGTATTAA	1	LTR	AMSBio	K113
69-91	CCATTTTGTTATGTATTAAGAAA	2	LTR	AMSBio	K113
75-97	TGTTATGTATTAAGAAAAATTCT	3	LTR	AMSBio	K113
350-372	CCATGTGATAGTCTGAAATATGG	4	LTR	AMSBio	K113
604-626	GGCAGCAATACTGCTTTGTAAAG	5	LTR	AMSBio	K113
861-883	CCTTATTTCTTTCTCTATACTTT	6	LTR	AMSBio	K113
878-900	TACTTTGTCTCTGTGTCTTTTTC	7	LTR	AMSBio	K113

888-910	CTGTGTCTTTTTCTTTTCCAAAT	8	LTR	AMSBio	K113
890-912	GTGTCTTTTTCTTTTCCAAATCT	9	LTR	AMSBio	K113
892-914	GTCTTTTTCTTTTCCAAATCTCT	10	LTR	AMSBio	K113
1114-1136	GGGCAAACTAAAAGTAAAATTAA	11	Gag	AMSBio	K113
1115-1137	GGCAAACTAAAAGTAAAATTAAA	12	Gag	AMSBio	K113
1190-1212	GAGTTAAAGTATCTACAAAAAAT	13	Gag	AMSBio	K113
2306-2328	GTCAAAATTGGAGTACTATTAGT	14	Gag	AMSBio	K113
2536-2558	GTGGAGTTAATGGCATATGAAAA	15	Gag	AMSBio	K113
7027-7049	CAGAAGTATATGTTAATGATAGT	16	Env	AMSBio	K108
7295-7317	TTCTTATCAAAGATCATTAAAAT	17	Env	AMSBio	K108
7353-7375	CCCAAAGAATCAAAAAATACAGA	18	Env	AMSBio	K108
7557-7579	GACAAACATAAGCATAAAAAATT	19	Env	AMSBio	K108
8313-8335	GACTGGAATACGTCAGATTTTTG	20	Env	AMSBio	K108
Negative control	GAATTCTTAACGACTACCA	shRNAc	-	System Biosciences	-
7157-7175	CCTGAACATCCAGAATTAT	shRNAenv	Env	System Biosciences	K10

AY037928.1, AC072054, and M14123.1 are accession numbers for K113, K108, and K10 respectively.

4.4.2.4 Overexpression of HERV-K Env in Schwann Cells and HMC Cells

HERV-K (HML-2) Env expressing lentiviral vector and the corresponding empty vector were produced elsewhere [17]. The production of lentiviral particles is explained in section 4.4.2.1. Schwann cells and HMC cells were seeded in a 6-well plate or 8-well Lab-Tek at high density (minimum 70% confluency). The cells were then incubated with fresh GFM containing HERV-K Env (HML-2) expressing lentiviral particles and protamine sulphate (21.3 µg/ml, Sigma) at 37°C for 72 hours. Protamine sulphate was added to increase the efficiency of lentiviral infection (see 4.4.2.2). Infected cells were selected with hygromycin b (63.2 µg/ml for Schwann cells, 50.6 µg/ml for HMC cells, Thermofisher Scientific) for 3-6 days. Cells that were seeded in a 6-well plate were lysed and subjected to Western blotting. Cells that were seeded in 8-well Lab-Tek were subjected to immunofluorescence staining.

4.5 Drug Treatments

4.5.1 Verteporfin

Cells were seeded in a 6-well plate or 8-well Lab-Tek at 70% confluency. Cells were then treated with 1 µM Verteporfin (Tocris, Bristol, UK) for 48 hours. Cells that were seeded in a 6-well plate were lysed and subjected to Western blotting. Cells that were seeded in 8-well Lab-Tek were subjected to immunofluorescence staining.

4.5.2 VT04153

VT04153 (Vivace Therapeutics, CA, USA) is a TEAD-specific auto-palmitoylation inhibitor [318]. Cells were seeded in a 6-well plate or 8-well Lab-Tek at 70% confluency. Cells were then treated with dosages of 1 µM and 2 µM VT04153 for 7 days. Cells that were seeded in a 6-well plate were lysed and subjected to Western blotting. Cells that were seeded in an 8-well Lab-Tek were subjected to immunofluorescence staining.

4.5.3 Anti-Retrovirals

Cells were seeded in a 6-well plate or 8-well Lab-Tek at 70% confluency. Cells were then treated with three different anti-retroviral drugs that are originally used against HIV: Ritonavir (Sigma), Lopinavir (Sigma), and Atazanavir (Caltag Medsystems, Buckingham, UK). All drugs were used at final concentrations of 0.1-10 µM, and the cells were treated for 72 hours (fresh dosage added every day). Cells that were seeded in a 6-well plate were lysed and subjected to Western blotting. Cells that were seeded in an 8-well Lab-Tek were subjected to immunofluorescence staining.

4.6 Immunohistochemistry (IHC)

Case slides were kindly provided by Derriford Hospital Neuropathology Department (David Hilton, Phil Edwards). Each slide contains a section from normal meninges or meningioma. Slides were initially baked at 60°C for an hour and dewaxed using 100% xylene and then 100% ethanol. The slides were then washed in running tap water for 5 minutes. The samples were blocked in methanol containing 3% hydrogen peroxide (H_2O_2), followed by washing in running tap water for 10 minutes. H_2O_2 blocks the endogenous peroxidase activity and prevent non-specific background staining. H_2O_2 is diluted in methanol to accelerate the blocking process and to prevent any H_2O_2 induced damage to the tissues. The slides were pre-treated in Tris-EDTA buffer (2.4 mg/ml Tris, 0.2 mg/ml EDTA, 2mM HCl pH 9.0) for anti-HERV-K Gag and in Citrate buffer (2.1 mg/ml citric acid, 10 mM NaOH, pH 6.0) for anti-HERV-K Env to unmask the antigens in paraffin-embedded tissue sections. Slides embedded in the pre-treatment buffer were heated in a microwave for 30 minutes. After cooling down in the water, a hydrophobic ring surrounding the tissue was drawn with ImmEdge pen (Vector Laboratories, Peterborough, UK). Subsequently, the slides were immersed in 0.05M Tris-HCl buffer (6.05 mg/ml Tris, 8 mg/ml sodium chloride, 1:1000 Tween 20 (Sigma); pH 7.6). Tissue sections were covered with Normal Horse Serum (diluted in 0.05M Tris-HCL buffer) from VECTASTAIN® Elite® ABC-HRP Kit (Vector Laboratories) to prevent non-specific binding of the secondary antibodies. Finally, tissue sections were incubated overnight with primary anti-HERV-K Gag and anti-HERV-K Env at 4°C. The next day, tissue sections were covered with secondary antibody solution (normal horse serum and biotinylated universal antibody diluted in 0.05M Tris-HCl buffer). 0.05M Tris-HCl

buffer was used for washing steps. Following washes, Streptavidin/Biotin Complex – ABC was applied on slides for 30 minutes to amplify the signal at the antigenic site. Slides were then washed, and tissue sections were covered with 3, 3′-Diaminobenzidine (DAB, Sigma) that ensures stable staining. Signals in tissue sections were increased using DAB enhancer solution if necessary to have more intense DAB staining. After washing slides with running tap water, they were washed using 100% ethanol and then 100% xylene. Finally, coverslips were mounted on top of sections using DPX mounting solution (Sigma). Staining is presented as brown, and intensity was scored by a third-party pathologist (Dr David Hilton): 0, no staining; 1, equivocal; 1+, weakly positive; 2, moderate; 3, strong.

4.7 Immunocytochemistry (ICC)

Pre-treated cells were fixed using 4% paraformaldehyde and permeabilised using 0.2% Triton X-100. Cells were then blocked using 10% normal goat serum and incubated with primary antibodies overnight at 4°C. Anti-HERV-K Env and anti-cJun were used at a concentration of 1:100. Anti-cJun antibody is a rabbit polyclonal antibody raised against amino acids 209-225 in the DNA binding domain in the C-terminal region of c-jun protein [319, 320]. Anti-Ki67 was used as a marker for proliferating cells, and anti-cleaved caspase-3 was used as a marker for cells undergoing apoptosis. Goat anti-mouse 594 and goat anti-rabbit 488 (Invitrogen, CA, USA) were used as secondary antibodies (concentration of 1:500), and DAPI (concentration of 1:500) was used to visualise cell nuclei. Quantification was done by dividing the total number of cells stained with the desired protein (HERV-K Env, cJun, caspase-3 or Ki67) with the total number of cells stained with DAPI.

4.8 Western Blotting

4.8.1 Sample Lysis

4.8.1.1 Cell Lysis

Cells were mechanically lysed on ice by cell scraping and chemically lysed using RIPA buffer (50mM Tris/HCl, 0.1% SDS, 1% NP-40, 150mM NaCl, 1mM EDTA, 0.5% sodium deoxycholate) with added 1% protease inhibitor cocktail (Thermofisher Scientific), 1% phosphatase inhibitors B and C (Santa Cruz Biotechnologies). Lysates were centrifuged at 4°C, 13000rpm for 15 minutes to remove cell debris, and the supernatant was stored at -80°C. Protein estimation was carried out using a colorimetric Pierce BCA Protein Assay Kit (Thermofisher Scientific).

4.8.1.2 Tissue Lysis

Frozen meningioma samples were homogenised using a centrifugal homogeniser. Samples were put inside tubes containing beads and RIPA buffer, and the tubes were centrifuged for 5 minutes. The weight of beads that were put inside the tubes was equal to the weight of the sample, and 2 µl of RIPA buffer was added per µg of the sample. After the centrifugal homogeniser step, the tubes were centrifuged at 4°C, 13000rpm for 15 minutes to remove cell debris and the beads. The collected supernatant was then stored at -80°C. Protein estimation was carried out using a colorimetric Pierce BCA Protein Assay Kit (Thermofisher Scientific).

4.8.2 SDS-PAGE and Transfer to PVDF membrane

8% and 10% polyacrylamide resolving gels topped with a 4% polyacrylamide stacking gel were made according to the protocol supplied with the 40% acrylamide solution (BioRad). Cell lysates were loaded after mixing with 4x concentrated reducing buffer (250mM Tris-HCL [pH6.8], 8% SDS, 40% glycerol, 200mM DTT and 0.4% bromophenol blue). A dual-colour protein ladder (BioRad) was used for molecular weight guidance. Proteins were separated according to molecular size via sodium dodecyl sulphate – polyacrylamide gel electrophoresis (SDS-PAGE) at a constant voltage of 120V for 90 minutes at room temperature. Proteins were transferred to a PVDF membrane (BioRad) in a transfer buffer made from 25 mM Tris, 19.2 mM glycine and 20% methanol at a constant amperage of 250mA and 100V for 90 minutes at 4°C or 175mA and 85V overnight at 4°C.

4.8.3 Immunoblotting

Unspecific binding to the membranes was blocked using 5% skimmed milk powder with 2% bovine serum albumin (BSA) in TBS-T (Tris-buffered saline with 0.1% Tween) for 60 minutes at room temperature. Membranes were then incubated overnight with primary antibodies (see Table 2). Application of primary antibodies was followed by incubation with the appropriate horseradish peroxidase (HRP)-conjugated secondary antibodies (goat anti-mouse, goat anti-rabbit, BioRad). Enhanced chemiluminescence (Thermofisher Scientific) was used for detection. Finally, the immunoblotting bands were quantified using ImageJ.

4.9 RNA Quantification

4.9.1 RNA Preparation

For studying HERV-K (HML2) transcription, RNA was extracted from cultured cells using the RNeasy mini kit (Qiagen, Germany) according to the manufacturer instructions. RNA was eluted in 50 µl nuclease-free water and quantitated using NanoDrop™ 2000 (Thermofisher Scientific). Extracted RNA was then subjected to DNase treatment using TURBO DNA-free™ Kit (Ambion, TX, USA) for the removal of DNA contaminants. 5 µl of 10X TURBO DNase buffer was added to 50 µl eluted RNA. Then, 1 µl of TURBO DNase was added and the solution was incubated for 1 hour at 37°C. Following DNase treatment, 10 µl of DNase inactivation reagent was added and the solution was incubated for 5 minutes at room temperature. Finally, the solution was centrifuged at 13000rpm for 2 minutes and the supernatant was stored in a freezer (-80°C).

4.9.2 Primers

Primer sequences for qRT-PCR were the following, given in 5'- 3' orientation:

Table 6. Primers.

Sequence	Forward	Reverse
HERV-K (HML2) *pol**	AATTGACTGTTATACATTTCTGC	CCGAATCCAATTAATATCTCC
HERV-K (HML2) *env* 1	GCGTGGTCATTGAGGACAAGTC	GGTGCTCGATTGCGGTGTCT
HERV-K (HML2) *env* 2	TTAGTTTGGGAAGAATGTGTGG	TTGGGGTAGAGATTCCTTTTTC
Human GAPDH (control)	CTTTTGCAGACCACAGTCCATG	TTTTCTAGACGGCAGGTCAGG

**pol* primers from Karamitros *et al.* [321]. Reference sequences used are:

HERV-K (HML2) (K113; NC_022518), human GAPDH (NC_000012.12).

4.9.3 qRT-PCR

Power SYBR™ Green RNA-to-CT™ 1-Step Kit (Applied Biosystems, CA, USA) was the qRT-PCR kit used for the quantification of cellular HERV-K (HML2) transcripts. Each RNA preparation was first diluted to 40 ng/µl. Then, 100 ng (2.5 µl) was added in each qRT-PCR reaction (20 µl). HERV-K (HML2) *pol*, *env* 1/2 and human *gapdh* primers were used at concentrations of 300 nM, 200 nM, and 300 nM respectively. qRT-PCR was conducted using a StepOnePlus™ Real-Time PCR System. The running program used for HERV-K *pol* and human *gapdh* was 48°C for 30 minutes (reverse transcription step), 95°C for 5 minutes (Hot start), 40 cycles of 95°C for 30 seconds, 47°C for 1 minute and 72°C for 1 minute, and melt curve (a single distinct peak in the plot of the negative derivative of fluorescence *vs.* temperature indicating a single discrete species of amplified double-stranded DNA product) as 95°C for 30 seconds, 47°C for 1 minute and 95°C for 30 seconds. The running program used for HERV-K *env* and human gapdh was 48°C for 30 minutes (reverse transcription step), 95°C for 10 minutes (Hot start), 35 cycles of 95°C for 15 seconds, 60°C for 1 minute, and melt curve as 95°C for 15 seconds, 60°C for 30 seconds and 95°C for 15 seconds. In the end, the $2^{-\Delta\Delta CT}$ method was used for data analysis.

4.10 Data Analysis

For statistical analysis student's two tailed t-tests were used. Experiments were performed in at least triplicates using at least three different batches of cells from different individuals where possible. In some experiments, samples from more than three different individuals were used. The p-value was used to determine significance of the results; ns (not significant) $p>0.05$, * $p<0.05$, ** $p<0.01$, *** $p<0.001$. The mean ± SEM is given in the figures. Scoring of IHC was done blind using a five-point scale (0, no staining; 1, equivocal; 1+, weakly positive; 2, moderate; 3, strong).

5 Results

5.1 Potential Role of HERV-K in Schwannoma Development

5.1.1 Attempts to Knockdown HERV-K in HEI193 cells

Dr Sylwia Ammoun and Dr Emmanuel A. Maze demonstrated HERV-K upregulation in Merlin-deficient schwannoma. Therefore, I initially started to work on getting a successful HERV-K knockdown in Merlin-deficient schwannoma to investigate the role of HERV-K in tumour development. shRNA constructs used in HERV-K knockdown experiments are explained in Section 4.4.2.3. HEI193 schwannoma cell line was used as a model to test all the shRNA constructs. Firstly, I infected the cells separately with 20 shRNA constructs (1-20) that were previously described and an additional published shRNA construct from Li *et al*. targeting *env* ORF [9]. Following transduction, I extracted RNA to run RT-qPCR using three different primer sets (2 for *env*; 1 for *pol*) to examine the effect on HERV-K Env and Pol mRNA levels. All AMSBIO constructs (1-20) failed to decrease HERV-K Env mRNA levels in HEI193 cells (shown by both *env* primers) compared to scr controls (Figure 8A, B). Interestingly, AMSBIO constructs 7, 8, 14 and 20 decreased the level of HERV-K Pol mRNA in HEI193 cells compared to scr control by 13.3%, 9.1%, 26.5%, and 19.5%, respectively. Even though these constructs demonstrated a slight decrease in HERV-K Pol mRNA levels, none showed a successful knockdown at the mRNA level which is ideally >50% (Figure 8C). The experiment was done only once as I did not have enough time to carry on with the knockdown experiments.

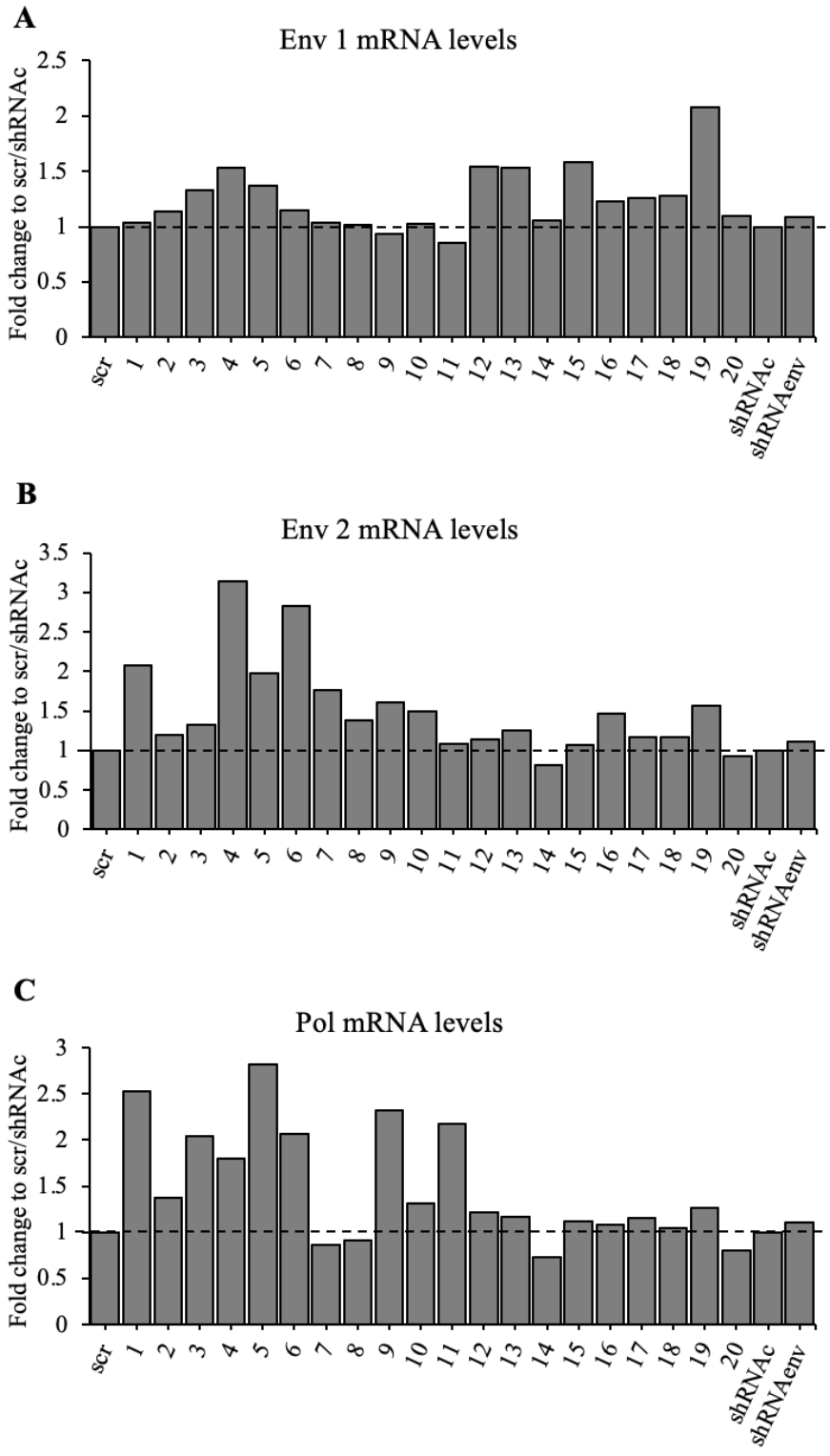

Figure 8. HERV-K Env and Pol mRNA levels after attempting to knockdown HERV-K in HEI193 cells using constructs from AMSBIO and Li et al. [9].

HEI193 cells were infected with shRNA lentiviral particles targeting LTRs (1-10), *gag* ORF (11-15), and *env* ORF (16-20; shRNAenv). Following infection, the cells were lysed and processed for RNA extraction. [A] Extracted RNA from each sample was analysed by RT-qPCR using a

HERV-K (HML-2) *env 1* primer set. The analysis did not show a significant reduction in HERV-K (HML-2) Env mRNA levels following knockdown attempt (n=1). [B] Extracted RNA from each sample was analysed by RT-qPCR using a HERV-K (HML-2) *env 2* primer set. Analysis did not show a significant reduction in HERV-K (HML-2) Env mRNA levels following the knockdown attempt (n=1). [C] Extracted RNA from each sample was analysed by RT-qPCR using a HERV-K (HML-2) *pol* primer set. The analysis did not show a significant reduction in HERV-K (HML-2) Pol mRNA levels following the knockdown attempt (n=1). Constructs 1-20 (AMSBIO) are normalised to scr control (AMSBIO), and construct shRNAenv (System Biosciences) is normalised to shRNAc control (System Biosciences). GAPDH was used as the housekeeping gene.

Finally, HERV-K Env protein expression in HEI193 cells following transduction with a shRNAenv construct was determined by immunoblotting. In contrast to the mRNA results (Figure 8), shRNAenv reduced HERV-K Env-FL protein expression by 45.2% and increased HERV-K Env-TM protein expression by 89.6% in HEI193 cells (Figure 9A, B). This result was unexpected as the mRNA results showed no effect on HERV-K Env mRNA levels. Additionally, it was unreliable that Env-FL protein expression was reduced while Env-TM protein expression was increased, following the knockdown. The experiment was done only once as I did not have enough time to carry on with the knockdown experiments. As a result, I stopped trying to achieve HERV-K knockdown and moved on to a new approach for investigating the role of HERV-K in schwannoma.

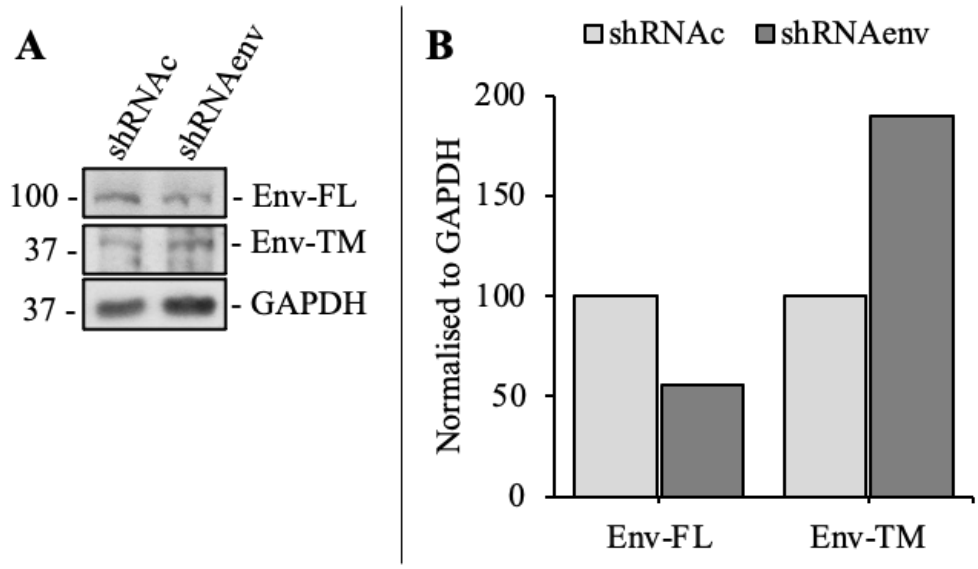

Figure 9. Published shRNA constructs from Li et al. [9] reduced HERV-K Env-Full Length (FL) protein expression but increased HERV-K Env-Transmembrane (TM) protein expression in HEI193 cells.

HEI193 cells were infected with shRNAc lentiviral particles (scr control) and with shRNAenv lentiviral particles targeting *env* ORF. [A] Extracted proteins were analysed by western blotting to measure the expression of HERV-K Env-FL and Env-TM proteins. GAPDH was used as the loading control. [B] Quantification of western blotting showed that shRNAenv reduced HERV-K Env-FL protein expression by 45.2%, and increased HERV-K Env-TM protein expression by 89.6% in HEI193 cells (n=1).

5.1.2 HERV-K Env Protein Contributes to Schwannoma Development

Next, I continued my investigation with an alternative approach. Instead of knocking down HERV-K in primary Sch-NF2-/- cells, I overexpressed HERV-K Env in primary Sch-NF2+/+ cells using HERV-K (HML-2) Env expressing lentiviral particles to examine the effects on cell proliferation and key oncogenic pathways. Initially, I confirmed the presence of both Env-FL and Env-TM proteins in primary Sch-NF2+/+ cells at the expected sizes of 98 kDa and 38 kDa bands, respectively [322] (Figure S2).

Subsequently, I infected HEK293T cells with HERV-K (HML-2) Env expressing lentiviral particles to overexpress HERV-K Env (Env o/e) and examined the effect on ERK1/2 activity which is an important regulator of cell proliferation [323]. HEK293T cells showed an increased expression of pERK1/2 following transduction (Figure 10). Thereby, I duplicated the result obtained by Lemaitre *et al*. [17] and ensured the efficacy of HERV-K (HML-2) Env expressing lentiviral particles I produced before starting to examine the effects of Env o/e in primary Sch-NF2+/+ cells. The experiment was done only once as it was a control experiment to confirm the effects of my lentiviral particles.

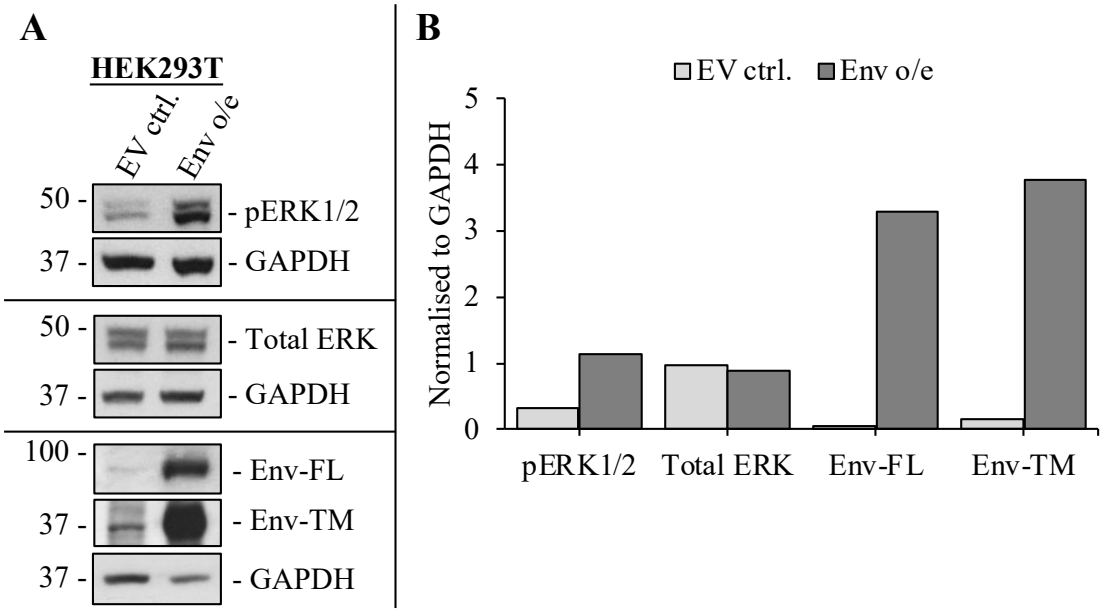

Figure 10. Overexpressing HERV-K Env in HEK293T cells activated ERK1/2.

HEK293T cells were infected with empty vector control lentiviral particles (EV ctrl.) and with HERV-K (HML-2) Env expressing lentiviral particles (Env o/e). Following infection, the cells were lysed and processed for protein extraction. [A] Extracted proteins were analysed by western blotting to measure the expression of pERK1/2, total ERK, HERV-K Env-FL and HERV-K Env-TM proteins. GAPDH was used as the loading control. [B] Quantification of western blotting results showed that overexpressing HERV-K Env in HEK293T cells increased phosphorylated ERK (pERK1/2) expression without any change in the total expression of ERK, indicating increased ERK1/2 activity (n=1).

Env o/e in primary Sch-NF2+/+ cells significantly increased cell proliferation measured as the number of Ki67+ cells (Figure 11B, C). In addition, Env o/e significantly elevated the expression of cJun in primary Sch-NF2+/+ cells (Figure 11D & 11E). The transcription factor cJun is a master regulator of Sch-NF2+/+ cell differentiation where it negatively regulates Sch-NF2+/+ cell myelination [324]. Furthermore, cJun and its upstream activator, phosphorylated cJun N-terminal kinase (pJNK), are upregulated in Sch-NF2-/- cells compared to Sch-NF2+/+ cells and contribute to cell proliferation and survival in vestibular schwannoma (VS) cells by suppressing superoxide accumulation in VS cell mitochondria [325, 326].

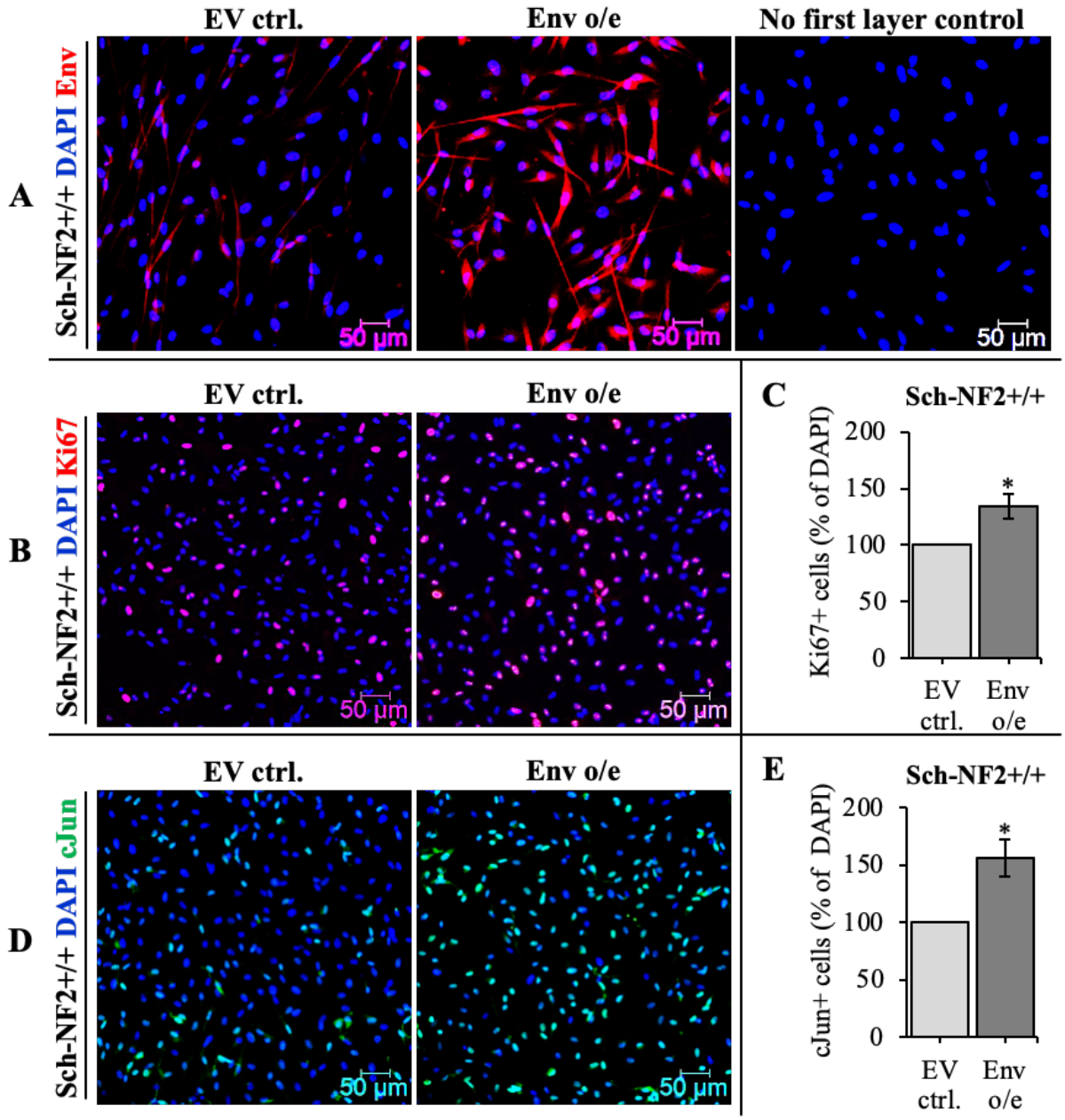

Figure 11. Overexpression of HERV-K Env in primary Sch-NF2+/+ cells significantly increased cell proliferation and expression of the transcription factor cJun.

Primary Schwann cells (Sch-NF2+/+) were infected with empty vector control lentiviral particles (EV ctrl.) and with HERV-K (HML-2) Env expressing lentiviral particles (Env o/e). After overnight incubation with primary antibodies, cells were incubated with secondary antibodies and DAPI (blue). [A] Immunocytochemistry (ICC) confirms increased HERV-K Env expression (red) in Sch-NF2+/+ cells following infection with Env o/e lentiviral particles. No first layer control was stained with DAPI and secondary antibodies. [B-C] ICC shows that HERV-K Env overexpression leads to increased Sch-NF2+/+ cell proliferation (measured as the number of Ki67+ cells (red), n=4). [D-E] ICC staining shows that HERV-K Env

overexpression increases cJun expression (green) in Sch-NF2+/+ cells (n=3). Student's two tailed t-test: *, $p<0.05$. Data presented as means ±SEM.

As expected, the immunoblotting analysis showed significantly increased pERK1/2 expression in primary Sch-NF2+/+ cells following Env o/e (Figure 13A, B). pERK1/2 is a component of the main pathway regulating proliferation in Sch-NF2-/- cells, where it has been shown to induce cyclin D1 expression via PDGF and *myc* resulting in cell cycle entry [151, 327-330]. Surprisingly, Env o/e decreased rather than increased the expression of cyclin D1 and increased the level of cyclin A2 instead (Figure 12A, B), suggesting that HERV-K Env increases proliferation via pERK1/2 mediated S phase cyclin A2 upregulation [331-333].

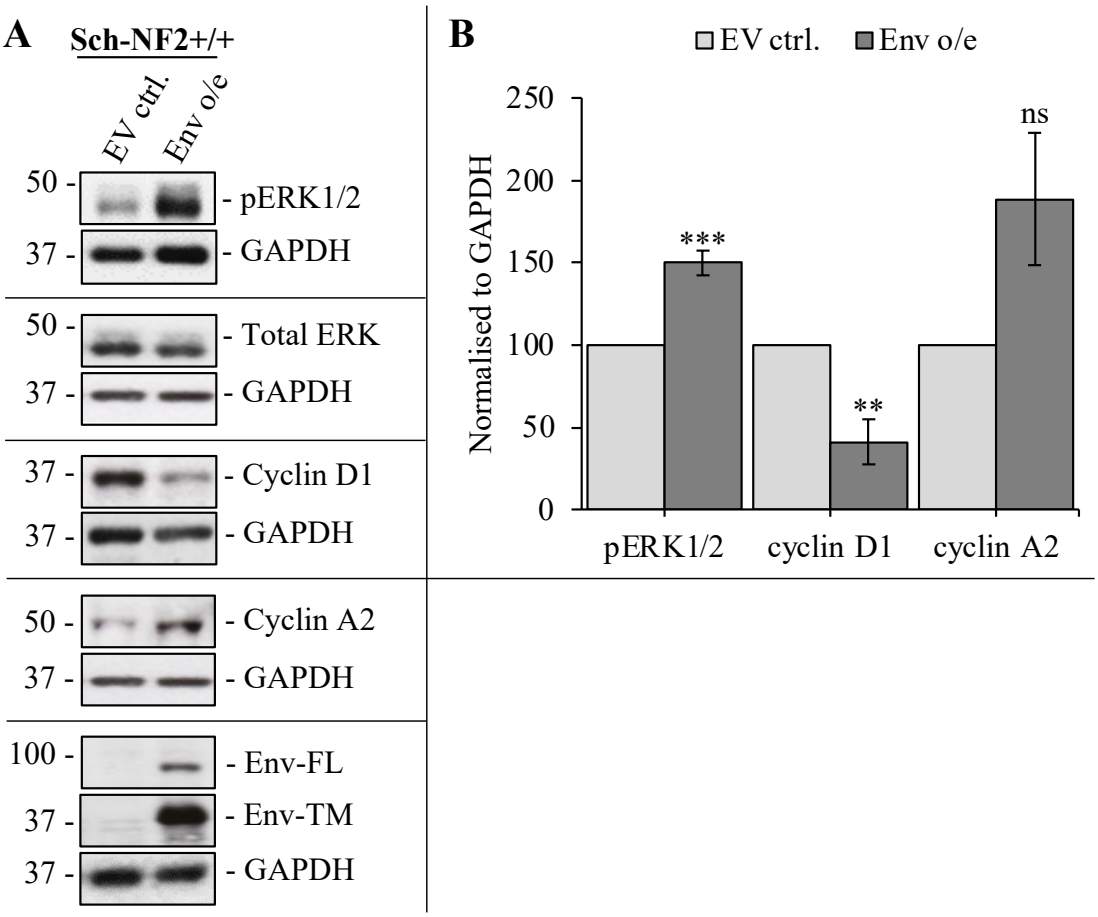

Figure 12. Overexpression of HERV-K Env in primary Sch-NF2+/+ cells increased ERK activity and cyclin A2 expression but decreased the expression of cyclin D1.

Primary Schwann cells (Sch-NF2+/+) were infected with empty vector control lentiviral particles (EV ctrl.) and with HERV-K (HML-2) Env expressing lentiviral particles (Env o/e).
[A-B] Western blotting results showed that overexpressing HERV-K Env in Sch-NF2+/+ cells increased phosphorylated ERK (pERK1/2) expression without any change in the total expression of ERK, indicating increased ERK1/2 activity (n=4). Western blotting results also showed reduced cyclin D1 levels (n=4) and increased cyclin A2 levels (n=4) in HERV-K Env overexpressing Sch-NF2+/+ cells. GAPDH was used as the loading control. Student's two tailed t-test: ns (not significant), $p>0.05$; **, $p<0.01$; ***, $p<0.001$. Data presented as means ±SEM.

5.2 HERV-K Proteins are Overexpressed in Merlin-Deficient Meningioma

My research also aimed to examine Merlin-deficient meningioma for HERV-K expression and expand the study further into understanding the connection between HERV-K and Merlin-deficient tumours. Firstly, I examined HERV-K expression in Merlin-deficient grade I meningioma (MN-GI-NF2-/-) tissues. Immunohistochemical analysis showed increased expression of HERV-K Env and Gag in MN-GI-NF2-/- compared to normal meninges (NMT-NF2+/+) (Figure 13, Table S1). 5 out of 12 HERV-K Env repetitions were performed by Dr Sylwia Ammoun.

I found moderate or strong expression of HERV-K Env in 12 of 12 MN-GI-NF2-/- biopsies and of HERV-K Gag in 6 of 7 MN-GI-NF2-/-, compared to 0 of 5 normal NMT-NF2+/+ biopsies (Figure 13A, B; Table S1). Dr Sylwia Ammoun also demonstrated strongly upregulated HERV-K Env in grade II and III meningioma (NF2-/-) compared to NMT-NF2+/+; however, higher grades of meningioma showed a decline in HERV-K Gag expression (data not shown).

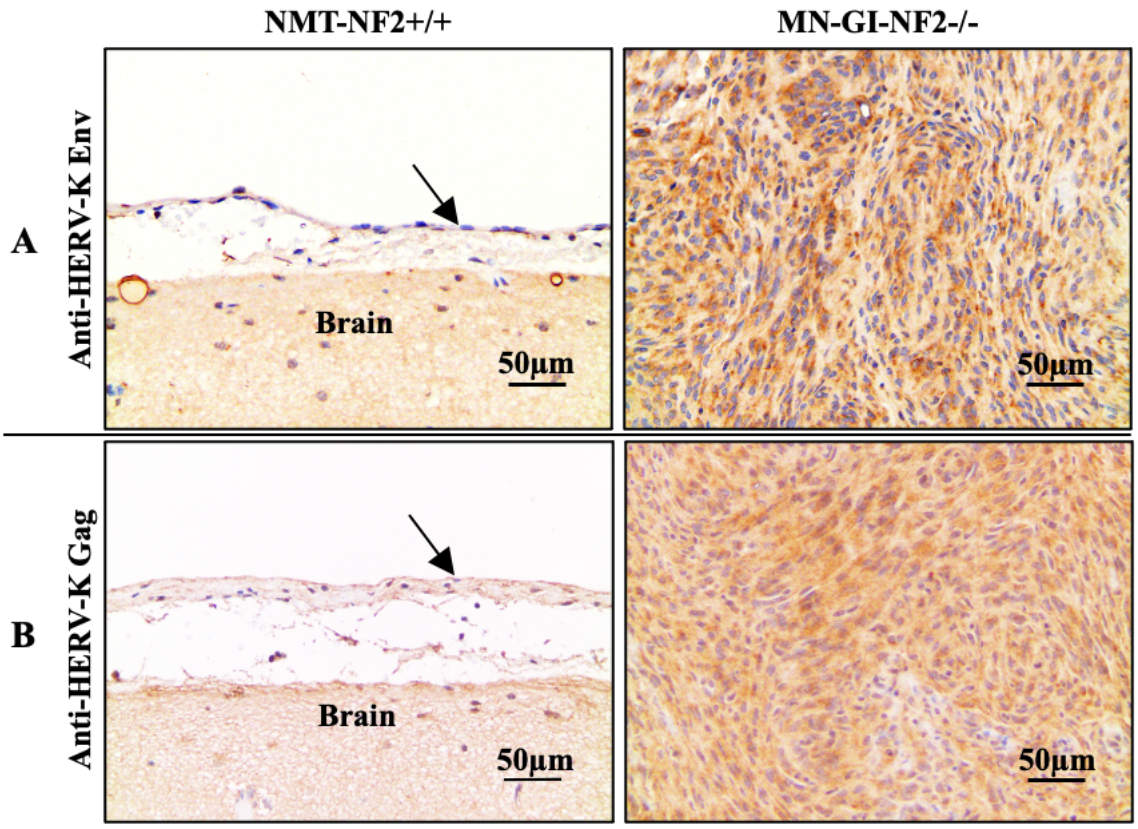

Figure 13. Immunohistochemical analysis showed increased HERV-K Env and Gag expression in grade I meningioma compared to normal meninges.

Sections of Merlin-deficient grade I meningioma (MN-GI-NF2-/-) and normal meninges (NMT-NF2+/+) were stained with anti-HERV-K Env and anti-HERV-K Gag. Staining intensity (brown) was scored as follows: 0, no staining; 1, equivocal to normal meninges; 1+, weakly positive; 2, moderate; 3, strong. NMT-NF2+/+ are indicated with arrows. Immunohistochemical analysis showed increased HERV-K Env (A, n=12, 5 were performed by Dr Sylwia Ammoun) and Gag (B, n=7) expression in MN-GI-NF2-/- compared to NMT-NF2+/+.

Next, HERV-K Env expression was analysed in lysates from 5 of the MN-GI-NF2-/- tissues previously used in immunohistochemistry analysis and 9 additional repeats that were performed by Dr Sylwia Ammoun. Overall, the immunoblotting analysis showed increased expression of HERV-K Env-FL (n=14) and Env-TM (n=14) in MN-GI-NF2-/- tissue lysates compared to NMT-NF2+/+ tissue lysates (Figure 14A, B). Dr Sylwia Ammoun also showed increased HERV-K rec and np9 expression in MN-GI-NF2-/- tissues compared to NMT-NF2+/+ (data not shown).

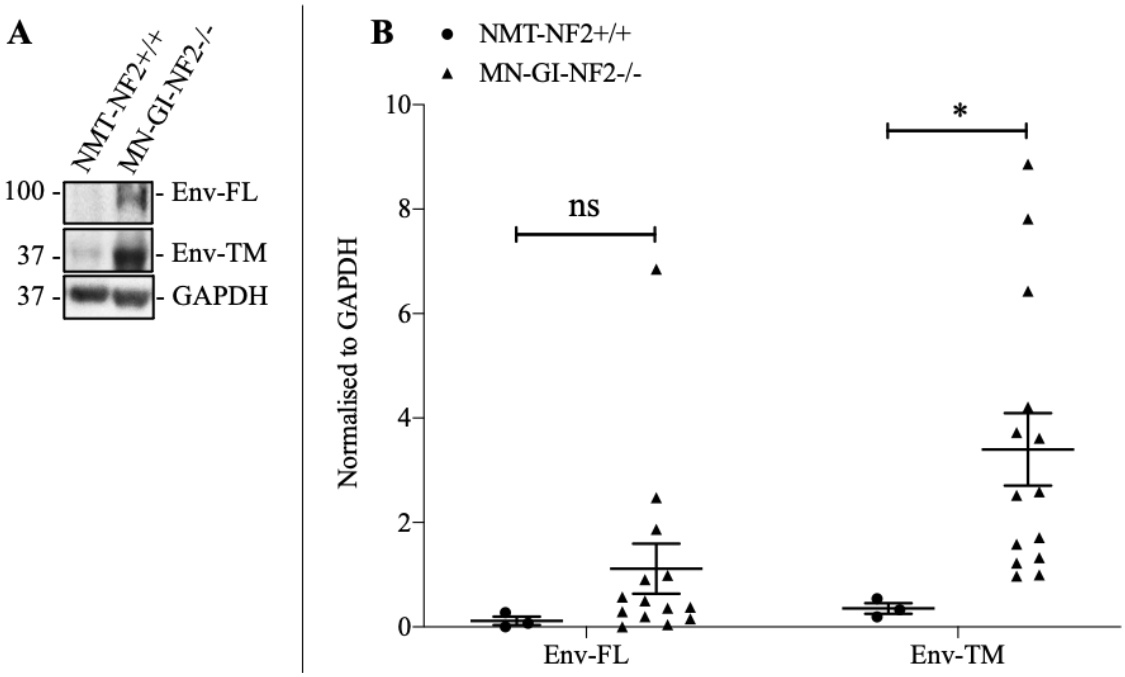

Figure 14. HERV-K Env is overexpressed in MN-GI-NF2-/- tissue lysates compared to normal meningeal tissue lysates.

Merlin-deficient grade I meningioma (MN-GI-NF2-/-) and normal meningeal (NMT-NF2+/+) tissues were lysed and processed for protein extraction. [A] Representative western blot (performed by myself) showing expression of HERV-K Env-Full Length (FL) and Env-Transmembrane (TM) proteins. GAPDH was used as the loading control. [B] Quantification of the western blotting showed increased HERV-K Env-FL and Env-TM expression in MN-GI-NF2-/- tissue lysates compared to NMT-NF2+/+ tissue lysates (n=14, 9 were lysed and analysed with western blotting by Dr Sylwia Ammoun). GAPDH was used as the loading control. Student's two tailed t-test: ns (not significant), $p>0.05$; *, $p<0.05$. Data presented as means ±SEM.

Finally, HERV-K Env expression in BenMen and primary MN-GI-NF2-/- cells was examined by immunoblotting. Significantly increased expression of HERV-K Env-FL was detected in primary MN-GI-NF2-/- cells compared to control HMC (Figure 15A, B). Conversely, there was no significant change in the expression of HERV-K Env-TM (Figure 15A, B). BenMen cells showed increased expression of HERV-K Env-FL and Env-TM compared to control HMC (Figure 15A, B). The specificity of the anti-HERV-K Env antibody for HERV-K Env-FL and Env-TM was confirmed by overexpressing HERV-K Env in HMC control cells (Figure 15C). HERV-K Env expression was also analysed in Merlin positive primary grade I meningioma cells (MN-GI-NF2+/+) as a comparative control. Although this was only performed as a single experiment, HERV-K Env was expressed in MN-GI-NF2+/+ cells (Figure 15D).

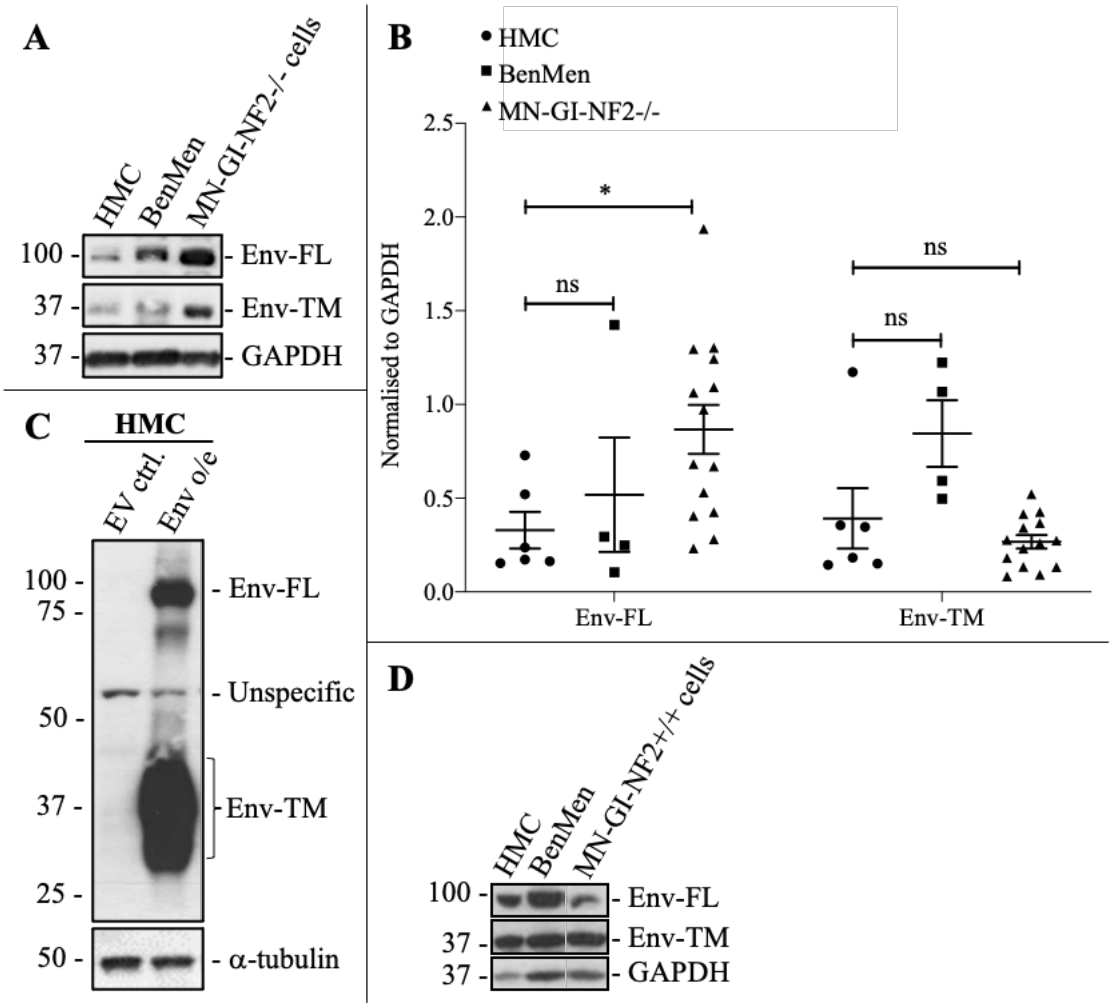

Figure 15. HERV-K Env is overexpressed in primary MN-GI-NF2-/- cells and BenMen cells compared to control HMC.

[A] Extracted proteins were analysed by western blotting to measure the expression of HERV-K Env-Full Length (FL) and Env-Transmembrane (TM) proteins. GAPDH was used as the loading control. [B] Quantification of the western blotting showed increased HERV-K Env-FL expression in primary Merlin-deficient grade I meningioma (MN-GI-NF2-/-, n=14) cells and Ben-Men-1 (BenMen, n=4) cells compared to control human meningeal cells (HMC, n=6). The results also showed increased Env-TM expression in BenMen cells (n=4) compared to HMC control cells (n=6). Conversely, there was no significant change in Env-TM expression in MN-GI-NF2-/- cells (n=14) compared to control HMC (n=6). GAPDH was used as the loading control. [C] The specificity of anti-HERV-K Env antibody for HERV-K Env-FL and Env-TM was confirmed by overexpressing HERV-K Env in control HMC. α-tubulin was used as the loading control. [D] Western blotting results showed that HERV-K Env was expressed in Merlin positive primary grade I meningioma cells (MN-GI-NF2+/+, n=1). GAPDH was used as the loading control. Student's two tailed t-test: ns (not significant), $p>0.05$; *, $p<0.05$. Data presented as means ±SEM.

5.3 Mechanisms of HERV-K Upregulation in Merlin-Deficient Tumours

5.3.1 HERV-K Overexpression in Schwannoma is Partially Merlin-Dependent

Next, I wanted to investigate the mechanisms of HERV-K upregulation in Merlin-deficient tumours. Since the preliminary data by Dr Sylwia Ammoun and Dr Emmanuel A. Maze demonstrated overexpressed HERV-K Env and Gag proteins in Sch-NF2-/-, it was important to check whether the upregulation was Merlin-dependent. Merlin re-introduction into primary Sch-NF2-/- cells using Merlin-expressing adenovirus (NF2 Ad) significantly decreased the expression of HERV-K Env-FL by ~30% and Env-TM by ~ 60% (Figure 16A, B). In addition, Merlin re-introduction into primary Sch-NF2-/- cells significantly reduced HERV-K Gag-FL by ~20%, CA+NC by ~18% and p15+CA by ~30% (Figure 16C, D). Therefore, HERV-K upregulation in schwannoma is partially Merlin-dependent. I contributed to only one repetition for both HERV-K Env and Gag. The remaining repetitions were performed by Dr Emmanuel A. Maze before I took over the project from Dr Emmanuel A. Maze.

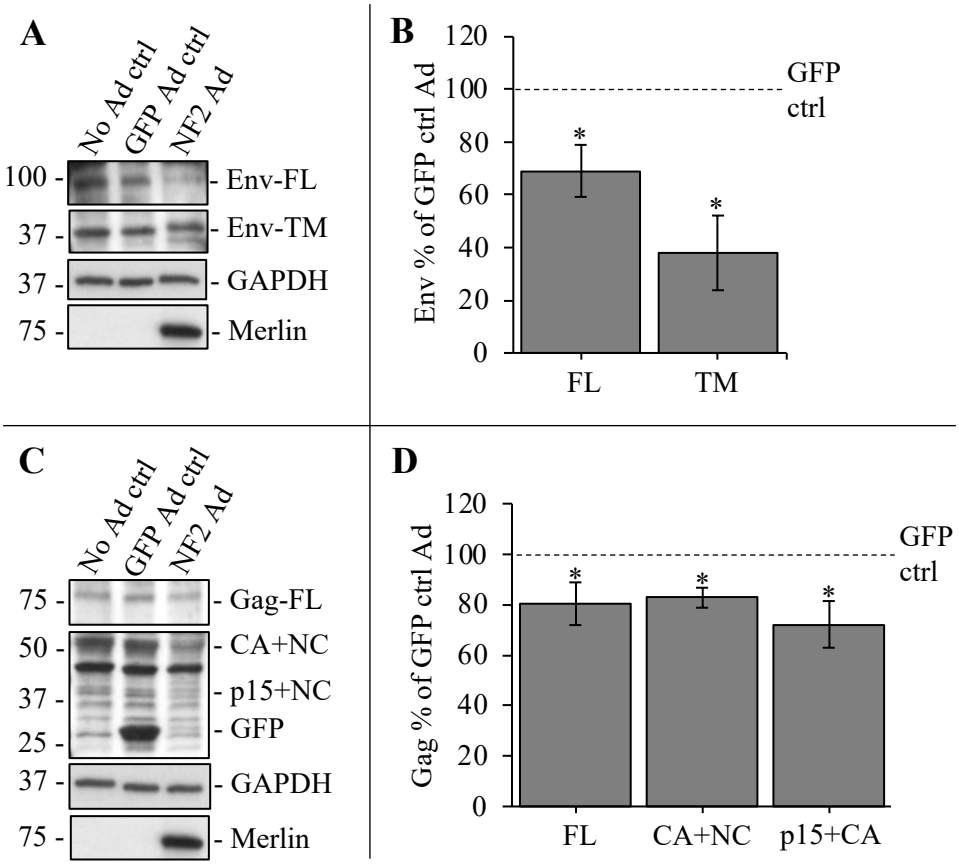

Figure 16. HERV-K upregulation in schwannoma is partially Merlin-dependent.

Merlin was re-introduced into primary Merlin-deficient schwannoma cells (Sch-NF2-/-) by infecting the cells with Merlin-expressing adenovirus (NF2 Ad) for 72 hours. [A] Extracted proteins were analysed by western blotting to measure the expression of HERV-K Env-Full Length (FL) and Env-Transmembrane (TM) proteins. Merlin was used as the positive control, no adenovirus (No Ad) was used as the negative control, and GFP adenovirus (GFP Ad) was used as the infection control examined by fluorescence microscope. Finally, GAPDH was used as the loading control. The western blotting result shown here belongs to me. [B] Quantification of the western blotting showed decreased HERV-K Env expression in Sch-NF2-/- cells following Merlin reintroduction (n=5, 4 were done by Dr Emmanuel A. Maze). [C] Extracted proteins were analysed by western blotting to measure the expression of HERV-K Gag-FL, CA+NC, and p15+NC proteins. Merlin was used as the positive control, No Ad was used as the negative control, and GFP Ad was the control for gene delivery, indicating the infection efficiency. Finally, GAPDH was used as the loading control. The western blotting result shown here belongs to me. [D] Quantification of the western blotting showed decreased HERV-K Gag expression in Sch-NF2-/- cells following Merlin reintroduction (n=6, 5 were performed by Dr Emmanuel A. Maze). Student's two tailed t-test: *, $p<0.05$. Data presented as means ±SEM.

5.3.2 $CRL4^{DCAF1}$/YAP/TEAD/Hippo Pathway is Involved in HERV-K Env Upregulation

Next, I wanted to check the downstream of Merlin for HERV-K upregulation in Sch-NF2-/-. $CRL4^{DCAF1}$ is derepressed in the absence of Merlin, thereby promoting oncogenic gene expression [160, 161, 163]. For that reason, it was important to check whether $CRL4^{DCAF1}$ regulates the expression of HERV-K in Sch-NF2-/-. Knocking down $CRL4^{DCAF1}$ in primary Sch-NF2-/- cells significantly decreased the expression of HERV-K Env-FL by ~30% with $CRL4^{DCAF1}$ shRNA1 construct and ~50% with $CRL4^{DCAF1}$ shRNA2 construct; and decreased the expression of Env-TM by ~15% with $CRL4^{DCAF1}$ shRNA1 construct and ~40% with $CRL4^{DCAF1}$ shRNA2 construct (Figure 17A, B), suggesting that $CRL4^{DCAF1}$ partially regulates the expression of HERV-K Env in Sch-NF2-/-. In contrast to Merlin re-introduction results (Figure 16C, D), knocking down $CRL4^{DCAF1}$ in primary Sch-NF2-/- cells using shRNA1 construct did not show any significant effect on the expression of HERV-K Gag-FL, p15+NC and CA (Figure 17C, D). Surprisingly, HERV-K CA+NC expression was significantly increased following knockdown with shRNA1 (Figure 17C, D). I contributed to one repetition of HERV-K Env expression in Sch-NF2-/- cells following knockdown with shRNA1, and all repetitions of HERV-K Gag expression in Sch-NF2-/- cells following knockdown with shRNA1. Dr Emmanuel A. Maze contributed to two repetitions of HERV-K Env expression in Sch-NF2-/- cells following knockdown with shRNA1 construct, and Dr Sylwia Ammoun contributed to all repetitions of HERV-K Env expression in Sch-NF2-/- cells following knockdown with shRNA2 construct.

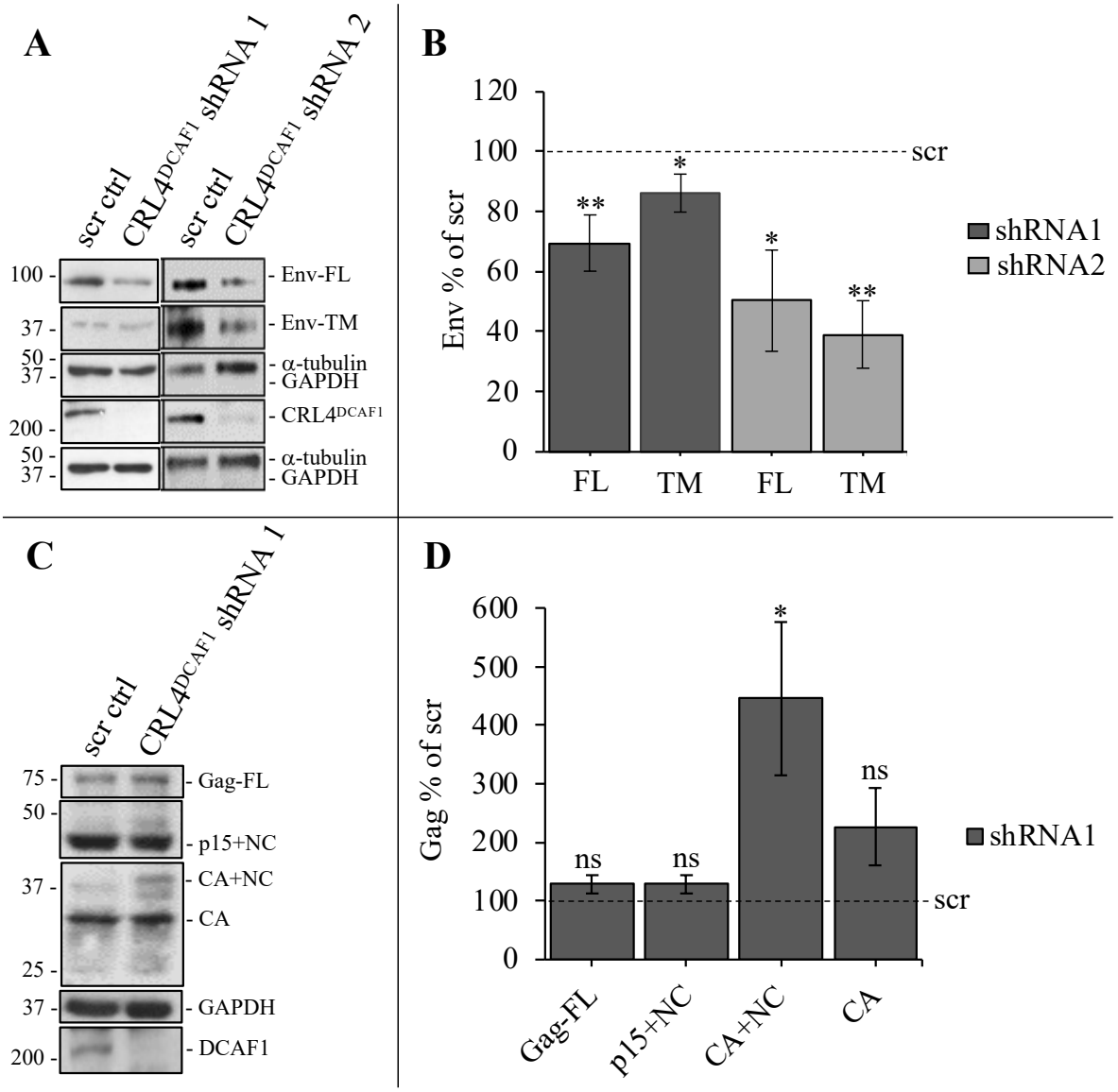

Figure 17. HERV-K Env upregulation in Sch-NF2-/- is partially regulated by CRL4^{DCAF1} whereas HERV-K Gag is not.

Primary Merlin-deficient schwannoma cells (Sch-NF2-/-) were infected with lentiviral particles containing scr control (ctrl), CRL4^{DCAF1} shRNA1, CRL4^{DCAF1} shRNA2 constructs. [A] Extracted proteins were analysed by western blotting to measure the expression of HERV-K Env-Full Length (FL) and Env-Transmembrane (TM) proteins. α-tubulin and GAPDH were used as the loading control. The western blotting results shown here belong to me (shRNA1) and Dr Sylwia Ammoun (shRNA2). [B] Quantification of the western blotting showed decreased HERV-K Env expression in Sch-NF2-/- cells following CRL4^{DCAF1} knockdown with shRNA1 (n=4, 2 repetitions were done by Dr Emmanuel A. Maze) and shRNA2 (n=3, all repetitions were performed by Dr Sylwia Ammoun). [C] Extracted proteins were analysed by western blotting (performed by myself) to measure the expression of HERV-K Gag-Full Length (FL),

p15+nucleocapsid (NC), capsid (CA)+nucleocapsid (NC), and capsid (CA). GAPDH was used as the loading control. [D] Quantification of the western blotting did not show any significant change in HERV-K Gag expression in Sch-NF2-/- cells following knockdown $CRL4^{DCAF1}$ knockdown with shRNA1 (n=3, all repetitions were performed by myself). Student's two tailed t-test: ns (not significant), $p>0.05$; *, $p<0.05$; **, $p<0.01$. Data presented as means ±SEM.

Upon this finding, it was hypothesised that HERV-K Env expression could possibly be regulated by YAP/TEAD-mediated transcription which was shown to be promoted by derepressed $CRL4^{DCAF1}$ in the absence of Merlin [160, 161, 163]. Therefore, I wanted to check whether YAP/TEAD mediated transcription is involved in HERV-K Env upregulation.

Two different drugs were used to inhibit TEAD-mediated transcription: Verteporfin, which promotes 14-3-3σ/YAP sequestration in the cytoplasm and its subsequent degradation [334]; and VT04153 (Vivace Therapeutics) which is a TEAD-specific auto-palmitoylation inhibitor (no published data by the company). Treating primary Sch-NF2-/- cells with Verteporfin significantly reduced the expression of HERV-K Env-FL by ~37% and Env-TM by ~40% (Figure 18A, B). Additionally, treating primary Sch-NF2-/- cells with Verteporfin significantly reduced cell proliferation [measured as the number of Ki67+ cells] by ~75% (Figure 19A, D), but had no significant effect on the proliferation of primary Sch-NF2+/+ cells (Figure 19C, F). Verteporfin also induced apoptosis [measured as the number of Casp3+ cells] in both Sch-NF2-/- (Figure 19B, E) and Sch-NF2+/+ cells (Figure 19 C, G).

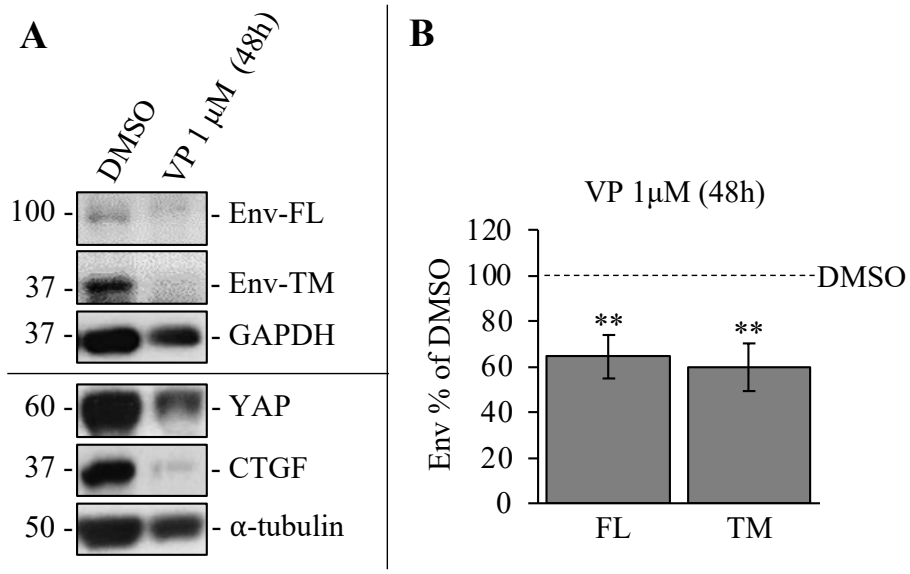

Figure 18. Verteporfin decreased the expression of HERV-K Env in Sch-NF2-/-.

Primary Merlin-deficient schwannoma cells (Sch-NF2-/-) were treated with Verteporfin (48h). Upon treatment, cells were lysed and processed for protein extraction. [A] Extracted proteins were analysed by western blotting to measure the expression of HERV-K Env-Full Length (FL) and Env-Transmembrane (TM) proteins. The efficacy of Verteporfin was demonstrated by decreased connective tissue growth factor (CTGF; target gene of YAP/TEAD transactivation, positive control) and YAP expression. α-tubulin and GAPDH were used as the loading control. [B] Quantification of the western blotting showed decreased expression of HERV-K Env-FL (n=6) and Env-TM (n=5) expression in primary Sch-NF2-/- cells following treatment with Verteporfin (48h). Student's two tailed t-test: **, $p<0.01$. Data presented as means ±SEM.

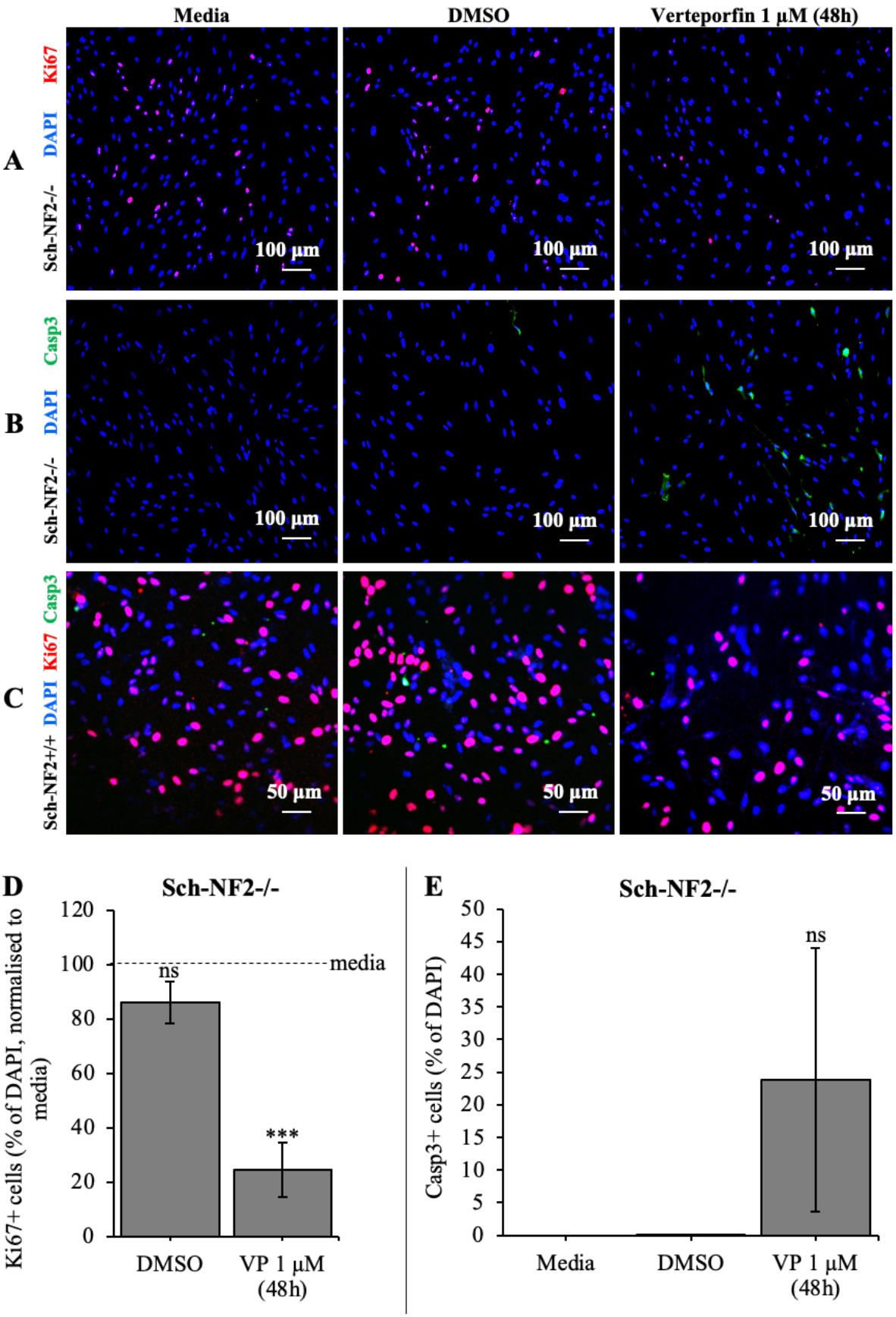
Media
DMSO
Verteporfin 1 µM (48h)
A
Ki67
DAPI
Sch-NF2-/-
100 µm
B
Casp3
DAPI
Sch-NF2-/-
100 µm
C
Casp3
Ki67
DAPI
Sch-NF2+/+
50 µm
D
Sch-NF2-/-
Ki67+ cells (% of DAPI, normalised to media)
120
100
80
60
40
20
0
media
ns
***
DMSO
VP 1 µM (48h)
E
Sch-NF2-/-
Casp3+ cells (% of DAPI)
50
45
40
35
30
25
20
15
10
5
0
ns
Media
DMSO
VP 1 µM (48h)

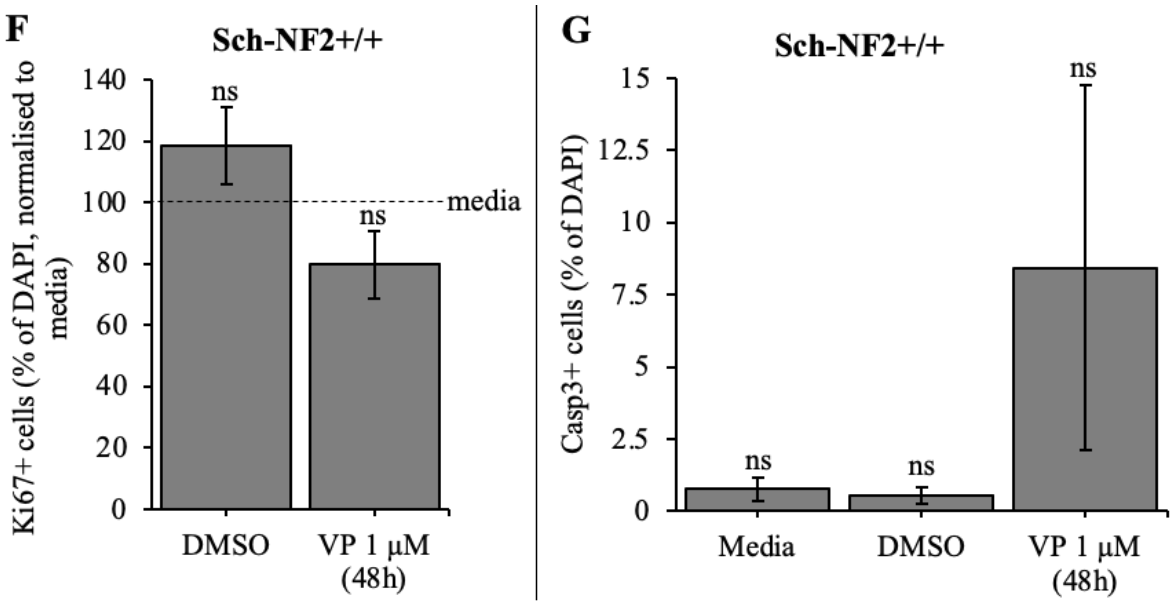

Figure 19. Verteporfin decreased Sch-NF2-/- proliferation and induced apoptosis.

Primary Merlin-deficient schwannoma cells (Sch-NF2-/-) and primary Schwan cells (Sch-NF2+/+) were treated with Verteporfin (48h). After overnight incubation with primary antibodies, cells were washed before having secondary antibodies and DAPI (blue staining) applied. [A, D] Immunocytochemistry (ICC) showed decreased Sch-NF2-/- cell proliferation (measured as number of Ki67+ cells, red) following Verteporfin treatment (n=4). [B, E] ICC showed induction of apoptosis (measured as number of Casp3+ cells, green) in Sch-NF2-/- cells following Verteporfin treatment (n=3). [C, F] ICC showed no effect on Sch-NF2+/+ cell proliferation (measured as number of Ki67+ cells, red) following Verteporfin treatment (n=3). [C, G] ICC showed induction of apoptosis (measured as number of Casp3+ cells, green) in Sch-NF2+/+ cells following Verteporfin treatment (n=3). Student's two tailed t-test: ns (not significant), $p>0.05$; ***, $p<0.001$. Data presented as means ±SEM.

Treating primary Sch-NF2-/- cells with Pan-TEAD inhibitor VT04153 significantly decreased the expression of both HERV-K Env-FL (1 repetition was done by Dr Sylwia Ammoun) and Env-TM (2 repetitions were done by Dr Sylwia Ammoun) by ~50% (Figure 20A, B). I contributed to three western blotting repetitions of HERV-K Env-FL and Env-TM expression following VT04153 treatment. However, the drug treatment was done by Liyam Laraba, and he kindly provided the samples for HERV-K Env analysis.

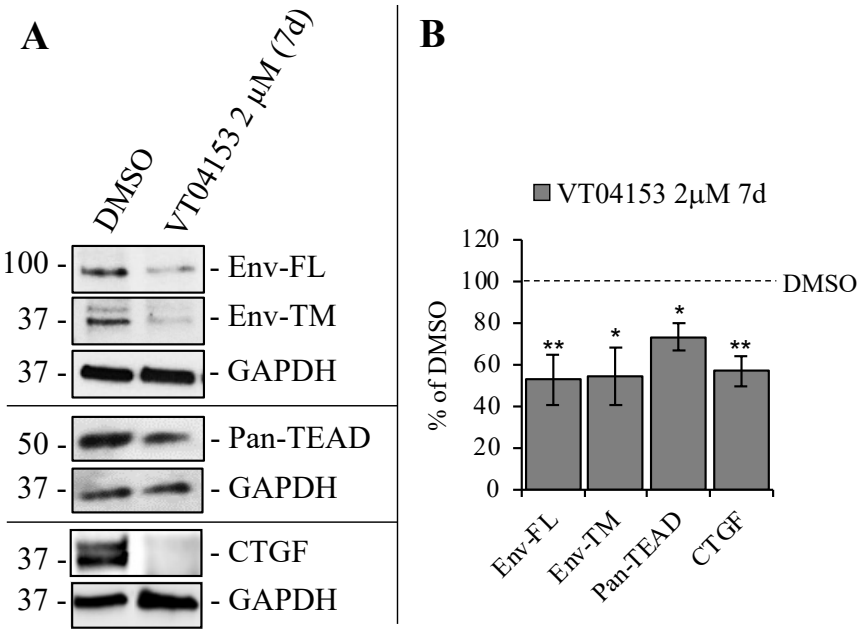

Figure 20. Pan-TEAD inhibitor VT04153 decreased the expression of HERV-K Env in Sch-NF2-/-.

Primary Merlin-deficient schwannoma cells (Sch-NF2-/-) were treated with VT04153 (7d). [A] Extracted proteins were analysed by western blotting to measure the expression of HERV-K Env-Full Length (FL) and Env-Transmembrane (TM) proteins. The efficacy of VT04135 was demonstrated by decreased connective tissue growth factor (CTGF; target gene of YAP/TEAD transactivation, positive control) and Pan-TEAD expression. GAPDH was used as the loading control. The western blotting result shown here for CTGF and its GAPDH control belongs to Liyam Laraba. The remaining results shown here were performed by myself. [B] Quantification of the western blotting showed decreased expression of HERV-K Env-FL (n=4, 1 was done by Dr Sylwia Ammoun) and Env-TM (n=5, 2 were done by Dr Sylwia Ammoun) expression in primary Sch-NF2-/- cells following treatment with VT04153 (7d). Student's two tailed t-test: *, $p<0.05$; **, $p<0.01$. Data presented as means ±SEM.

In addition, treating primary MN-GI-NF2-/- cells with Pan-TEAD inhibitor VT04153 significantly decreased the expression of HERV-K Env-FL by 40% and Env-TM by ~38% (Figure 21A, B).

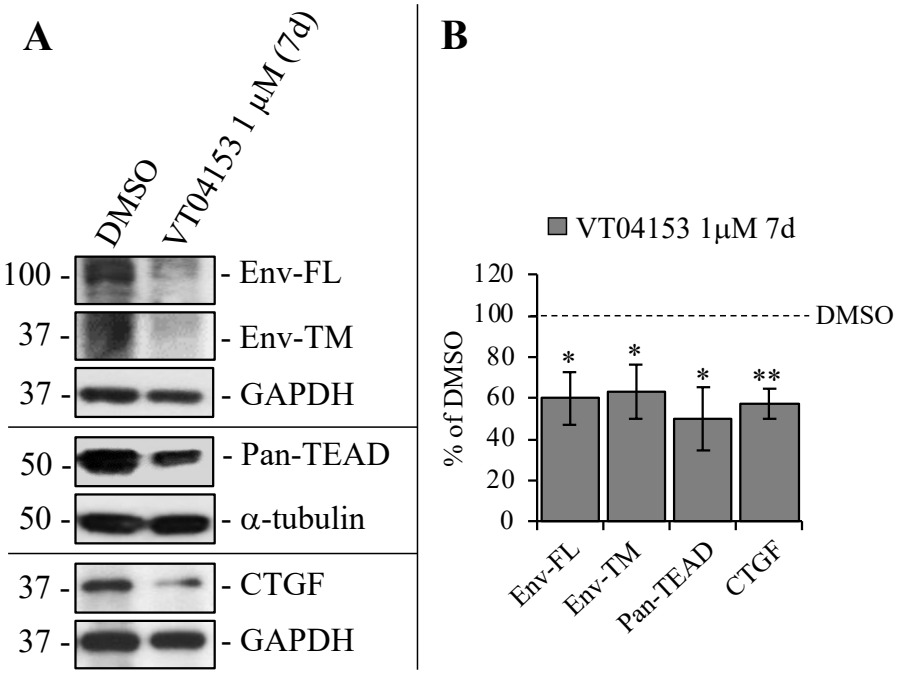

Figure 21. Pan-TEAD inhibitor VT04153 decreased the expression of HERV-K Env in MN-GI-NF2-/-.

Primary Merlin-deficient grade I meningioma (MN-GI-NF2-/-) cells were treated with VT04153 (7d). [A] Extracted proteins were analysed by western blotting to measure the expression of HERV-K Env-Full Length (FL) and Env-Transmembrane (TM) proteins. The efficacy of VT04135 was demonstrated by decreased connective tissue growth factor (CTGF; target gene of YAP/TEAD transactivation, positive control) and Pan-TEAD expression. α-tubulin and GAPDH were used as the loading control. [B] Quantification of the western blotting showed decreased expression of HERV-K Env-FL (n=5) and Env-TM (n=5) expression in primary MN-GI-NF2-/- cells following treatment with VT04153 (7d). Student's two tailed t-test: *, $p<0.05$; **, $p<0.01$. Data presented as means ±SEM.

Finally, treating primary MN-GI-NF2-/- cells with Pan-TEAD inhibitor VT04153 significantly reduced proliferation (measured as the number of Ki67+ cells) by ~80% (Figure 22A, B). Taken together, these results show evidence for the involvement of TEAD-mediated transcription in HERV-K Env upregulation, and this is further supported by the presence of TEAD binding site on HERV-K LTR which was shown *in silico* by Dr Emmanuel A. Maze (Figure S4).

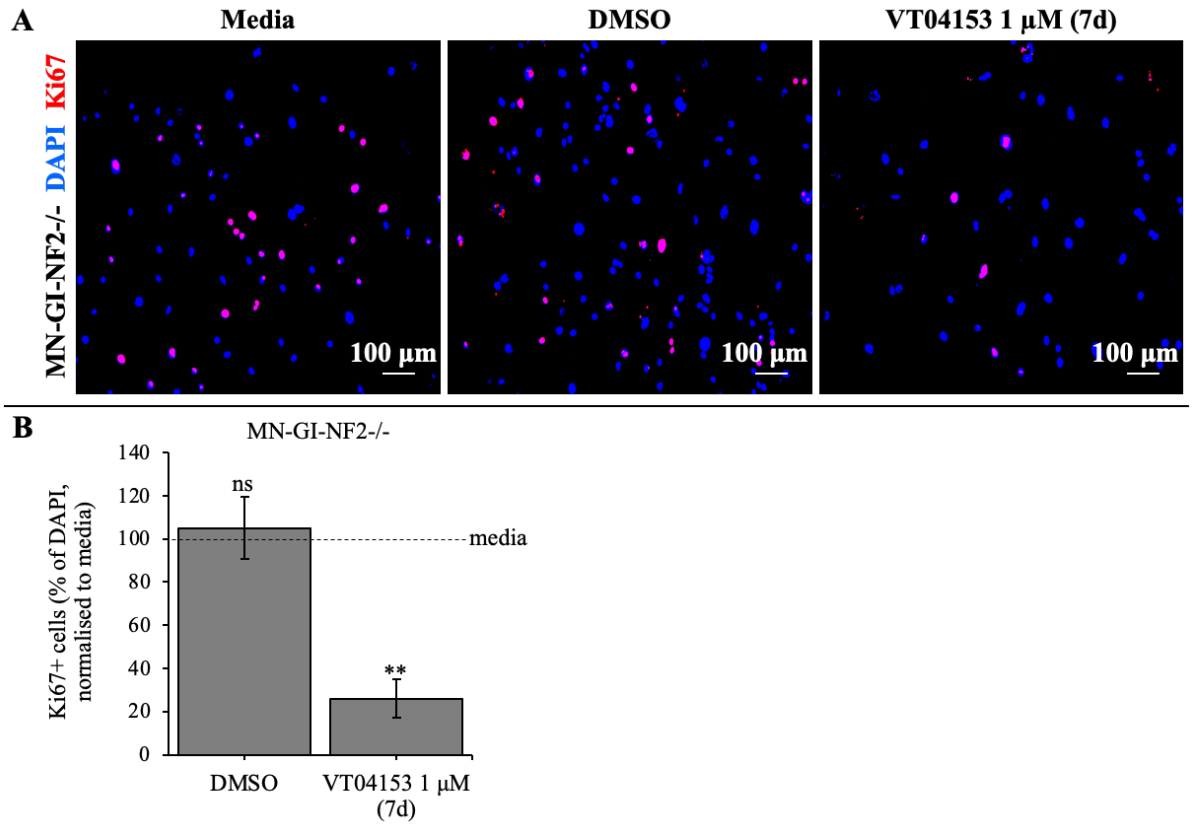

Figure 22. Pan-TEAD inhibitor VT04153 significantly decreased MN-GI-NF2-/- proliferation.

Primary Merlin-deficient grade I meningioma (MN-GI-NF2-/-) cells were treated with VT04153 (7d). After overnight incubation with primary antibodies, cells were incubated with secondary antibodies and DAPI (blue). [A, B] Immunocytochemistry (ICC) showed decreased MN-GI-NF2-/- cell proliferation (measured as the number of Ki67+ cells, red) following VT04153 treatment (n=3). Student's two tailed t-test: **, $p<0.01$. Data presented as means ±SEM.

5.4 Repurposing Anti-Retroviral Drugs to Treat Merlin-Deficient Tumours

Ritonavir, Lopinavir, and Atazanavir are FDA-approved retroviral protease inhibitors (PI) that bind to HIV-1 protease and block the enzyme catalytic site, thereby preventing the processing of Gag and Gag-Pol polyprotein precursor into mature capsid and active reverse transcriptase proteins which are all crucial for the maturity of HIV-1 virions [335-338]. These drugs are also capable of binding to HERV-K protease, although they have lower potency against it compared to that of HIV-1 [339-341].

Dr Sylwia Ammoun and Dr Emmanuel A. Maze initially started testing Ritonavir for HERV-K protease inhibition and anti-tumour effects in primary Sch-NF2-/- cells. Their data shows inhibition of HERV-K protease in primary Sch-NF2-/- cells causing an increase in the expression of uncleaved Gag-FL precursor protein. Dr Sylwia Ammoun also demonstrated reduced expression of pERK1/2 (IC50: 3.17 μM), cyclin D1 (IC50: 21.02 μM), HERV-K Env-FL (IC50: 17.73 μM) and Env-TM (IC50: 2.18 μM) in primary Sch-NF2-/- cells after 72h treatment with Ritonavir (data not shown).

5.4.1 Retroviral Protease Inhibitors Ritonavir, Atazanavir and Lopinavir Reduce Schwannoma Cell Proliferation

My project aimed to measure the effects of Ritonavir on cell proliferation and test other PI on primary Sch-NF2-/- cells. Ritonavir strongly reduced the proliferation of primary Sch-NF2-/- cells (measured as the number of Ki67+ cells) with a half-maximal inhibitory concentration (IC50) of 3.9 µM (Figure 23A, C), which is nearly six-fold lower than the peak serum concentration (C_{max}) of 22.5 µM and two-fold lower than through serum concentration (C_{min}, lowest concentration observed after drug administration before the next dose) of 10.4 µM, observed in HIV patients without side effects [342]. Moreover, Ritonavir had no effect on primary Sch-NF2+/+ cells (Figure 23B, C), suggesting that the drug is tumour-selective.

Treating primary Sch-NF2-/- cells with Atazanavir decreased cell proliferation (measured as the number of Ki67+ cells) with an IC50 of 7.29 µM (Figure 24A, C), which is ~two-fold higher than the C_{max} of ~4.1 µM and ~ten-fold higher than C_{min} of ~0.7 µM, observed in a pharmacokinetic study [343]. Lopinavir appears to be even more effective than Ritonavir and Atazanavir. This drug reduced the proliferation of primary Sch-NF2-/- cells (measured as the number of Ki67+ cells) with an IC50 of 2.04 µM (Figure 24B, C), which is ~eight-fold lower than the C_{max} of ~16.9 µM and ~5-fold lower than the C_{min} of ~9.4 µM, observed in a pharmacokinetic study [343].

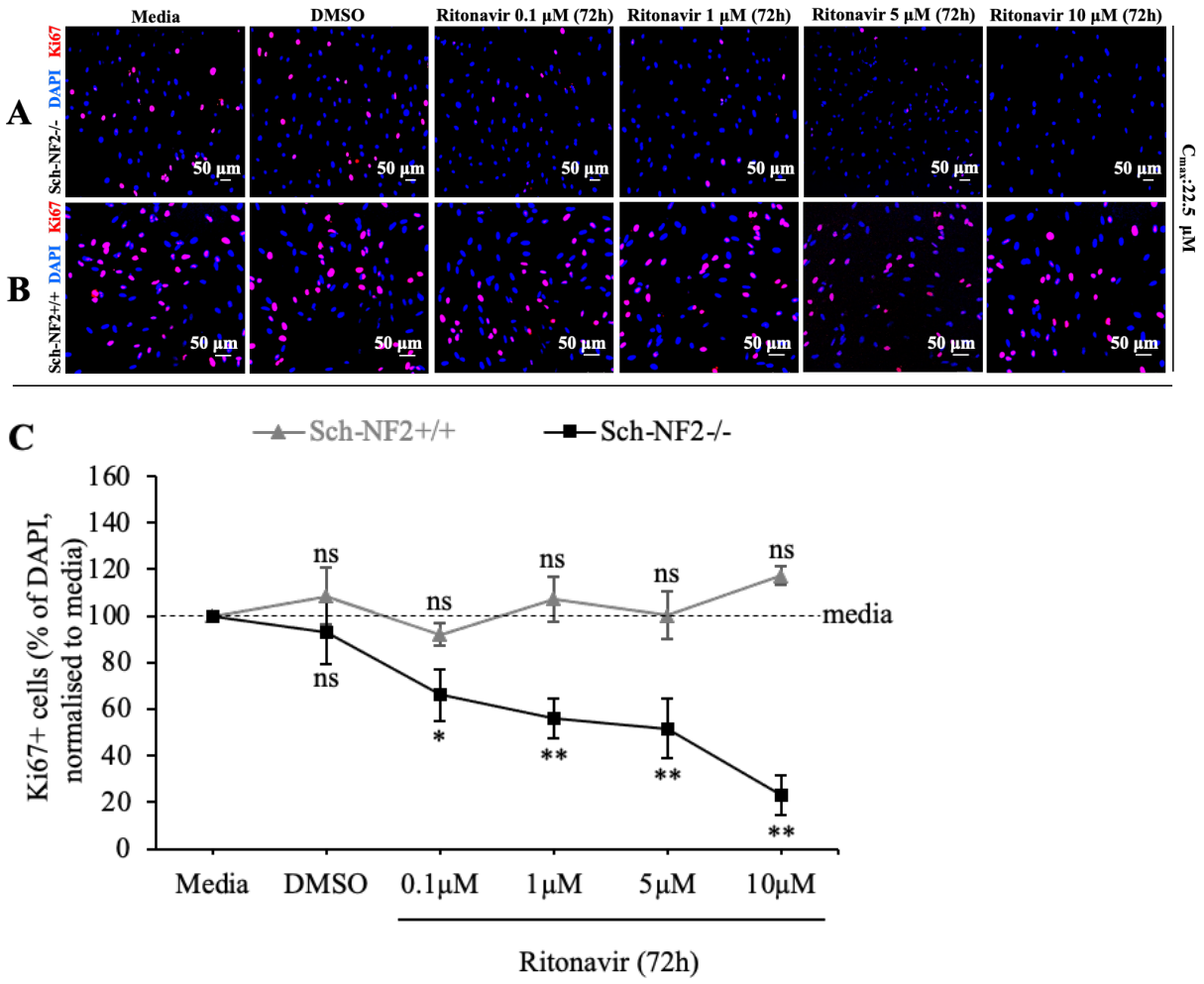

Figure 23. Ritonavir significantly decreased primary Sch-NF2-/- cell proliferation but had no effect on primary Sch-NF2+/+ cells.

Primary Merlin-deficient schwannoma cells (Sch-NF2-/-) and primary Schwann cells (Sch-NF2+/+) were treated with Ritonavir (72h). After overnight incubation with primary antibodies, cells were washed and incubated with secondary antibodies and DAPI (blue). [A, C] Immunocytochemistry (ICC) showed decreased Sch-NF2-/- cell proliferation (measured as the number of Ki67+ cells, red) following Ritonavir treatment (n=3). [B, C] ICC showed no effect on Sch-NF2+/+ cell proliferation (measured as the number of Ki67+ cells, red) following Ritonavir treatment (n=3). Student's two tailed t-test: ns (not significant), $p>0.05$; *, $p<0.05$; **, $p<0.01$. Data presented as means ±SEM.

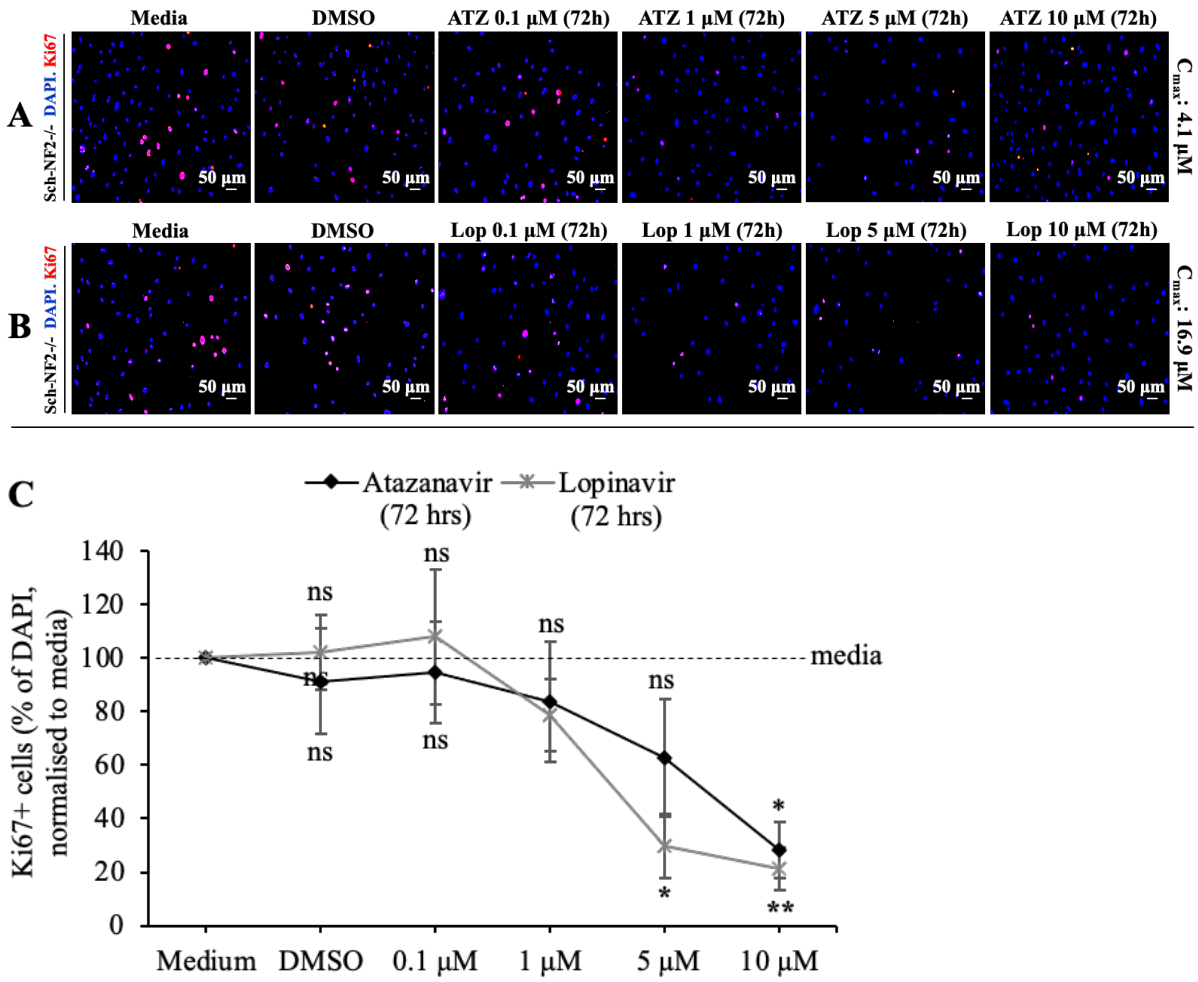

Figure 24. Lopinavir and Atazanavir decreased Sch-NF2-/- proliferation.

Primary Merlin-deficient schwannoma cells (Sch-NF2-/-) were treated with Atazanavir (72h) or Lopinavir (72h). After overnight incubation with primary antibodies, cells were incubated with secondary antibodies and DAPI (blue). [A, C] Immunocytochemistry (ICC) showed decreased Sch-NF2-/- cell proliferation (measured as the number of Ki67+ cells) following Atazanavir treatment (n=3). [B, C] ICC showed decreased Sch-NF2-/- cell proliferation (measured as the number of Ki67+ cells) following Lopinavir treatment (n=3). Student's two tailed t-test: ns (not significant), $p>0.05$; *, $p<0.05$; **, $p<0.01$. Data presented as means ±SEM.

Overall, Ritonavir and Lopinavir appear to be significantly effective against primary Sch-NF2-/- cells and could potentially be used for schwannoma treatment. Unlike Ritonavir and Lopinavir, Atazanavir had higher IC50 than C_{max} and C_{min} observed in a pharmacokinetic study [343].

5.4.2 Ritonavir and Atazanavir Reduce BenMen Cell Proliferation

My research also aimed to test PI in MN-GI-NF2-/-. BenMen was used as a cell line model to test Ritonavir and Atazanavir in MN-GI-NF2-/-. Ritonavir treatment (7d) effectively decreased BenMen cell proliferation (measured as the number of Ki67+ cells) with an IC50 of 1 µM (Figure 25A, C). Similarly, Atazanavir (7d) decreased BenMen cell proliferation (measured as the number of Ki67+ cells) with an IC50 of 1.08 µM (Figure 25A, B). Both drugs also reduced BenMen cell proliferation (measured as the number of Ki67+ cells) after 72h treatment (Figure 25A-C). However, 7d treatment appeared to be more effective.

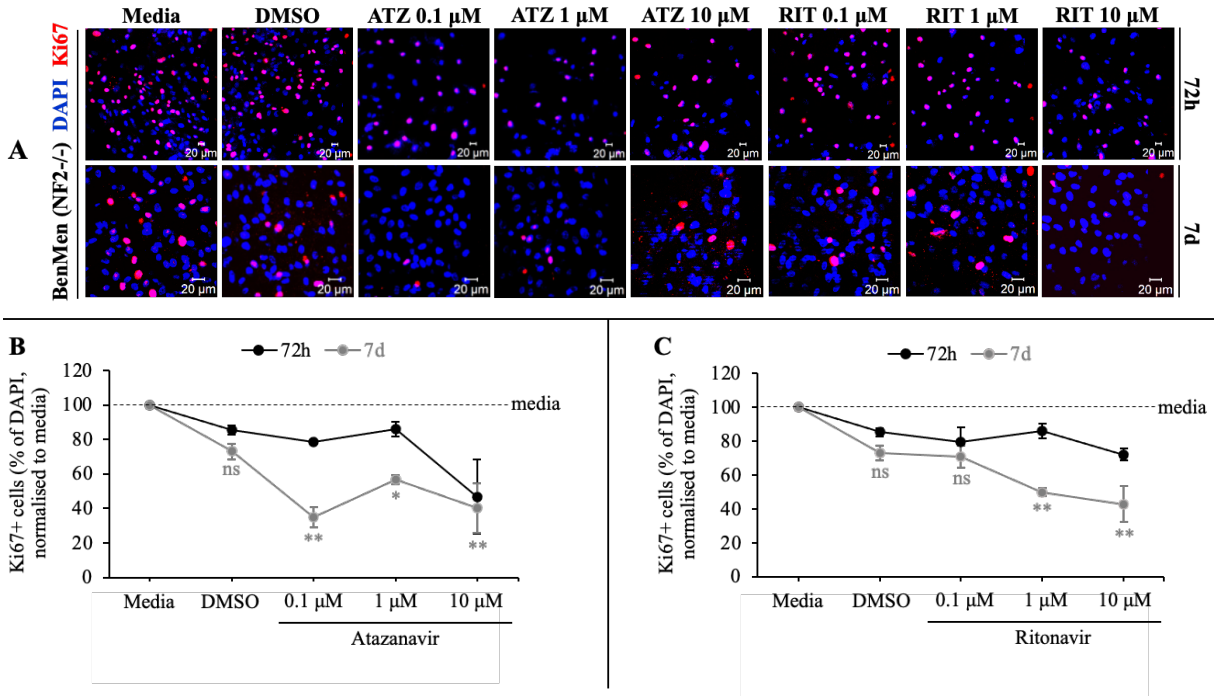

Figure 25. Atazanavir and Ritonavir decreased BenMen cell proliferation.

Ben-Men-1 (BenMen) cells were treated with Atazanavir (72h/7d) or Ritonavir (72h/7d). After overnight incubation with primary antibodies, cells were incubated with secondary antibodies and DAPI (blue). [A, B] Immunocytochemistry (ICC) showed decreased BenMen cell proliferation (measured as the number of Ki67+ cells, red) following Atazanavir treatment for 7d (n=3) and 72h (n=2). [A, C] ICC showed decreased BenMen cell proliferation (measured as the number of Ki67+ cells, red) following Ritonavir treatment for 7d (n=3) and 72h (n=2).

Student's two tailed t-test: ns (not significant), $p>0.05$; *, $p<0.05$; **, $p<0.01$. Data presented as means ±SEM.

Following my results (Figure 25), Dr Sylwia Ammoun tested the effects of PI in primary MN-GI-NF2-/- cells. Ritonavir, Atazanavir and Lopinavir significantly reduced primary MN-GI-NF2-/- cell proliferation (measured as the number of Ki67+ cells) with IC50s of 1.36 μM, 0.2 μM and 0.02 μM, respectively (data not shown). In addition, Ritonavir, Atazanavir and Lopinavir reduced the expression pERK1/2 (IC50s for Ritonavir and Lopinavir are 12.43 μM and 8.94 μM, respectively. More repeats are required to calculate the IC50 for Atazanavir), cyclin D1 (IC50s: 9.09 μM, 8.98 μM and 7.26 μM, respectively), HERV-K Env-FL (IC50s: 28.21 μM, 8.7 μM and 8.8 μM, respectively) and Env-TM (IC50 for Lopinavir is 2.29 μM. More repeats are needed to calculate the IC50 for Ritonavir and Atazanavir) in primary MN-GI-NF2-/- cells (data not shown).

6 Discussion

Our group is working with human primary schwannoma, meningioma, and Schwann cells to improve our understanding of the development of these tumours. Clinical trials to test candidate therapeutic compounds are expensive and require many patients. Human primary cells provide a validated preclinical model with a highly predictive value of therapeutic efficacy [344].

Current treatments for Merlin-deficient tumours are surgical resection and adjuvant radiotherapy which are both partially effective yet may lead to neurological complications such as nerve damage. Gamma knife surgery (GKS) was shown to have long-term local tumour control for small- to medium-sized vestibular schwannomas. However, GKS was confirmed to be less effective in NF2 related vestibular schwannomas compared to unilateral sporadic vestibular schwannomas. Therefore, new drug-based treatments are urgently required [5, 345, 346]. Several studies have shown the transcriptional activity and tumourigenic potential of HERV-K in various types of cancer [7-18]. Furthermore, several groups have tested the potential of targeting HERV-K *in vivo* using monoclonal antibodies [347], recombinant vaccinia virus vaccination [348] and CAR-T cells [349], which all caused tumour regression in mouse models.

Dr Sylwia Ammoun and Dr Emmanuel A. Maze demonstrated the presence of HERV-K in Merlin-deficient schwannoma. Therefore, I investigated the contribution of HERV-K in Merlin-deficient schwannoma and grade I meningioma tumourigenesis and examined the potential of HERV-K to be used as a novel therapeutic target as well as

testing retroviral protease inhibitors' efficacy for the potential treatment of these tumours.

6.1 HERV-K Env Signalling Pathway in Merlin-Deficient Schwannoma

Here, I demonstrate that HERV-K Env overexpression (Env o/e) induces the proliferation (measured as the number of Ki67+ cells) of Sch-NF2+/+ cells and leads to upregulation of the transcription factor cJun in Sch-NF2+/+ cells. Moreover, these results are associated with an upregulation of pERK1/2 and cyclin A2. Surprisingly, Env o/e reduces the levels of cyclin D1 in Sch-NF2+/+, whilst it increases the levels of cyclin A2. Reduced levels of cyclin D1 was unexpected as it is upregulated in Sch-NF2-/- [156-158]. More importantly, pERK1/2 has been shown to induce cyclin D1 expression via PDGF and *myc* which results in cell cycle entry and increased Sch-NF2-/- cell proliferation [151, 327-330]. Cyclin A2 is a crucial regulator of the S phase as well as the mitotic entry [332, 350-352], and it is deregulated in a variety of cancers where it is related to increased tumour proliferation [353-355]. Dr Sylwia Ammoun demonstrated decreased cyclin D1 levels in NF2+/+ schwannoma and increased cyclin D1 levels in NF2-/- schwannoma, following Env o/e. Additionally, Dr Sylwia Ammoun showed a stronger increase of cyclin A2 levels in NF2+/+ schwannoma than in NF2-/- schwannoma cells. More experimental repeats are required to confirm these results; however, the presence of Merlin could explain the reduction in cyclin D1 levels in Sch-NF2+/+ or NF2+/+ schwannoma cells, following Env o/e. One way to validate this data is to initially knockdown Merlin in primary NF2+/+ schwannoma and Sch-NF2+/+ cells

and to subsequently overexpress HERV-K Env in the same cells. Upon Merlin knockdown and Env o/e, cyclin D1 and cyclin A2 levels should be measured.

The signalling pathway from HERV-K Env to the upregulation of cyclin A2 is unknown. However, proto-oncogene *c-myc* is a potential candidate for several reasons. Firstly, *c-myc* mediated cell cycle progression from G1 to S phase and *c-myc* mediated cell proliferation was shown to be primarily dependent on cyclin A but not dependent on cyclin D1 [356, 357]. Secondly, myc protein has been shown to repress the cyclin D1 gene [358]. This is also supported by the disappearance of cyclin D1 protein as the cell progresses into the S phase [359]. Lastly, Merlin deficiency leads to upregulated Wnt signalling in Sch-NF2-/- cells causing an increased transcription of *c-myc* [158, 360]. Consequently, it should be investigated whether Env o/e upregulates *c-myc* levels in Sch-NF2+/+ cells. For that reason, *c-myc* levels should be measured in both transcriptional and protein levels using qRT-PCR and western blotting, respectively. Lastly, it is important to mention that examining the effects of Env o/e on cyclin D1 and cyclin A2 was a limited analysis of the cell cycle. Other cyclins involved in cell cycle progression and their binding partners CDKs must be examined.

My work failed to achieve a successful HERV-K knockdown in Sch-NF2-/- using shRNA constructs targeting LTRs, *env* ORF and *gag* ORF. As such, I could not validate the results I obtained from Env o/e experiments in primary Sch-NF2+/+ cells. The shRNA constructs used also included one that reduces HERV-K Env expression in pancreatic cell lines, which resulted in reduced pERK1/2 expression [9]. Using the HEI193 cell line as a model, I was unable to achieve such a knockdown. Tatkiewicz *et*

al. has shown that only 10% of the HERV-K Env-encoding proviruses can produce a functional Env protein [361]. However, this should not have been an issue here, as the shRNA used was in excess. Additionally, 19 HERV-K (HML-2) proviruses were aligned using MEGAX software and searched for the shRNA target sequences used in knockdown experiments. Search results showed that most of these sequences are also present in other proviruses, suggesting that the shRNA sequences should target other proviruses as well. shRNA construct 18 (see Table 5, Materials and Methods) was searched in all proviruses to demonstrate an example (Figure S3). Despite all this, the knockdown trials failed.

6.2 HERV-K Env Upregulation in Merlin-Deficient Schwannoma and Grade I Meningioma

As in preliminary group data on Sch-NF2-/-, I found the expression of HERV-K Env to be upregulated in primary MN-GI-NF2-/- cells, but it is more variable than primary Sch-NF2-/- cells. Firstly, this outcome was expected as meningiomas are known to be relatively heterogeneous. Secondly, HMC cells are derived from embryonal cells and cannot reflect adult normal MN-NF2+/+ cells. However, they were the only control that could be used in this experiment and their origin could be one of the reasons why the results are heterogeneous (Figure 15). In contrast, IHC and western blotting results obtained using MN-GI-NF2-/- tissues demonstrate more homogenous results (Figure 13 and 14).

Combined with the data from Dr Sylwia Ammoun and Dr Emmanuel A. Maze, I show that HERV-K Env upregulation in Sch-NF2-/- is partially Merlin dependent. Dr Sylwia Ammoun also demonstrated the same result in MN-GI-NF2-/- (data not shown). A similar observation, the dependence on a tumour suppressor, was made with another HERV, HERV-E, which is upregulated in the absence of a tumour suppressor: Von Hippel-Lindau (VHL) [362]. Downstream of Merlin, I demonstrate that HERV-K Env expression in both Sch-NF2-/- and MN-GI-NF2-/- is regulated by the transcription factor TEAD via binding to YAP. These findings are further supported by the presence of a TEAD binding site on HERV-K LTR, demonstrated *in silico* (Figure S4). Therefore, chromatin immunoprecipitation followed by HERV-K LTR-specific PCR is required to fully characterise such transcription binding site. Interestingly, identified TEAD binding site overlaps with one NFκB binding site on HERV-K LTR (Figure S4), which was recently tested by Gonzales-Hernandez *et al*. using chromatin immunoprecipitation [276]. To check whether NFκB is involved in HERV-K upregulation, Dr Sylwia Ammoun and Dr Emmanuel A. Maze have tested a cell-permeable recombinant peptide, SN50, which prevents the nuclear translocation of NFκB [363]. However, SN50 did not show any effect on HERV-K Env protein expression in primary Sch-NF2-/- cells (data not shown).

Hypomethylation is also a method of HERV-K transactivation [364, 365]; however, in some cell lines, it is not sufficient to induce HERV-K transcription [271, 366]. In addition, Torres-Martín *et al*. detected homeobox (HOX) gene cluster hypomethylation in vestibular schwannoma [367], but HOX gene has no known interaction with HERV-

K LTR. Therefore, transcription factors need to be considered for HERV-K upregulation.

Knocking down $CRL4^{DCAF1}$ did not block HERV-K Env expression completely, suggesting that other factors are involved in the process. Src is a potential candidate as it has been shown to activate YAP [368, 369]. In addition, Src is involved in the increased proliferation of Sch-NF2-/- cells downstream of PDGFRβ [151] and integrin β1 [370]. Whether Src is also involved in HERV-K Env upregulation could be investigated by knocking down Src in primary Sch-NF2-/- and MN-GI-NF2-/- cells and measuring HERV-K Env protein expression by western blotting. Finally, the proposed mechanism of the HERV-K upregulation in Sch-NF2-/- and MN-GI-NF2-/- is summarised in Figure 26.

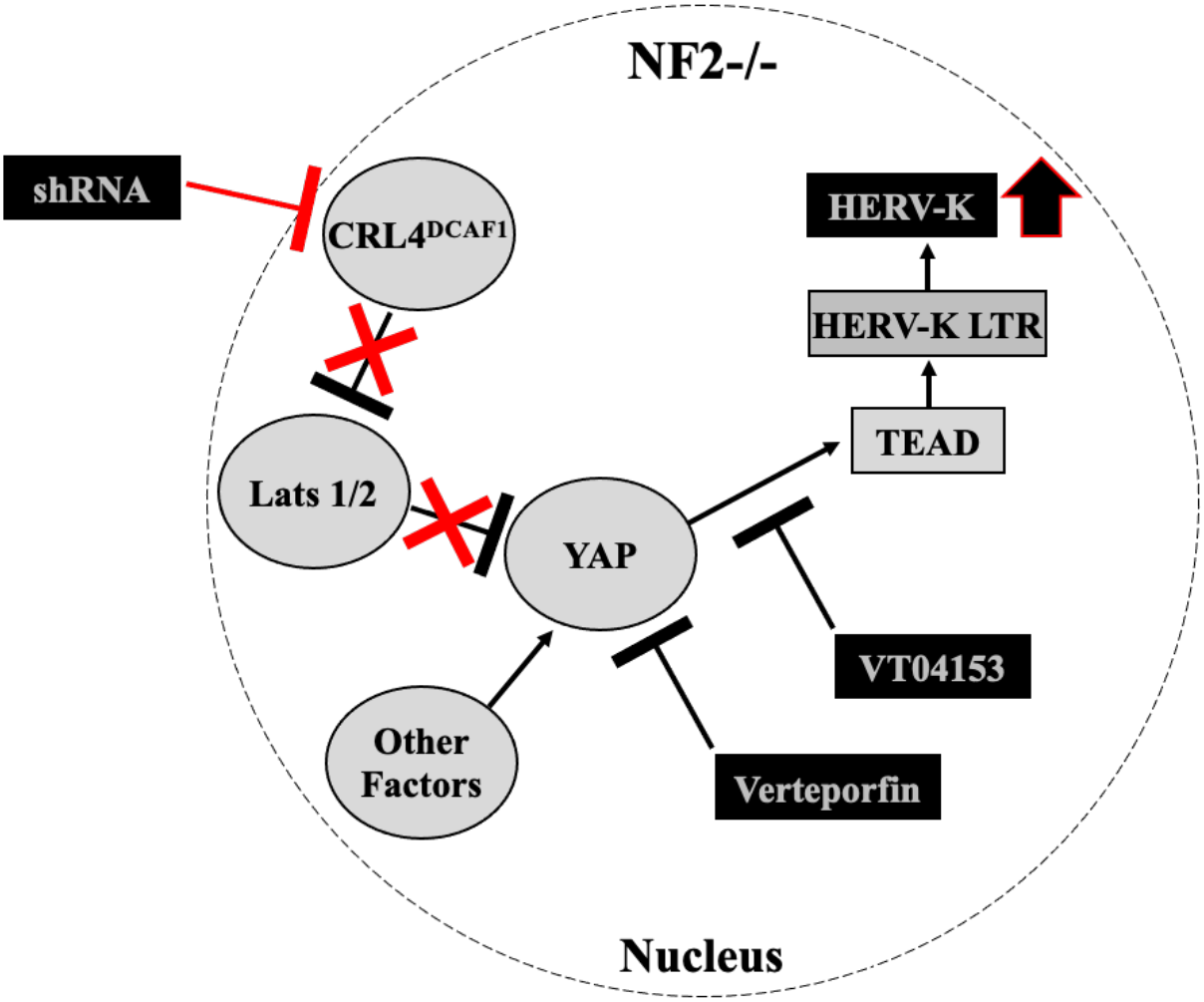

Figure 26. Mechanism of HERV-K upregulation.

HERV-K upregulation was shown to be partially Merlin-dependent. Therefore, downstream pathways regulated by Merlin were investigated. $CRL4^{DCAF1}$ is known to be derepressed in the absence of Merlin, leading to increased oncogenic gene expression via promoting YAP/TEAD-mediated transcription [163]; however, knocking down $CRL4^{DCAF1}$ did not block HERV-K expression completely. Consequently, the YAP/TEAD protein interaction was investigated. TEAD inhibitors Verteporfin and VT04153 significantly decreased the expression of HERV-K Env in Sch-NF2-/- and MN-GI-NF2-/-, providing evidence for the involvement of TEAD-mediated transcription in HERV-K upregulation. These findings were further supported by the presence of a TEAD binding site on HERV-K LTR, which was demonstrated *in silico* (Figure S4). Finally, it should be noted that there are other factors that are potentially involved in HERV-K Env upregulation.

6.3 Potential Therapeutics for Schwannomas and Meningiomas

Here, I suggest the use of retroviral protease inhibitors, Ritonavir and Lopinavir, for the treatment of patients suffering from Merlin-deficient schwannomas and meningiomas. For both drugs, IC50 that affects the cell proliferation were much lower than the drug concentration used in HIV patients [342, 343], which could mean minimal side effects. More importantly, Ritonavir showed no effect on primary Sch-NF2+/+ cell proliferation, suggesting that the drug is tumour-selective. Lopinavir was not tested on primary Sch-NF2+/+ cells, thus it is not known whether it is tumour-selective or not. In Atazanavir, IC50 was higher than C_{max} and C_{min} used in HIV patients [343]. As such, it is not ideal to use this drug for schwannoma treatment because most protease inhibitors were accompanied by side effects in long-term treatment [335, 371].

Anti-cancer effects of these drugs are clearly discussed in Section 3.8. So far, there have been at least 20 clinical trials involving Ritonavir in a broad range of therapies and cancers [372]. Three of these trials also involve Lopinavir, which has not been trialled alone due to its low bioavailability without Ritonavir. In one phase II trial (NCT01095094), Ritonavir combined with Lopinavir was tested in 19 patients suffering from high-grade gliomas. However, only 2/19 patients had a 6-months progression-free survival and the study failed to meet primary efficacy endpoint [373].

Treating NF2 related schwannomas and meningiomas require prolonged periods and there is a risk of developing long-term adverse effects in patients. *In vitro* treatment of Sch-NF2-/- and MN-GI-NF2-/- cells demonstrate a relatively low IC50, allowing us to use a low dose in the medication regimen. Additionally, both schwannoma and meningioma tumours are located outside the blood-brain barrier and thus tumour

delivery for these drugs should not be problematic. Dr Sylwia Ammoun has shown that Ritonavir has an additive effect in combination with the PDGFR/Raf inhibitor Sorafenib or the MEK inhibitor Selumetinib that were recently shown to reduce the proliferation of schwannoma cells *in vitro* [151, 327]. Also, a recent phase 0 clinical trial of orally administrated Sorafenib in NF2 patients achieved a high intratumoural drug concentration [374]. Lastly, similar additive effects of Ritonavir were observed in other studies involving Ritonavir/Non-PI drug combinations [301-303].

Regarding the mechanism of these drugs, Dr Sylwia Ammoun and Dr Emmanuel A. Maze demonstrated a reduction in pERK1/2 and cyclin D1 expression in Sch-NF2-/- and MN-GI-NF2-/- cells treated with Ritonavir, Atazanavir and Lopinavir (data not shown), which explains the reduction in cell proliferation. Dr Emmanuel A. Maze also confirmed the effect of these drugs on HERV-K protease (data not shown), which cleaves HERV-K Gag protein. In addition to the inhibitory effect on HERV-K protease, Ritonavir is known to inhibit the proteasome activity, although achievable only at higher concentrations (>10 μM) [375]. In a study, Ritonavir induced cytostatic and cytotoxic effects on glioblastoma-derived cells via inhibiting the chymotrypsin-like activity of the proteasome, and induced resistances *in vitro* [376]. However, Ritonavir cannot have such effects in Sch-NF2-/- and MN-GI-NF2-/- cells as the drug concentrations used are much lower than needed for effective proteasome inhibition suggesting that proteasome inhibitory effect of Ritonavir would be a minimal contribution. Dr Sylwia Ammoun also showed that the protease inhibitors reduce the expression of HERV-K Env in Sch-NF2-/- and MN-GI-NF2-/- cells (data not shown), which could partly aid the reduction in pERK1/2. HERV-K Env is known to be cleaved by a cellular furin-like endoprotease

[267], and the protease inhibitors decreased the levels of both uncleaved Env-FL precursor and cleaved Env-TM, suggesting that the drugs did not affect the cleavage efficiency as for Gag but rather the overall expression of HERV-K Env. This is possibly consistent with the broad range effects of seen in these drugs (discussed in section 3.8).

Overall, Ritonavir and Lopinavir could be potentially repurposed for the treatment of Merlin-deficient schwannoma and meningioma, but more *in vitro* experiments with a larger sample size should be done. Clinical testing of Ritonavir and Lopinavir for the treatment of these tumours should have minimal side effects because the measured IC50s for these drugs (*in vitro*) are much lower than the C_{max} used in HIV patients [342, 343]. The side effect profile, monitoring and doses for pre-approved medications help the clinicians feel more confident and prepared for potential issues when prescribing them. Additionally, pre-approved drugs are advantageous in terms of saving time, effort, and money to get them re-purposed for other diseases as the process is streamlined. Finally, the possibility of using protease inhibitors in combination with other anti-cancer drugs such as Sorafenib and Selumetinib means that lower doses of each drug might be used which could reduce the side effect/toxicity profile of these drugs.

7 Conclusion

The main findings of the thesis are as follow: (i) HERV-K Env is upregulated in Merlin-deficient grade I meningioma; (ii) HERV-K Env contributes to schwannoma tumourigenesis; (iii) HERV-K Env upregulation in Merlin-deficient schwannoma and grade I meningioma is partly regulated by the transcription factor TEAD via binding to the Hippo signalling pathway coactivator YAP; (iv) Retroviral protease inhibitors Ritonavir and Lopinavir could be potentially repurposed for the treatment of NF2 related schwannoma and meningioma; however, they need further testing.

8 Future Work

Further work needed to be done are as follow: (i) Signalling pathway from HERV-K Env to the upregulation of cyclin A2 need to be investigated. (ii) Whether the presence of Merlin plays a role in reduced cyclin D1 levels after Env o/e in Merlin-positive schwannoma and Schwann cells need to be validated. (iii) Other cyclins involved in cell cycle progression and their binding partners CDKs must be examined after Env o/e in Sch-NF2+/+ cells. (iv) TEAD binding site on HERV-K LTR need to be confirmed experimentally. (v) Involvement of other factors in HERV-K upregulation, especially Src, need to be investigated. (vi) Ritonavir and Lopinavir need to be tested *in vitro* with larger sample size.

9 References

1. Rouleau, G.A., et al., *Alteration in a new gene encoding a putative membrane-organizing protein causes neuro-fibromatosis type 2.* Nature, 1993. **363**(6429): p. 515-21.
2. Trofatter, J.A., et al., *A novel moesin-, ezrin-, radixin-like gene is a candidate for the neurofibromatosis 2 tumor suppressor.* Cell, 1993. **75**(4): p. 826.
3. Narod, S.A., et al., *Neurofibromatosis type 2 appears to be a genetically homogeneous disease.* Am J Hum Genet, 1992. **51**(3): p. 486-96.
4. Gutmann, D.H., et al., *Loss of merlin expression in sporadic meningiomas, ependymomas and schwannomas.* Neurology, 1997. **49**(1): p. 267-70.
5. Hanemann, C.O. and D.G. Evans, *News on the genetics, epidemiology, medical care and translational research of Schwannomas.* J Neurol, 2006. **253**(12): p. 1533-41.
6. Blakeley, J.O., et al., *Consensus recommendations for current treatments and accelerating clinical trials for patients with neurofibromatosis type 2.* Am J Med Genet A, 2012. **158A**(1): p. 24-41.
7. Goering, W., T. Ribarska, and W.A. Schulz, *Selective changes of retroelement expression in human prostate cancer.* Carcinogenesis, 2011. **32**(10): p. 1484-92.
8. Ishida, T., et al., *Identification of the HERV-K gag antigen in prostate cancer by SEREX using autologous patient serum and its immunogenicity.* Cancer Immun, 2008. **8**: p. 15.
9. Li, M., et al., *Downregulation of Human Endogenous Retrovirus Type K (HERV-K) Viral env RNA in Pancreatic Cancer Cells Decreases Cell Proliferation and Tumor Growth.* Clin Cancer Res, 2017. **23**(19): p. 5892-5911.
10. Wang-Johanning, F., et al., *Expression of human endogenous retrovirus k envelope transcripts in human breast cancer.* Clin Cancer Res, 2001. **7**(6): p. 1553-60.
11. Wang-Johanning, F., et al., *Expression of multiple human endogenous retrovirus surface envelope proteins in ovarian cancer.* Int J Cancer, 2007. **120**(1): p. 81-90.
12. Armbruester, V., et al., *Np9 protein of human endogenous retrovirus K interacts with ligand of numb protein X.* J Virol, 2004. **78**(19): p. 10310-9.
13. Denne, M., et al., *Physical and functional interactions of human endogenous retrovirus proteins Np9 and rec with the promyelocytic leukemia zinc finger protein.* J Virol, 2007. **81**(11): p. 5607-16.
14. Galli, U.M., et al., *Human endogenous retrovirus rec interferes with germ cell development in mice and may cause carcinoma in situ, the predecessor lesion of germ cell tumors.* Oncogene, 2005. **24**(19): p. 3223-8.
15. Hanke, K., et al., *The Rec protein of HERV-K(HML-2) upregulates androgen receptor activity by binding to the human small glutamine-rich tetratricopeptide repeat protein (hSGT).* Int J Cancer, 2013. **132**(3): p. 556-67.

16. Johanning, G.L., et al., *Expression of human endogenous retrovirus-K is strongly associated with the basal-like breast cancer phenotype.* Sci Rep, 2017. **7**: p. 41960.
17. Lemaitre, C., et al., *A human endogenous retrovirus-derived gene that can contribute to oncogenesis by activating the ERK pathway and inducing migration and invasion.* PLoS Pathog, 2017. **13**(6): p. e1006451.
18. Zhou, F., et al., *Activation of HERV-K Env protein is essential for tumorigenesis and metastasis of breast cancer cells.* Oncotarget, 2016. **7**(51): p. 84093-84117.
19. Evans, D.G., et al., *Somatic mosaicism: a common cause of classic disease in tumor-prone syndromes? Lessons from type 2 neurofibromatosis.* Am J Hum Genet, 1998. **63**(3): p. 727-36.
20. Kluwe, L., et al., *Molecular study of frequency of mosaicism in neurofibromatosis 2 patients with bilateral vestibular schwannomas.* J Med Genet, 2003. **40**(2): p. 109-14.
21. Evans, D.G., et al., *Mosaicism in neurofibromatosis type 2: an update of risk based on uni/bilaterality of vestibular schwannoma at presentation and sensitive mutation analysis including multiple ligation-dependent probe amplification.* J Med Genet, 2007. **44**(7): p. 424-8.
22. Evans, D.G., et al., *Incidence of mosaicism in 1055 de novo NF2 cases: much higher than previous estimates with high utility of next-generation sequencing.* Genet Med, 2020. **22**(1): p. 53-59.
23. Evans, D.G., *Neurofibromatosis type 2.* Handb Clin Neurol, 2015. **132**: p. 87-96.
24. Evans, D.G., *Neurofibromatosis type 2 (NF2): a clinical and molecular review.* Orphanet J Rare Dis, 2009. **4**: p. 16.
25. Hilton, D.A. and C.O. Hanemann, *Schwannomas and their pathogenesis.* Brain Pathol, 2014. **24**(3): p. 205-20.
26. Upadhyaya, M., et al., *Germline and somatic NF1 gene mutation spectrum in NF1-associated malignant peripheral nerve sheath tumors (MPNSTs).* Hum Mutat, 2008. **29**(1): p. 74-82.
27. Ferner, R.E. and D.H. Gutmann, *International consensus statement on malignant peripheral nerve sheath tumors in neurofibromatosis.* Cancer Res, 2002. **62**(5): p. 1573-7.
28. Ferner, R.E., et al., *Guidelines for the diagnosis and management of individuals with neurofibromatosis 1.* J Med Genet, 2007. **44**(2): p. 81-8.
29. Johansson, G., et al., *Effective in vivo targeting of the mammalian target of rapamycin pathway in malignant peripheral nerve sheath tumors.* Mol Cancer Ther, 2008. **7**(5): p. 1237-45.
30. Verdijk, R.M., et al., *TP53 mutation analysis of malignant peripheral nerve sheath tumors.* J Neuropathol Exp Neurol, 2010. **69**(1): p. 16-26.
31. Nielsen, G.P., et al., *Malignant transformation of neurofibromas in neurofibromatosis 1 is associated with CDKN2A/p16 inactivation.* Am J Pathol, 1999. **155**(6): p. 1879-84.
32. De Raedt, T., et al., *PRC2 loss amplifies Ras-driven transcription and confers sensitivity to BRD4-based therapies.* Nature, 2014. **514**(7521): p. 247-51.

33. Sohier, P., et al., *Confirmation of mutation landscape of NF1-associated malignant peripheral nerve sheath tumors.* Genes Chromosomes Cancer, 2017. **56**(5): p. 421-426.
34. Lee, W., et al., *PRC2 is recurrently inactivated through EED or SUZ12 loss in malignant peripheral nerve sheath tumors.* Nat Genet, 2014. **46**(11): p. 1227-32.
35. Evans, D.G., S.M. Huson, and J.M. Birch, *Malignant peripheral nerve sheath tumours in inherited disease.* Clin Sarcoma Res, 2012. **2**(1): p. 17.
36. Pelton, P.D., et al., *Ruffling membrane, stress fiber, cell spreading and proliferation abnormalities in human Schwannoma cells.* Oncogene, 1998. **17**(17): p. 2195-209.
37. Rosenbaum, C., et al., *Isolation and characterization of Schwann cells from neurofibromatosis type 2 patients.* Neurobiol Dis, 1998. **5**(1): p. 55-64.
38. Utermark, T., K. Kaempchen, and C.O. Hanemann, *Pathological adhesion of primary human schwannoma cells is dependent on altered expression of integrins.* Brain Pathol, 2003. **13**(3): p. 352-63.
39. Flaiz, C., et al., *Actin-rich protrusions and nonlocalized GTPase activation in Merlin-deficient schwannomas.* J Neuropathol Exp Neurol, 2007. **66**(7): p. 608-16.
40. Utermark, T., S.J. Schubert, and C.O. Hanemann, *Rearrangements of the intermediate filament GFAP in primary human schwannoma cells.* Neurobiol Dis, 2005. **19**(1-2): p. 1-9.
41. Utermark, T., et al., *Reduced apoptosis rates in human schwannomas.* Brain Pathol, 2005. **15**(1): p. 17-22.
42. Petrilli, A.M. and C. Fernandez-Valle, *Role of Merlin/NF2 inactivation in tumor biology.* Oncogene, 2016. **35**(5): p. 537-48.
43. Antinheimo, J., et al., *Population-based analysis of sporadic and type 2 neurofibromatosis-associated meningiomas and schwannomas.* Neurology, 2000. **54**(1): p. 71-6.
44. Evans, D.G., et al., *Management of the patient and family with neurofibromatosis 2: a consensus conference statement.* Br J Neurosurg, 2005. **19**(1): p. 5-12.
45. Schneider, J., et al., *[Tumors of the central nervous system in biopsy and autopsy material. 7th communication: neurinomas and neurofibromatoses with CNS involvement].* Zentralbl Allg Pathol, 1983. **127**(5-6): p. 305-14.
46. Hanemann, C.O., *Magic but treatable? Tumours due to loss of merlin.* Brain, 2008. **131**(Pt 3): p. 606-15.
47. Mautner, V.F., et al., *[Ophthalmologic spectrum of neurofibromatosis type 2 in childhood].* Klin Monbl Augenheilkd, 1996. **208**(1): p. 58-62.
48. Mautner, V.F., et al., *The neuroimaging and clinical spectrum of neurofibromatosis 2.* Neurosurgery, 1996. **38**(5): p. 880-5; discussion 885-6.
49. MacCollin, M., et al., *Diagnostic criteria for schwannomatosis.* Neurology, 2005. **64**(11): p. 1838-45.

50. Hulsebos, T.J., et al., *Germline mutation of INI1/SMARCB1 in familial schwannomatosis.* Am J Hum Genet, 2007. **80**(4): p. 805-10.
51. Paganini, I., et al., *Expanding the mutational spectrum of LZTR1 in schwannomatosis.* Eur J Hum Genet, 2015. **23**(7): p. 963-8.
52. Piotrowski, A., et al., *Germline loss-of-function mutations in LZTR1 predispose to an inherited disorder of multiple schwannomas.* Nat Genet, 2014. **46**(2): p. 182-7.
53. Smith, M.J., et al., *Mutations in LZTR1 add to the complex heterogeneity of schwannomatosis.* Neurology, 2015. **84**(2): p. 141-7.
54. Evans, D.G., et al., *Spinal and cutaneous schwannomatosis is a variant form of type 2 neurofibromatosis: a clinical and molecular study.* J Neurol Neurosurg Psychiatry, 1997. **62**(4): p. 361-6.
55. MacCollin, M., et al., *Schwannomatosis: a clinical and pathologic study.* Neurology, 1996. **46**(4): p. 1072-9.
56. MacCollin, M., et al., *Familial schwannomatosis: exclusion of the NF2 locus as the germline event.* Neurology, 2003. **60**(12): p. 1968-74.
57. Blakeley, J.O. and S.R. Plotkin, *Therapeutic advances for the tumors associated with neurofibromatosis type 1, type 2, and schwannomatosis.* Neuro Oncol, 2016. **18**(5): p. 624-38.
58. Kehrer-Sawatzki, H., et al., *The molecular pathogenesis of schwannomatosis, a paradigm for the co-involvement of multiple tumour suppressor genes in tumorigenesis.* Hum Genet, 2017. **136**(2): p. 129-148.
59. Roberts, D.S., et al., *Linked-read Sequencing Analysis Reveals Tumor-specific Genome Variation Landscapes in Neurofibromatosis Type 2 (NF2) Patients.* Otol Neurotol, 2019. **40**(2): p. e150-e159.
60. Carlson, M.L., et al., *Next Generation Sequencing of Sporadic Vestibular Schwannoma: Necessity of Biallelic NF2 Inactivation and Implications of Accessory Non-NF2 Variants.* Otol Neurotol, 2018. **39**(9): p. e860-e871.
61. Pathmanaban, O.N., et al., *Association of Genetic Predisposition With Solitary Schwannoma or Meningioma in Children and Young Adults.* JAMA Neurol, 2017. **74**(9): p. 1123-1129.
62. Lin, A.L. and D.H. Gutmann, *Advances in the treatment of neurofibromatosis-associated tumours.* Nat Rev Clin Oncol, 2013. **10**(11): p. 616-24.
63. Smith, M.J., et al., *Frequency of SMARCB1 mutations in familial and sporadic schwannomatosis.* Neurogenetics, 2012. **13**(2): p. 141-5.
64. Paganini, I., et al., *Double somatic SMARCB1 and NF2 mutations in sporadic spinal schwannoma.* J Neurooncol, 2018. **137**(1): p. 33-38.
65. Agnihotri, S., et al., *The genomic landscape of schwannoma.* Nat Genet, 2016. **48**(11): p. 1339-1348.

66. Havik, A.L., et al., *Genetic landscape of sporadic vestibular schwannoma.* J Neurosurg, 2018. **128**(3): p. 911-922.
67. Gao, X., et al., *Whole Genome Sequencing Identifies Key Genes in Spinal Schwannoma.* Front Genet, 2020. **11**: p. 507816.
68. Ostrom, Q.T., et al., *CBTRUS Statistical Report: Primary Brain and Central Nervous System Tumors Diagnosed in the United States in 2008-2012.* Neuro Oncol, 2015. **17 Suppl 4**: p. iv1-iv62.
69. Gallagher, M.J., et al., *WHO grade 1 meningioma recurrence: Are location and Simpson grade still relevant?* Clin Neurol Neurosurg, 2016. **141**: p. 117-21.
70. Hansson, C.M., et al., *Comprehensive genetic and epigenetic analysis of sporadic meningioma for macro-mutations on 22q and micro-mutations within the NF2 locus.* BMC Genomics, 2007. **8**: p. 16.
71. Louis, D.N., et al., *The 2016 World Health Organization Classification of Tumors of the Central Nervous System: a summary.* Acta Neuropathol, 2016. **131**(6): p. 803-20.
72. Claus, E.B., et al., *Epidemiology of intracranial meningioma.* Neurosurgery, 2005. **57**(6): p. 1088-95; discussion 1088-95.
73. Baser, M.E., et al., *The location of constitutional neurofibromatosis 2 (NF2) splice site mutations is associated with the severity of NF2.* J Med Genet, 2005. **42**(7): p. 540-6.
74. Goutagny, S. and M. Kalamarides, *Meningiomas and neurofibromatosis.* J Neurooncol, 2010. **99**(3): p. 341-7.
75. Yuzawa, S., et al., *Clinical impact of targeted amplicon sequencing for meningioma as a practical clinical-sequencing system.* Mod Pathol, 2016. **29**(7): p. 708-16.
76. Yuzawa, S., H. Nishihara, and S. Tanaka, *Genetic landscape of meningioma.* Brain Tumor Pathol, 2016. **33**(4): p. 237-247.
77. Zotti, T., P. Vito, and R. Stilo, *The seventh ring: exploring TRAF7 functions.* J Cell Physiol, 2012. **227**(3): p. 1280-4.
78. Carpten, J.D., et al., *A transforming mutation in the pleckstrin homology domain of AKT1 in cancer.* Nature, 2007. **448**(7152): p. 439-44.
79. Bleeker, F.E., et al., *AKT1(E17K) in human solid tumours.* Oncogene, 2008. **27**(42): p. 5648-50.
80. Takahashi, K. and S. Yamanaka, *Induction of pluripotent stem cells from mouse embryonic and adult fibroblast cultures by defined factors.* Cell, 2006. **126**(4): p. 663-76.
81. Tetreault, M.P., Y. Yang, and J.P. Katz, *Kruppel-like factors in cancer.* Nat Rev Cancer, 2013. **13**(10): p. 701-13.
82. Clark, V.E., et al., *Genomic analysis of non-NF2 meningiomas reveals mutations in TRAF7, KLF4, AKT1, and SMO.* Science, 2013. **339**(6123): p. 1077-80.

83. Bujko, M., et al., *EGFR, PIK3CA, KRAS and BRAF mutations in meningiomas.* Oncol Lett, 2014. **7**(6): p. 2019-2022.
84. Abedalthagafi, M., et al., *Oncogenic PI3K mutations are as common as AKT1 and SMO mutations in meningioma.* Neuro Oncol, 2016. **18**(5): p. 649-55.
85. Karakas, B., K.E. Bachman, and B.H. Park, *Mutation of the PIK3CA oncogene in human cancers.* Br J Cancer, 2006. **94**(4): p. 455-9.
86. Aavikko, M., et al., *Loss of SUFU function in familial multiple meningioma.* Am J Hum Genet, 2012. **91**(3): p. 520-6.
87. Clark, V.E., et al., *Recurrent somatic mutations in POLR2A define a distinct subset of meningiomas.* Nat Genet, 2016. **48**(10): p. 1253-9.
88. Suppiah, S., et al., *Molecular and translational advances in meningiomas.* Neuro Oncol, 2019. **21**(Suppl 1): p. i4-i17.
89. Karsy, M., et al., *Clinical potential of meningioma genomic insights: a practical review for neurosurgeons.* Neurosurg Focus, 2018. **44**(6): p. E10.
90. Pawloski, J.A., et al., *Genomic Biomarkers of Meningioma: A Focused Review.* Int J Mol Sci, 2021. **22**(19).
91. Gilbert, M.R., R. Ruda, and R. Soffietti, *Ependymomas in adults.* Curr Neurol Neurosci Rep, 2010. **10**(3): p. 240-7.
92. Rodriguez, D., et al., *Outcomes of malignant CNS ependymomas: an examination of 2408 cases through the Surveillance, Epidemiology, and End Results (SEER) database (1973-2005).* J Surg Res, 2009. **156**(2): p. 340-51.
93. Oppenheim, J.S., et al., *Ependymomas of the third ventricle.* Neurosurgery, 1994. **34**(2): p. 350-2; discussion 352-3.
94. Reni, M., et al., *Ependymoma.* Crit Rev Oncol Hematol, 2007. **63**(1): p. 81-9.
95. McGuire, C.S., K.L. Sainani, and P.G. Fisher, *Incidence patterns for ependymoma: a surveillance, epidemiology, and end results study.* J Neurosurg, 2009. **110**(4): p. 725-9.
96. Korshunov, A., et al., *The histologic grade is a main prognostic factor for patients with intracranial ependymomas treated in the microneurosurgical era: an analysis of 258 patients.* Cancer, 2004. **100**(6): p. 1230-7.
97. Reni, M. and A.A. Brandes, *Current management and prognostic factors for adult ependymoma.* Expert Rev Anticancer Ther, 2002. **2**(5): p. 537-45.
98. Guyotat, J., et al., *Intracranial ependymomas in adult patients: analyses of prognostic factors.* J Neurooncol, 2002. **60**(3): p. 255-68.
99. Nagasawa, D.T., et al., *Complications associated with the treatment for spinal ependymomas.* Neurosurg Focus, 2011. **31**(4): p. E13.
100. Rajaram, V., et al., *Alterations of protein 4.1 family members in ependymomas: a study of 84 cases.* Mod Pathol, 2005. **18**(7): p. 991-7.

101. Lamszus, K., et al., *Molecular genetic alterations on chromosomes 11 and 22 in ependymomas.* Int J Cancer, 2001. **91**(6): p. 803-8.
102. Guyotat, J., et al., *Infratentorial ependymomas: prognostic factors and outcome analysis in a multi-center retrospective series of 106 adult patients.* Acta Neurochir (Wien), 2009. **151**(8): p. 947-60.
103. Godfraind, C., *Classification and controversies in pathology of ependymomas.* Childs Nerv Syst, 2009. **25**(10): p. 1185-93.
104. Gusella, J.F., et al., *Merlin: the neurofibromatosis 2 tumor suppressor.* Biochim Biophys Acta, 1999. **1423**(2): p. M29-36.
105. Seizinger, B.R., R.L. Martuza, and J.F. Gusella, *Loss of genes on chromosome 22 in tumorigenesis of human acoustic neuroma.* Nature, 1986. **322**(6080): p. 644-7.
106. Ahronowitz, I., et al., *Mutational spectrum of the NF2 gene: a meta-analysis of 12 years of research and diagnostic laboratory findings.* Hum Mutat, 2007. **28**(1): p. 1-12.
107. Chang, L.S., et al., *Multiple transcription initiation sites, alternative splicing, and differential polyadenylation contribute to the complexity of human neurofibromatosis 2 transcripts.* Genomics, 2002. **79**(1): p. 63-76.
108. *The Human Gene Mutation Database*. 2020; Available from: http://www.hgmd.cf.ac.uk/ac/gene.php?gene=NF2.
109. Evans, D.G., et al., *A genetic study of type 2 neurofibromatosis in the United Kingdom. I. Prevalence, mutation rate, fitness, and confirmation of maternal transmission effect on severity.* J Med Genet, 1992. **29**(12): p. 841-6.
110. Jacoby, L.B., et al., *Frequency and distribution of NF2 mutations in schwannomas.* Genes Chromosomes Cancer, 1996. **17**(1): p. 45-55.
111. Irving, R.M., et al., *Somatic neurofibromatosis type 2 gene mutations and growth characteristics in vestibular schwannoma.* Am J Otol, 1997. **18**(6): p. 754-60.
112. Evans, D.G., et al., *Genotype/phenotype correlations in type 2 neurofibromatosis (NF2): evidence for more severe disease associated with truncating mutations.* J Med Genet, 1998. **35**(6): p. 450-5.
113. Ruttledge, M.H., et al., *Type of mutation in the neurofibromatosis type 2 gene (NF2) frequently determines severity of disease.* Am J Hum Genet, 1996. **59**(2): p. 331-42.
114. Trofatter, J.A., et al., *A novel moesin-, ezrin-, radixin-like gene is a candidate for the neurofibromatosis 2 tumor suppressor.* Cell, 1993. **72**(5): p. 791-800.
115. Kang, B.S., et al., *The structure of the FERM domain of merlin, the neurofibromatosis type 2 gene product.* Acta Crystallogr D Biol Crystallogr, 2002. **58**(Pt 3): p. 381-91.
116. Xu, H.M. and D.H. Gutmann, *Merlin differentially associates with the microtubule and actin cytoskeleton.* J Neurosci Res, 1998. **51**(3): p. 403-15.

117. Kissil, J.L., et al., *Merlin phosphorylation by p21-activated kinase 2 and effects of phosphorylation on merlin localization.* J Biol Chem, 2002. **277**(12): p. 10394-9.
118. Alfthan, K., et al., *Cyclic AMP-dependent protein kinase phosphorylates merlin at serine 518 independently of p21-activated kinase and promotes merlin-ezrin heterodimerization.* J Biol Chem, 2004. **279**(18): p. 18559-66.
119. Xiao, G.H., et al., *p21-activated kinase links Rac/Cdc42 signaling to merlin.* J Biol Chem, 2002. **277**(2): p. 883-6.
120. Shaw, R.J., et al., *The Nf2 tumor suppressor, merlin, functions in Rac-dependent signaling.* Dev Cell, 2001. **1**(1): p. 63-72.
121. Rong, R., et al., *Serine 518 phosphorylation modulates merlin intramolecular association and binding to critical effectors important for NF2 growth suppression.* Oncogene, 2004. **23**(52): p. 8447-54.
122. Kissil, J.L., et al., *Merlin, the product of the Nf2 tumor suppressor gene, is an inhibitor of the p21-activated kinase, Pak1.* Mol Cell, 2003. **12**(4): p. 841-9.
123. Jin, H., et al., *Tumorigenic transformation by CPI-17 through inhibition of a merlin phosphatase.* Nature, 2006. **442**(7102): p. 576-9.
124. Yin, F., et al., *Spatial organization of Hippo signaling at the plasma membrane mediated by the tumor suppressor Merlin/NF2.* Cell, 2013. **154**(6): p. 1342-55.
125. Chinthalapudi, K., et al., *Lipid binding promotes the open conformation and tumor-suppressive activity of neurofibromin 2.* Nat Commun, 2018. **9**(1): p. 1338.
126. Li, Y., et al., *Angiomotin binding-induced activation of Merlin/NF2 in the Hippo pathway.* Cell Res, 2015. **25**(7): p. 801-17.
127. Guo, L., et al., *Rac1 controls Schwann cell myelination through cAMP and NF2/merlin.* J Neurosci, 2012. **32**(48): p. 17251-61.
128. Sobue, G., S. Shuman, and D. Pleasure, *Schwann cell responses to cyclic AMP: proliferation, change in shape, and appearance of surface galactocerebroside.* Brain Res, 1986. **362**(1): p. 23-32.
129. Yoon, C., Z. Korade, and B.D. Carter, *Protein kinase A-induced phosphorylation of the p65 subunit of nuclear factor-kappaB promotes Schwann cell differentiation into a myelinating phenotype.* J Neurosci, 2008. **28**(14): p. 3738-46.
130. Kim, H.A., J.E. DeClue, and N. Ratner, *cAMP-dependent protein kinase A is required for Schwann cell growth: interactions between the cAMP and neuregulin/tyrosine kinase pathways.* J Neurosci Res, 1997. **49**(2): p. 236-47.
131. Howe, D.G. and K.D. McCarthy, *Retroviral inhibition of cAMP-dependent protein kinase inhibits myelination but not Schwann cell mitosis stimulated by interaction with neurons.* J Neurosci, 2000. **20**(10): p. 3513-21.

132. Morrison, H., et al., *The NF2 tumor suppressor gene product, merlin, mediates contact inhibition of growth through interactions with CD44.* Genes Dev, 2001. **15**(8): p. 968-80.
133. Ponta, H., L. Sherman, and P.A. Herrlich, *CD44: from adhesion molecules to signalling regulators.* Nat Rev Mol Cell Biol, 2003. **4**(1): p. 33-45.
134. Carroll, S.L., *Molecular mechanisms promoting the pathogenesis of Schwann cell neoplasms.* Acta Neuropathol, 2012. **123**(3): p. 321-48.
135. Stamenkovic, I. and Q. Yu, *Merlin, a "magic" linker between extracellular cues and intracellular signaling pathways that regulate cell motility, proliferation, and survival.* Curr Protein Pept Sci, 2010. **11**(6): p. 471-84.
136. Fraenzer, J.T., et al., *Overexpression of the NF2 gene inhibits schwannoma cell proliferation through promoting PDGFR degradation.* Int J Oncol, 2003. **23**(6): p. 1493-500.
137. Lallemand, D., et al., *Merlin regulates transmembrane receptor accumulation and signaling at the plasma membrane in primary mouse Schwann cells and in human schwannomas.* Oncogene, 2009. **28**(6): p. 854-65.
138. Ahmad, Z., et al., *Merlin knockdown in human Schwann cells: clues to vestibular schwannoma tumorigenesis.* Otol Neurotol, 2010. **31**(3): p. 460-6.
139. Ammoun, S., et al., *ErbB/HER receptor activation and preclinical efficacy of lapatinib in vestibular schwannoma.* Neuro Oncol, 2010. **12**(8): p. 834-43.
140. Ammoun, S., et al., *The role of insulin-like growth factors signaling in merlin-deficient human schwannomas.* Glia, 2012. **60**(11): p. 1721-33.
141. Okada, T., M. Lopez-Lago, and F.G. Giancotti, *Merlin/NF-2 mediates contact inhibition of growth by suppressing recruitment of Rac to the plasma membrane.* J Cell Biol, 2005. **171**(2): p. 361-71.
142. Yi, C., et al., *A tight junction-associated Merlin-angiomotin complex mediates Merlin's regulation of mitogenic signaling and tumor suppressive functions.* Cancer Cell, 2011. **19**(4): p. 527-40.
143. Beeser, A., et al., *Role of group A p21-activated kinases in activation of extracellular-regulated kinase by growth factors.* J Biol Chem, 2005. **280**(44): p. 36609-15.
144. Kaempchen, K., et al., *Upregulation of the Rac1/JNK signaling pathway in primary human schwannoma cells.* Hum Mol Genet, 2003. **12**(11): p. 1211-21.
145. Clark, E.A. and R.O. Hynes, *Ras activation is necessary for integrin-mediated activation of extracellular signal-regulated kinase 2 and cytosolic phospholipase A2 but not for cytoskeletal organization.* J Biol Chem, 1996. **271**(25): p. 14814-8.
146. Mainiero, F., et al., *The coupling of alpha6beta4 integrin to Ras-MAP kinase pathways mediated by Shc controls keratinocyte proliferation.* EMBO J, 1997. **16**(9): p. 2365-75.
147. Stewart, H.J., et al., *Expression and regulation of alpha1beta1 integrin in Schwann cells.* J Neurobiol, 1997. **33**(7): p. 914-28.

148. Flaiz, C., et al., *Altered adhesive structures and their relation to RhoGTPase activation in merlin-deficient Schwannoma.* Brain Pathol, 2009. **19**(1): p. 27-38.
149. Fernandez-Valle, C., et al., *Paxillin binds schwannomin and regulates its density-dependent localization and effect on cell morphology.* Nat Genet, 2002. **31**(4): p. 354-62.
150. James, M.F., et al., *A NHERF binding site links the betaPDGFR to the cytoskeleton and regulates cell spreading and migration.* J Cell Sci, 2004. **117**(Pt 14): p. 2951-61.
151. Ammoun, S., et al., *Dissecting and targeting the growth factor-dependent and growth factor-independent extracellular signal-regulated kinase pathway in human schwannoma.* Cancer Res, 2008. **68**(13): p. 5236-45.
152. Morrison, H., et al., *Merlin/neurofibromatosis type 2 suppresses growth by inhibiting the activation of Ras and Rac.* Cancer Res, 2007. **67**(2): p. 520-7.
153. Hassan, B., et al., *Targeting the PI3-kinase/Akt/mTOR signaling pathway.* Surg Oncol Clin N Am, 2013. **22**(4): p. 641-64.
154. Lopez-Lago, M.A., et al., *Loss of the tumor suppressor gene NF2, encoding merlin, constitutively activates integrin-dependent mTORC1 signaling.* Mol Cell Biol, 2009. **29**(15): p. 4235-49.
155. Rong, R., et al., *Neurofibromatosis 2 (NF2) tumor suppressor merlin inhibits phosphatidylinositol 3-kinase through binding to PIKE-L.* Proc Natl Acad Sci U S A, 2004. **101**(52): p. 18200-5.
156. James, M.F., et al., *NF2/merlin is a novel negative regulator of mTOR complex 1, and activation of mTORC1 is associated with meningioma and schwannoma growth.* Mol Cell Biol, 2009. **29**(15): p. 4250-61.
157. Kim, S. and E.H. Jho, *Merlin, a regulator of Hippo signaling, regulates Wnt/beta-catenin signaling.* BMB Rep, 2016. **49**(7): p. 357-8.
158. Zhou, L., et al., *Merlin-deficient human tumors show loss of contact inhibition and activation of Wnt/beta-catenin signaling linked to the PDGFR/Src and Rac/PAK pathways.* Neoplasia, 2011. **13**(12): p. 1101-12.
159. Saucedo, L.J. and B.A. Edgar, *Filling out the Hippo pathway.* Nat Rev Mol Cell Biol, 2007. **8**(8): p. 613-21.
160. Cooper, J., et al., *Merlin/NF2 functions upstream of the nuclear E3 ubiquitin ligase CRL4DCAF1 to suppress oncogenic gene expression.* Sci Signal, 2011. **4**(188): p. pt6.
161. Li, W., et al., *Merlin/NF2 loss-driven tumorigenesis linked to CRL4(DCAF1)-mediated inhibition of the hippo pathway kinases Lats1 and 2 in the nucleus.* Cancer Cell, 2014. **26**(1): p. 48-60.
162. Zhao, B., et al., *TEAD mediates YAP-dependent gene induction and growth control.* Genes Dev, 2008. **22**(14): p. 1962-71.

163. Li, W., et al., *Merlin/NF2 suppresses tumorigenesis by inhibiting the E3 ubiquitin ligase CRL4(DCAF1) in the nucleus.* Cell, 2010. **140**(4): p. 477-90.
164. Muranen, T., et al., *Cell cycle-dependent nucleocytoplasmic shuttling of the neurofibromatosis 2 tumour suppressor merlin.* Oncogene, 2005. **24**(7): p. 1150-8.
165. Zhou, L. and C.O. Hanemann, *Merlin, a multi-suppressor from cell membrane to the nucleus.* FEBS Lett, 2012. **586**(10): p. 1403-8.
166. Nurse, P., Y. Masui, and L. Hartwell, *Understanding the cell cycle.* Nat Med, 1998. **4**(10): p. 1103-6.
167. Planas-Silva, M.D. and R.A. Weinberg, *The restriction point and control of cell proliferation.* Curr Opin Cell Biol, 1997. **9**(6): p. 768-72.
168. Murray, A.W., *Recycling the cell cycle: cyclins revisited.* Cell, 2004. **116**(2): p. 221-34.
169. Bartek, J., C. Lukas, and J. Lukas, *Checking on DNA damage in S phase.* Nat Rev Mol Cell Biol, 2004. **5**(10): p. 792-804.
170. Musacchio, A. and E.D. Salmon, *The spindle-assembly checkpoint in space and time.* Nat Rev Mol Cell Biol, 2007. **8**(5): p. 379-93.
171. Malumbres, M. and M. Barbacid, *Cell cycle, CDKs and cancer: a changing paradigm.* Nat Rev Cancer, 2009. **9**(3): p. 153-66.
172. Sherr, C.J. and J.M. Roberts, *Living with or without cyclins and cyclin-dependent kinases.* Genes Dev, 2004. **18**(22): p. 2699-711.
173. Beroukhim, R., et al., *The landscape of somatic copy-number alteration across human cancers.* Nature, 2010. **463**(7283): p. 899-905.
174. Corcoran, M.M., et al., *Dysregulation of cyclin dependent kinase 6 expression in splenic marginal zone lymphoma through chromosome 7q translocations.* Oncogene, 1999. **18**(46): p. 6271-7.
175. Schmidt, E.E., et al., *CDKN2 (p16/MTS1) gene deletion or CDK4 amplification occurs in the majority of glioblastomas.* Cancer Res, 1994. **54**(24): p. 6321-4.
176. Wolfel, T., et al., *A p16INK4a-insensitive CDK4 mutant targeted by cytolytic T lymphocytes in a human melanoma.* Science, 1995. **269**(5228): p. 1281-4.
177. Ma, T., et al., *Cell cycle-regulated phosphorylation of p220(NPAT) by cyclin E/Cdk2 in Cajal bodies promotes histone gene transcription.* Genes Dev, 2000. **14**(18): p. 2298-313.
178. Okuda, M., et al., *Nucleophosmin/B23 is a target of CDK2/cyclin E in centrosome duplication.* Cell, 2000. **103**(1): p. 127-40.
179. Strohmaier, H., et al., *Human F-box protein hCdc4 targets cyclin E for proteolysis and is mutated in a breast cancer cell line.* Nature, 2001. **413**(6853): p. 316-22.
180. Koepp, D.M., et al., *Phosphorylation-dependent ubiquitination of cyclin E by the SCFFbw7 ubiquitin ligase.* Science, 2001. **294**(5540): p. 173-7.

181. Otto, T. and P. Sicinski, *Cell cycle proteins as promising targets in cancer therapy.* Nat Rev Cancer, 2017. **17**(2): p. 93-115.
182. Scaltriti, M., et al., *Cyclin E amplification/overexpression is a mechanism of trastuzumab resistance in HER2+ breast cancer patients.* Proc Natl Acad Sci U S A, 2011. **108**(9): p. 3761-6.
183. Etemadmoghadam, D., et al., *Synthetic lethality between CCNE1 amplification and loss of BRCA1.* Proc Natl Acad Sci U S A, 2013. **110**(48): p. 19489-94.
184. Spruck, C.H., et al., *hCDC4 gene mutations in endometrial cancer.* Cancer Res, 2002. **62**(16): p. 4535-9.
185. Kemp, Z., et al., *CDC4 mutations occur in a subset of colorectal cancers but are not predicted to cause loss of function and are not associated with chromosomal instability.* Cancer Res, 2005. **65**(24): p. 11361-6.
186. Akli, S., et al., *Cdk2 is required for breast cancer mediated by the low-molecular-weight isoform of cyclin E.* Cancer Res, 2011. **71**(9): p. 3377-86.
187. Chao, Y., et al., *Overexpression of cyclin A but not Skp 2 correlates with the tumor relapse of human hepatocellular carcinoma.* Cancer Res, 1998. **58**(5): p. 985-90.
188. Handa, K., et al., *Expression of cell cycle markers in colorectal carcinoma: superiority of cyclin A as an indicator of poor prognosis.* Int J Cancer, 1999. **84**(3): p. 225-33.
189. Michalides, R., et al., *Cyclin A is a prognostic indicator in early stage breast cancer with and without tamoxifen treatment.* Br J Cancer, 2002. **86**(3): p. 402-8.
190. Campaner, S., et al., *Cdk2 suppresses cellular senescence induced by the c-myc oncogene.* Nat Cell Biol, 2010. **12**(1): p. 54-9; sup pp 1-14.
191. Hydbring, P., et al., *Phosphorylation by Cdk2 is required for Myc to repress Ras-induced senescence in cotransformation.* Proc Natl Acad Sci U S A, 2010. **107**(1): p. 58-63.
192. Du, J., et al., *Critical role of CDK2 for melanoma growth linked to its melanocyte-specific transcriptional regulation by MITF.* Cancer Cell, 2004. **6**(6): p. 565-76.
193. Santamaria, D., et al., *Cdk1 is sufficient to drive the mammalian cell cycle.* Nature, 2007. **448**(7155): p. 811-5.
194. Gavet, O. and J. Pines, *Progressive activation of CyclinB1-Cdk1 coordinates entry to mitosis.* Dev Cell, 2010. **18**(4): p. 533-43.
195. Krek, W. and E.A. Nigg, *Mutations of p34cdc2 phosphorylation sites induce premature mitotic events in HeLa cells: evidence for a double block to p34cdc2 kinase activation in vertebrates.* EMBO J, 1991. **10**(11): p. 3331-41.
196. Ravindran Menon, D., et al., *CDK1 Interacts with Sox2 and Promotes Tumor Initiation in Human Melanoma.* Cancer Res, 2018. **78**(23): p. 6561-6574.
197. Liu, Y., et al., *Pleiotropic Effects of PPARD Accelerate Colorectal Tumorigenesis, Progression, and Invasion.* Cancer Res, 2019. **79**(5): p. 954-969.

198. Wu, C.X., et al., *Blocking CDK1/PDK1/beta-Catenin signaling by CDK1 inhibitor RO3306 increased the efficacy of sorafenib treatment by targeting cancer stem cells in a preclinical model of hepatocellular carcinoma.* Theranostics, 2018. **8**(14): p. 3737-3750.
199. Kuang, Y., et al., *Iron-dependent CDK1 activity promotes lung carcinogenesis via activation of the GP130/STAT3 signaling pathway.* Cell Death Dis, 2019. **10**(4): p. 297.
200. Sarafan-Vasseur, N., et al., *Overexpression of B-type cyclins alters chromosomal segregation.* Oncogene, 2002. **21**(13): p. 2051-7.
201. Yin, X.Y., et al., *Inverse regulation of cyclin B1 by c-Myc and p53 and induction of tetraploidy by cyclin B1 overexpression.* Cancer Res, 2001. **61**(17): p. 6487-93.
202. Jin, P., S. Hardy, and D.O. Morgan, *Nuclear localization of cyclin B1 controls mitotic entry after DNA damage.* J Cell Biol, 1998. **141**(4): p. 875-85.
203. Park, M., et al., *Constitutive activation of cyclin B1-associated cdc2 kinase overrides p53-mediated G2-M arrest.* Cancer Res, 2000. **60**(3): p. 542-5.
204. Santana, C., E. Ortega, and A. Garcia-Carranca, *Oncogenic H-ras induces cyclin B1 expression in a p53-independent manner.* Mutat Res, 2002. **508**(1-2): p. 49-58.
205. Takeno, S., et al., *Prognostic value of cyclin B1 in patients with esophageal squamous cell carcinoma.* Cancer, 2002. **94**(11): p. 2874-81.
206. Hassan, K.A., et al., *Cyclin B1 overexpression and resistance to radiotherapy in head and neck squamous cell carcinoma.* Cancer Res, 2002. **62**(22): p. 6414-7.
207. Li, J.Q., et al., *Cyclin B1, unlike cyclin G1, increases significantly during colorectal carcinogenesis and during later metastasis to lymph nodes.* Int J Oncol, 2003. **22**(5): p. 1101-10.
208. Hunter, E., *Retroviruses*, in *Encylopedia of Virology*, M.H.V.v.R. Brian W.J., Editor. 2008, Academic Press. p. 459-467.
209. Ryu, W.-S., *Retroviruses*, in *Molecular Virology of Human Pathogenic Viruses*. 2017, Academic Press. p. 227-246.
210. Varmus, H., *Retroviruses.* Science, 1988. **240**(4858): p. 1427-35.
211. Hallenberger, S., et al., *Inhibition of furin-mediated cleavage activation of HIV-1 glycoprotein gp160.* Nature, 1992. **360**(6402): p. 358-61.
212. Checkley, M.A., B.G. Luttge, and E.O. Freed, *HIV-1 envelope glycoprotein biosynthesis, trafficking, and incorporation.* J Mol Biol, 2011. **410**(4): p. 582-608.
213. Fenner, F., *Retroviridae*, in *Fenner's Veterinary Virology*, E.J.D. N. James Maclachlan, Editor. 2017, Academic Press. p. 269-297.
214. Johnson, W.E., *Origins and evolutionary consequences of ancient endogenous retroviruses.* Nat Rev Microbiol, 2019. **17**(6): p. 355-370.
215. Temin, H.M., *Separation of morphological conversion and virus production in Rous sarcoma virus infection.* Cold Spring Harb Symp Quant Biol, 1962. **27**: p. 407-14.

216. Temin, H.M. and S. Mizutani, *RNA-dependent DNA polymerase in virions of Rous sarcoma virus.* Nature, 1970. **226**(5252): p. 1211-3.
217. Baltimore, D., *RNA-dependent DNA polymerase in virions of RNA tumour viruses.* Nature, 1970. **226**(5252): p. 1209-11.
218. Weiss, R.A., *The discovery of endogenous retroviruses.* Retrovirology, 2006. **3**: p. 67.
219. Callahan, R., et al., *Detection and cloning of human DNA sequences related to the mouse mammary tumor virus genome.* Proc Natl Acad Sci U S A, 1982. **79**(18): p. 5503-7.
220. Ono, M., *Molecular cloning and long terminal repeat sequences of human endogenous retrovirus genes related to types A and B retrovirus genes.* J Virol, 1986. **58**(3): p. 937-44.
221. Martin, M.A., et al., *Identification and cloning of endogenous retroviral sequences present in human DNA.* Proc Natl Acad Sci U S A, 1981. **78**(8): p. 4892-6.
222. Horn, T.M., et al., *Chromosomal locations of members of a family of novel endogenous human retroviral genomes.* J Virol, 1986. **58**(3): p. 955-9.
223. Nelson, P.N., et al., *Demystified. Human endogenous retroviruses.* Mol Pathol, 2003. **56**(1): p. 11-8.
224. Tristem, M., *Identification and characterization of novel human endogenous retrovirus families by phylogenetic screening of the human genome mapping project database.* J Virol, 2000. **74**(8): p. 3715-30.
225. Jern, P., G.O. Sperber, and J. Blomberg, *Use of endogenous retroviral sequences (ERVs) and structural markers for retroviral phylogenetic inference and taxonomy.* Retrovirology, 2005. **2**: p. 50.
226. Boller, K., et al., *Evidence that HERV-K is the endogenous retrovirus sequence that codes for the human teratocarcinoma-derived retrovirus HTDV.* Virology, 1993. **196**(1): p. 349-53.
227. Lower, R., et al., *Identification of human endogenous retroviruses with complex mRNA expression and particle formation.* Proc Natl Acad Sci U S A, 1993. **90**(10): p. 4480-4.
228. Boller, K., et al., *Structural organization of unique retrovirus-like particles budding from human teratocarcinoma cell lines.* J Gen Virol, 1983. **64 (Pt 12)**: p. 2549-59.
229. Lower, R., et al., *Human teratocarcinomas cultured in vitro produce unique retrovirus-like viruses.* J Gen Virol, 1984. **65 (Pt 5)**: p. 887-98.
230. Bieda, K., A. Hoffmann, and K. Boller, *Phenotypic heterogeneity of human endogenous retrovirus particles produced by teratocarcinoma cell lines.* J Gen Virol, 2001. **82**(Pt 3): p. 591-596.
231. Muster, T., et al., *An endogenous retrovirus derived from human melanoma cells.* Cancer Res, 2003. **63**(24): p. 8735-41.
232. Boller, K., et al., *Human endogenous retrovirus HERV-K113 is capable of producing intact viral particles.* J Gen Virol, 2008. **89**(Pt 2): p. 567-572.

233. Gifford, R. and M. Tristem, *The evolution, distribution and diversity of endogenous retroviruses.* Virus Genes, 2003. **26**(3): p. 291-315.
234. Barbulescu, M., et al., *Many human endogenous retrovirus K (HERV-K) proviruses are unique to humans.* Curr Biol, 1999. **9**(16): p. 861-8.
235. Turner, G., et al., *Insertional polymorphisms of full-length endogenous retroviruses in humans.* Curr Biol, 2001. **11**(19): p. 1531-5.
236. Ruda, V.M., et al., *Tissue specificity of enhancer and promoter activities of a HERV-K(HML-2) LTR.* Virus Res, 2004. **104**(1): p. 11-6.
237. Yi, J.M., H.M. Kim, and H.S. Kim, *Molecular cloning and phylogenetic analysis of the human endogenous retrovirus HERV-K long terminal repeat elements in various cancer cells.* Mol Cells, 2001. **12**(1): p. 137-41.
238. Ehlhardt, S., et al., *Human endogenous retrovirus HERV-K(HML-2) Rec expression and transcriptional activities in normal and rheumatoid arthritis synovia.* J Rheumatol, 2006. **33**(1): p. 16-23.
239. Fuchs, N.V., et al., *Human endogenous retrovirus K (HML-2) RNA and protein expression is a marker for human embryonic and induced pluripotent stem cells.* Retrovirology, 2013. **10**: p. 115.
240. Buscher, K., et al., *Expression of the human endogenous retrovirus-K transmembrane envelope, Rec and Np9 proteins in melanomas and melanoma cell lines.* Melanoma Res, 2006. **16**(3): p. 223-34.
241. Buscher, K., et al., *Expression of human endogenous retrovirus K in melanomas and melanoma cell lines.* Cancer Res, 2005. **65**(10): p. 4172-80.
242. Contreras-Galindo, R., et al., *Human endogenous retrovirus K (HML-2) elements in the plasma of people with lymphoma and breast cancer.* J Virol, 2008. **82**(19): p. 9329-36.
243. Sauter, M., et al., *Human endogenous retrovirus K10: expression of Gag protein and detection of antibodies in patients with seminomas.* J Virol, 1995. **69**(1): p. 414-21.
244. Wang-Johanning, F., et al., *Human endogenous retrovirus K triggers an antigen-specific immune response in breast cancer patients.* Cancer Res, 2008. **68**(14): p. 5869-77.
245. Subramanian, R.P., et al., *Identification, characterization, and comparative genomic distribution of the HERV-K (HML-2) group of human endogenous retroviruses.* Retrovirology, 2011. **8**: p. 90.
246. Wildschutte, J.H., et al., *Discovery of unfixed endogenous retrovirus insertions in diverse human populations.* Proc Natl Acad Sci U S A, 2016. **113**(16): p. E2326-34.
247. Marchi, E., et al., *Unfixed endogenous retroviral insertions in the human population.* J Virol, 2014. **88**(17): p. 9529-37.
248. Xue, B., et al., *Identification of the distribution of human endogenous retroviruses K (HML-2) by PCR-based target enrichment sequencing.* Retrovirology, 2020. **17**(1): p. 10.

249. Hohn, O., K. Hanke, and N. Bannert, *HERV-K(HML-2), the Best Preserved Family of HERVs: Endogenization, Expression, and Implications in Health and Disease.* Front Oncol, 2013. **3**: p. 246.

250. Kovalskaya, E., et al., *Functional human endogenous retroviral LTR transcription start sites are located between the R and U5 regions.* Virology, 2006. **346**(2): p. 373-8.

251. Lower, R., et al., *Identification of a Rev-related protein by analysis of spliced transcripts of the human endogenous retroviruses HTDV/HERV-K.* J Virol, 1995. **69**(1): p. 141-9.

252. Armbruester, V., et al., *A novel gene from the human endogenous retrovirus K expressed in transformed cells.* Clin Cancer Res, 2002. **8**(6): p. 1800-7.

253. Garcia-Montojo, M., et al., *Human endogenous retrovirus-K (HML-2): a comprehensive review.* Crit Rev Microbiol, 2018. **44**(6): p. 715-738.

254. Flockerzi, A., et al., *Expression patterns of transcribed human endogenous retrovirus HERV-K(HML-2) loci in human tissues and the need for a HERV Transcriptome Project.* BMC Genomics, 2008. **9**: p. 354.

255. Reus, K., et al., *HERV-K(OLD): ancestor sequences of the human endogenous retrovirus family HERV-K(HML-2).* J Virol, 2001. **75**(19): p. 8917-26.

256. Hughes, J.F. and J.M. Coffin, *Evidence for genomic rearrangements mediated by human endogenous retroviruses during primate evolution.* Nat Genet, 2001. **29**(4): p. 487-9.

257. Ono, M., M. Kawakami, and H. Ushikubo, *Stimulation of expression of the human endogenous retrovirus genome by female steroid hormones in human breast cancer cell line T47D.* J Virol, 1987. **61**(6): p. 2059-62.

258. Macfarlane, C. and P. Simmonds, *Allelic variation of HERV-K(HML-2) endogenous retroviral elements in human populations.* J Mol Evol, 2004. **59**(5): p. 642-56.

259. Costas, J., *Evolutionary dynamics of the human endogenous retrovirus family HERV-K inferred from full-length proviral genomes.* J Mol Evol, 2001. **53**(3): p. 237-43.

260. Belshaw, R., et al., *Genomewide screening reveals high levels of insertional polymorphism in the human endogenous retrovirus family HERV-K(HML2): implications for present-day activity.* J Virol, 2005. **79**(19): p. 12507-14.

261. Tonjes, R.R., F. Czauderna, and R. Kurth, *Genome-wide screening, cloning, chromosomal assignment, and expression of full-length human endogenous retrovirus type K.* J Virol, 1999. **73**(11): p. 9187-95.

262. George, M., et al., *Identification of the protease cleavage sites in a reconstituted Gag polyprotein of an HERV-K(HML-2) element.* Retrovirology, 2011. **8**: p. 30.

263. Schommer, S., et al., *Characterization of the human endogenous retrovirus K proteinase.* J Gen Virol, 1996. **77 (Pt 2)**: p. 375-9.

264. Ono, M., et al., *Nucleotide sequence of human endogenous retrovirus genome related to the mouse mammary tumor virus genome.* J Virol, 1986. **60**(2): p. 589-98.

265. Berkhout, B., M. Jebbink, and J. Zsiros, *Identification of an active reverse transcriptase enzyme encoded by a human endogenous HERV-K retrovirus.* J Virol, 1999. **73**(3): p. 2365-75.

266. Kitamura, Y., et al., *Human endogenous retrovirus K10 encodes a functional integrase.* J Virol, 1996. **70**(5): p. 3302-6.

267. Ruggieri, A., et al., *Human endogenous retrovirus HERV-K(HML-2) encodes a stable signal peptide with biological properties distinct from Rec.* Retrovirology, 2009. **6**: p. 17.

268. Kammerer, U., et al., *Human endogenous retrovirus K (HERV-K) is expressed in villous and extravillous cytotrophoblast cells of the human placenta.* J Reprod Immunol, 2011. **91**(1-2): p. 1-8.

269. Wodrich, H. and H.G. Krausslich, *Nucleocytoplasmic RNA transport in retroviral replication.* Results Probl Cell Differ, 2001. **34**: p. 197-217.

270. Buzdin, A., et al., *At least 50% of human-specific HERV-K (HML-2) long terminal repeats serve in vivo as active promoters for host nonrepetitive DNA transcription.* J Virol, 2006. **80**(21): p. 10752-62.

271. Fuchs, N.V., et al., *Expression of the human endogenous retrovirus (HERV) group HML-2/HERV-K does not depend on canonical promoter elements but is regulated by transcription factors Sp1 and Sp3.* J Virol, 2011. **85**(7): p. 3436-48.

272. Katoh, I., et al., *Activation of the long terminal repeat of human endogenous retrovirus K by melanoma-specific transcription factor MITF-M.* Neoplasia, 2011. **13**(11): p. 1081-92.

273. Tomlins, S.A., et al., *Distinct classes of chromosomal rearrangements create oncogenic ETS gene fusions in prostate cancer.* Nature, 2007. **448**(7153): p. 595-9.

274. Guasch, G., et al., *Endogenous retroviral sequence is fused to FGFR1 kinase in the 8p12 stem-cell myeloproliferative disorder with t(8;19)(p12;q13.3).* Blood, 2003. **101**(1): p. 286-8.

275. Grow, E.J., et al., *Intrinsic retroviral reactivation in human preimplantation embryos and pluripotent cells.* Nature, 2015. **522**(7555): p. 221-5.

276. Gonzalez-Hernandez, M.J., et al., *Expression of human endogenous retrovirus type K (HML-2) is activated by the Tat protein of HIV-1.* J Virol, 2012. **86**(15): p. 7790-805.

277. Knossl, M., R. Lower, and J. Lower, *Expression of the human endogenous retrovirus HTDV/HERV-K is enhanced by cellular transcription factor YY1.* J Virol, 1999. **73**(2): p. 1254-61.

278. Wang, Y.J. and M. Herlyn, *The emerging roles of Oct4 in tumor-initiating cells.* Am J Physiol Cell Physiol, 2015. **309**(11): p. C709-18.

279. Xia, L., et al., *Role of the NFkappaB-signaling pathway in cancer.* Onco Targets Ther, 2018. **11**: p. 2063-2073.

280. Qin, J.J., et al., *NFAT as cancer target: mission possible?* Biochim Biophys Acta, 2014. **1846**(2): p. 297-311.

281. Urban, P., et al., *[The Importance of MITF Signaling Pathway in the Regulation of Proliferation and Invasiveness of Malignant Melanoma].* Klin Onkol. **29**(5): p. 347-350.
282. Hedrick, E., et al., *Specificity protein (Sp) transcription factors Sp1, Sp3 and Sp4 are non-oncogene addiction genes in cancer cells.* Oncotarget, 2016. **7**(16): p. 22245-56.
283. Sarvagalla, S., S.P. Kolapalli, and S. Vallabhapurapu, *The Two Sides of YY1 in Cancer: A Friend and a Foe.* Front Oncol, 2019. **9**: p. 1230.
284. Morozov, V.A., V.L. Dao Thi, and J. Denner, *The transmembrane protein of the human endogenous retrovirus--K (HERV-K) modulates cytokine release and gene expression.* PLoS One, 2013. **8**(8): p. e70399.
285. Moore, K.W., et al., *Interleukin-10 and the interleukin-10 receptor.* Annu Rev Immunol, 2001. **19**: p. 683-765.
286. Chen, T., et al., *The viral oncogene Np9 acts as a critical molecular switch for co-activating beta-catenin, ERK, Akt and Notch1 and promoting the growth of human leukemia stem/progenitor cells.* Leukemia, 2013. **27**(7): p. 1469-78.
287. Liang, X., et al., *beta-catenin mediates tumor-induced immunosuppression by inhibiting cross-priming of CD8(+) T cells.* J Leukoc Biol, 2014. **95**(1): p. 179-90.
288. Schmitt, K., et al., *HERV-K(HML-2) rec and np9 transcripts not restricted to disease but present in many normal human tissues.* Mob DNA, 2015. **6**: p. 4.
289. Seaberg, E.C., et al., *Cancer incidence in the multicenter AIDS Cohort Study before and during the HAART era: 1984 to 2007.* Cancer, 2010. **116**(23): p. 5507-16.
290. Sgadari, C., et al., *Use of HIV protease inhibitors to block Kaposi's sarcoma and tumour growth.* Lancet Oncol, 2003. **4**(9): p. 537-47.
291. Dewan, M.Z., et al., *Efficient intervention of growth and infiltration of primary adult T-cell leukemia cells by an HIV protease inhibitor, ritonavir.* Blood, 2006. **107**(2): p. 716-24.
292. Srirangam, A., et al., *Effects of HIV protease inhibitor ritonavir on Akt-regulated cell proliferation in breast cancer.* Clin Cancer Res, 2006. **12**(6): p. 1883-96.
293. Laurent, N., et al., *Effects of the proteasome inhibitor ritonavir on glioma growth in vitro and in vivo.* Mol Cancer Ther, 2004. **3**(2): p. 129-36.
294. Maggiorella, L., et al., *Combined radiation sensitizing and anti-angiogenic effects of ionizing radiation and the protease inhibitor ritonavir in a head and neck carcinoma model.* Anticancer Res, 2005. **25**(6B): p. 4357-62.
295. Kumar, S., et al., *Ritonavir blocks AKT signaling, activates apoptosis and inhibits migration and invasion in ovarian cancer cells.* Mol Cancer, 2009. **8**: p. 26.
296. Batchu, R.B., et al., *Ritonavir-Mediated Induction of Apoptosis in Pancreatic Cancer Occurs via the RB/E2F-1 and AKT Pathways.* Pharmaceuticals (Basel), 2014. **7**(1): p. 46-57.
297. Srirangam, A., et al., *The human immunodeficiency virus protease inhibitor ritonavir inhibits lung cancer cells, in part, by inhibition of survivin.* J Thorac Oncol, 2011. **6**(4): p. 661-70.

298. Hampson, L., H.C. Kitchener, and I.N. Hampson, *Specific HIV protease inhibitors inhibit the ability of HPV16 E6 to degrade p53 and selectively kill E6-dependent cervical carcinoma cells in vitro.* Antivir Ther, 2006. **11**(6): p. 813-25.

299. Pyrko, P., et al., *HIV-1 protease inhibitors nelfinavir and atazanavir induce malignant glioma death by triggering endoplasmic reticulum stress.* Cancer Res, 2007. **67**(22): p. 10920-8.

300. Okubo, K., et al., *Lopinavir-Ritonavir Combination Induces Endoplasmic Reticulum Stress and Kills Urological Cancer Cells.* Anticancer Res, 2019. **39**(11): p. 5891-5901.

301. Ikezoe, T., et al., *HIV-1 protease inhibitor, ritonavir: a potent inhibitor of CYP3A4, enhanced the anticancer effects of docetaxel in androgen-independent prostate cancer cells in vitro and in vivo.* Cancer Res, 2004. **64**(20): p. 7426-31.

302. Ikezoe, T., et al., *HIV-1 protease inhibitor ritonavir potentiates the effect of 1,25-dihydroxyvitamin D3 to induce growth arrest and differentiation of human myeloid leukemia cells via down-regulation of CYP24.* Leuk Res, 2006. **30**(8): p. 1005-11.

303. Olson, D.P., et al., *The protease inhibitor ritonavir inhibits the functional activity of the multidrug resistance related-protein 1 (MRP-1).* AIDS, 2002. **16**(13): p. 1743-7.

304. Halum, S.L., et al., *Gene discovery using a human vestibular schwannoma cDNA library constructed from a patient with neurofibromatosis type 2 (NF2).* Otolaryngol Head Neck Surg, 2003. **128**(3): p. 364-71.

305. Bhat, R.K., et al., *Human endogenous retrovirus-K(II) envelope induction protects neurons during HIV/AIDS.* PLoS One, 2014. **9**(7): p. e97984.

306. Lokossou, A.G., C. Toudic, and B. Barbeau, *Implication of human endogenous retrovirus envelope proteins in placental functions.* Viruses, 2014. **6**(11): p. 4609-27.

307. Tolosa, J.M., et al., *The endogenous retroviral envelope protein syncytin-1 inhibits LPS/PHA-stimulated cytokine responses in human blood and is sorted into placental exosomes.* Placenta, 2012. **33**(11): p. 933-41.

308. Vargas, A., et al., *Syncytin proteins incorporated in placenta exosomes are important for cell uptake and show variation in abundance in serum exosomes from patients with preeclampsia.* FASEB J, 2014. **28**(8): p. 3703-19.

309. Azmi, A.S., B. Bao, and F.H. Sarkar, *Exosomes in cancer development, metastasis, and drug resistance: a comprehensive review.* Cancer Metastasis Rev, 2013. **32**(3-4): p. 623-42.

310. Rosenbaum, C., et al., *Enhanced proliferation and potassium conductance of Schwann cells isolated from NF2 schwannomas can be reduced by quinidine.* Neurobiol Dis, 2000. **7**(4): p. 483-91.

311. Puttmann, S., et al., *Establishment of a benign meningioma cell line by hTERT-mediated immortalization.* Lab Invest, 2005. **85**(9): p. 1163-71.

312. Hung, G., et al., *Establishment of primary vestibular schwannoma cultures from neurofibromatosis type-2 patients.* Int J Oncol, 1999. **14**(3): p. 409-15.

313. Sainio, M., et al., *Mild familial neurofibromatosis 2 associates with expression of merlin with altered COOH-terminus.* Neurology, 2000. **54**(5): p. 1132-8.
314. Thomson, B.J., *Viruses and apoptosis.* Int J Exp Pathol, 2001. **82**(2): p. 65-76.
315. Ui-Tei, K., et al., *Thermodynamic stability and Watson-Crick base pairing in the seed duplex are major determinants of the efficiency of the siRNA-based off-target effect.* Nucleic Acids Res, 2008. **36**(22): p. 7100-9.
316. Reynolds, A., et al., *Rational siRNA design for RNA interference.* Nat Biotechnol, 2004. **22**(3): p. 326-30.
317. Amarzguioui, M. and H. Prydz, *An algorithm for selection of functional siRNA sequences.* Biochem Biophys Res Commun, 2004. **316**(4): p. 1050-8.
318. Tang, T.T., et al., *Small Molecule Inhibitors of TEAD Auto-palmitoylation Selectively Inhibit Proliferation and Tumor Growth of NF2-deficient Mesothelioma.* Mol Cancer Ther, 2021. **20**(6): p. 986-998.
319. Bos, T.J., et al., *v-jun encodes a nuclear protein with enhancer binding properties of AP-1.* Cell, 1988. **52**(5): p. 705-12.
320. Oo, T.F., et al., *Expression of c-fos, c-jun, and c-jun N-terminal kinase (JNK) in a developmental model of induced apoptotic death in neurons of the substantia nigra.* J Neurochem, 1999. **72**(2): p. 557-64.
321. Karamitros, T., et al., *A contaminant-free assessment of Endogenous Retroviral RNA in human plasma.* Sci Rep, 2016. **6**: p. 33598.
322. Hanke, K., et al., *Reconstitution of the ancestral glycoprotein of human endogenous retrovirus k and modulation of its functional activity by truncation of the cytoplasmic domain.* J Virol, 2009. **83**(24): p. 12790-800.
323. Sun, Y., et al., *Signaling pathway of MAPK/ERK in cell proliferation, differentiation, migration, senescence and apoptosis.* J Recept Signal Transduct Res, 2015. **35**(6): p. 600-4.
324. Parkinson, D.B., et al., *c-Jun is a negative regulator of myelination.* J Cell Biol, 2008. **181**(4): p. 625-37.
325. Shivane, A., et al., *Expression of c-Jun and Sox-2 in human schwannomas and traumatic neuromas.* Histopathology, 2013. **62**(4): p. 651-6.
326. Yue, W.Y., et al., *Contribution of persistent C-Jun N-terminal kinase activity to the survival of human vestibular schwannoma cells by suppression of accumulation of mitochondrial superoxides.* Neuro Oncol, 2011. **13**(9): p. 961-73.
327. Ammoun, S., et al., *Targeting ERK1/2 activation and proliferation in human primary schwannoma cells with MEK1/2 inhibitor AZD6244.* Neurobiol Dis, 2010. **37**(1): p. 141-6.
328. Chambard, J.C., et al., *ERK implication in cell cycle regulation.* Biochim Biophys Acta, 2007. **1773**(8): p. 1299-310.

329. Weber, J.D., et al., *Sustained activation of extracellular-signal-regulated kinase 1 (ERK1) is required for the continued expression of cyclin D1 in G1 phase.* Biochem J, 1997. **326 (Pt 1)**: p. 61-8.
330. Daksis, J.I., et al., *Myc induces cyclin D1 expression in the absence of de novo protein synthesis and links mitogen-stimulated signal transduction to the cell cycle.* Oncogene, 1994. **9**(12): p. 3635-45.
331. Handra-Luca, A., et al., *Extra-cellular signal-regulated ERK-1/ERK-2 pathway activation in human salivary gland mucoepidermoid carcinoma: association to aggressive tumor behavior and tumor cell proliferation.* Am J Pathol, 2003. **163**(3): p. 957-67.
332. Loukil, A., et al., *Cyclin A2: At the crossroads of cell cycle and cell invasion.* World J Biol Chem, 2015. **6**(4): p. 346-50.
333. Pagano, M., et al., *Cyclin A is required at two points in the human cell cycle.* EMBO J, 1992. **11**(3): p. 961-71.
334. Wang, C., et al., *Verteporfin inhibits YAP function through up-regulating 14-3-3sigma sequestering YAP in the cytoplasm.* Am J Cancer Res, 2016. **6**(1): p. 27-37.
335. Wood, R., *Atazanavir: its role in HIV treatment.* Expert Rev Anti Infect Ther, 2008. **6**(6): p. 785-96.
336. Hartman, T.L. and R.W. Buckheit, Jr., *The Continuing Evolution of HIV-1 Therapy: Identification and Development of Novel Antiretroviral Agents Targeting Viral and Cellular Targets.* Mol Biol Int, 2012. **2012**: p. 401965.
337. Chandwani, A. and J. Shuter, *Lopinavir/ritonavir in the treatment of HIV-1 infection: a review.* Ther Clin Risk Manag, 2008. **4**(5): p. 1023-33.
338. Wlodawer, A. and J.W. Erickson, *Structure-based inhibitors of HIV-1 protease.* Annu Rev Biochem, 1993. **62**: p. 543-85.
339. Tyagi, R., et al., *Inhibition of human endogenous retrovirus-K by antiretroviral drugs.* Retrovirology, 2017. **14**(1): p. 21.
340. Towler, E.M., et al., *Functional characterization of the protease of human endogenous retrovirus, K10: can it complement HIV-1 protease?* Biochemistry, 1998. **37**(49): p. 17137-44.
341. Kuhelj, R., et al., *Inhibition of human endogenous retrovirus-K10 protease in cell-free and cell-based assays.* J Biol Chem, 2001. **276**(20): p. 16674-82.
342. Gatti, G., et al., *The relationship between ritonavir plasma levels and side-effects: implications for therapeutic drug monitoring.* AIDS, 1999. **13**(15): p. 2083-9.
343. Zhu, L., et al., *Pharmacokinetics and inhibitory quotient of atazanavir/ritonavir versus lopinavir/ritonavir in HIV-infected, treatment-naive patients who participated in the CASTLE Study.* J Antimicrob Chemother, 2012. **67**(2): p. 465-8.
344. Decaudin, D., *Primary human tumor xenografted models ('tumorgrafts') for good management of patients with cancer.* Anticancer Drugs, 2011. **22**(9): p. 827-41.

345. Sun, S. and A. Liu, *Long-term follow-up studies of Gamma Knife surgery for patients with neurofibromatosis Type 2.* J Neurosurg, 2014. **121 Suppl**: p. 143-9.
346. Kruyt, I.J., et al., *Gamma Knife radiosurgery for treatment of growing vestibular schwannomas in patients with neurofibromatosis Type 2: a matched cohort study with sporadic vestibular schwannomas.* J Neurosurg, 2018. **128**(1): p. 49-59.
347. Wang-Johanning, F., et al., *Immunotherapeutic potential of anti-human endogenous retrovirus-K envelope protein antibodies in targeting breast tumors.* J Natl Cancer Inst, 2012. **104**(3): p. 189-210.
348. Kraus, B., et al., *Vaccination directed against the human endogenous retrovirus-K (HERV-K) gag protein slows HERV-K gag expressing cell growth in a murine model system.* Virol J, 2014. **11**: p. 58.
349. Zhou, F., et al., *Chimeric antigen receptor T cells targeting HERV-K inhibit breast cancer and its metastasis through downregulation of Ras.* Oncoimmunology, 2015. **4**(11): p. e1047582.
350. Gong, D. and J.E. Ferrell, Jr., *The roles of cyclin A2, B1, and B2 in early and late mitotic events.* Mol Biol Cell, 2010. **21**(18): p. 3149-61.
351. Gong, D., et al., *Cyclin A2 regulates nuclear-envelope breakdown and the nuclear accumulation of cyclin B1.* Curr Biol, 2007. **17**(1): p. 85-91.
352. De Boer, L., et al., *Cyclin A/cdk2 coordinates centrosomal and nuclear mitotic events.* Oncogene, 2008. **27**(31): p. 4261-8.
353. Gopinathan, L., et al., *Loss of Cdk2 and cyclin A2 impairs cell proliferation and tumorigenesis.* Cancer Res, 2014. **74**(14): p. 3870-9.
354. Yam, C.H., T.K. Fung, and R.Y. Poon, *Cyclin A in cell cycle control and cancer.* Cell Mol Life Sci, 2002. **59**(8): p. 1317-26.
355. Bukholm, I.R., G. Bukholm, and J.M. Nesland, *Over-expression of cyclin A is highly associated with early relapse and reduced survival in patients with primary breast carcinomas.* Int J Cancer, 2001. **93**(2): p. 283-7.
356. Garcia-Gutierrez, L., et al., *Myc stimulates cell cycle progression through the activation of Cdk1 and phosphorylation of p27.* Sci Rep, 2019. **9**(1): p. 18693.
357. Qi, Y., et al., *Cyclin A but not cyclin D1 is essential for c-myc-modulated cell-cycle progression.* J Cell Physiol, 2007. **210**(1): p. 63-71.
358. Philipp, A., et al., *Repression of cyclin D1: a novel function of MYC.* Mol Cell Biol, 1994. **14**(6): p. 4032-43.
359. Baldin, V., et al., *Cyclin D1 is a nuclear protein required for cell cycle progression in G1.* Genes Dev, 1993. **7**(5): p. 812-21.
360. Kim, M., et al., *Merlin inhibits Wnt/beta-catenin signaling by blocking LRP6 phosphorylation.* Cell Death Differ, 2016. **23**(10): p. 1638-47.

361. Tatkiewicz, W., et al., *Characterising a human endogenous retrovirus(HERV)-derived tumour-associated antigen: enriched RNA-Seq analysis of HERV-K(HML-2) in mantle cell lymphoma cell lines.* Mob DNA, 2020. **11**: p. 9.

362. Cherkasova, E., et al., *Inactivation of the von Hippel-Lindau tumor suppressor leads to selective expression of a human endogenous retrovirus in kidney cancer.* Oncogene, 2011. **30**(47): p. 4697-706.

363. Qin, Z.H., et al., *Nuclear factor-kappa B contributes to excitotoxin-induced apoptosis in rat striatum.* Mol Pharmacol, 1998. **53**(1): p. 33-42.

364. Hurst, T.P. and G. Magiorkinis, *Epigenetic Control of Human Endogenous Retrovirus Expression: Focus on Regulation of Long-Terminal Repeats (LTRs).* Viruses, 2017. **9**(6).

365. Depil, S., et al., *Expression of a human endogenous retrovirus, HERV-K, in the blood cells of leukemia patients.* Leukemia, 2002. **16**(2): p. 254-9.

366. St Laurent, G., et al., *VlincRNAs controlled by retroviral elements are a hallmark of pluripotency and cancer.* Genome Biol, 2013. **14**(7): p. R73.

367. Torres-Martin, M., et al., *Genome-wide methylation analysis in vestibular schwannomas shows putative mechanisms of gene expression modulation and global hypomethylation at the HOX gene cluster.* Genes Chromosomes Cancer, 2015. **54**(4): p. 197-209.

368. Lamar, J.M., et al., *SRC tyrosine kinase activates the YAP/TAZ axis and thereby drives tumor growth and metastasis.* J Biol Chem, 2019. **294**(7): p. 2302-2317.

369. Warren, J.S.A., Y. Xiao, and J.M. Lamar, *YAP/TAZ Activation as a Target for Treating Metastatic Cancer.* Cancers (Basel), 2018. **10**(4).

370. Ammoun, S., et al., *Insulin-like growth factor-binding protein-1 (IGFBP-1) regulates human schwannoma proliferation, adhesion and survival.* Oncogene, 2012. **31**(13): p. 1710-22.

371. Lv, Z., Y. Chu, and Y. Wang, *HIV protease inhibitors: a review of molecular selectivity and toxicity.* HIV AIDS (Auckl), 2015. **7**: p. 95-104.

372. Maksimovic-Ivanic, D., et al., *HIV-protease inhibitors for the treatment of cancer: Repositioning HIV protease inhibitors while developing more potent NO-hybridized derivatives?* Int J Cancer, 2017. **140**(8): p. 1713-1726.

373. Ahluwalia, M.S., et al., *Phase II trial of ritonavir/lopinavir in patients with progressive or recurrent high-grade gliomas.* J Neurooncol, 2011. **102**(2): p. 317-21.

374. Ammoun, S., et al., *Phase 0 trial investigating the intratumoural concentration and activity of sorafenib in neurofibromatosis type 2.* J Neurol Neurosurg Psychiatry, 2019. **90**(10): p. 1184-1187.

375. Chow, W.A., C. Jiang, and M. Guan, *Anti-HIV drugs for cancer therapeutics: back to the future?* Lancet Oncol, 2009. **10**(1): p. 61-71.

376. Laurent, N., et al., *Effects of the proteasome inhibitor ritonavir on glioma growth in vitro and in vivo.* 2004. **3**(2): p. 129-36.

377. Vassilev, A., et al., *TEAD/TEF transcription factors utilize the activation domain of YAP65, a Src/Yes-associated protein localized in the cytoplasm.* Genes Dev, 2001. **15**(10): p. 1229-41.

10 Supplementary Information

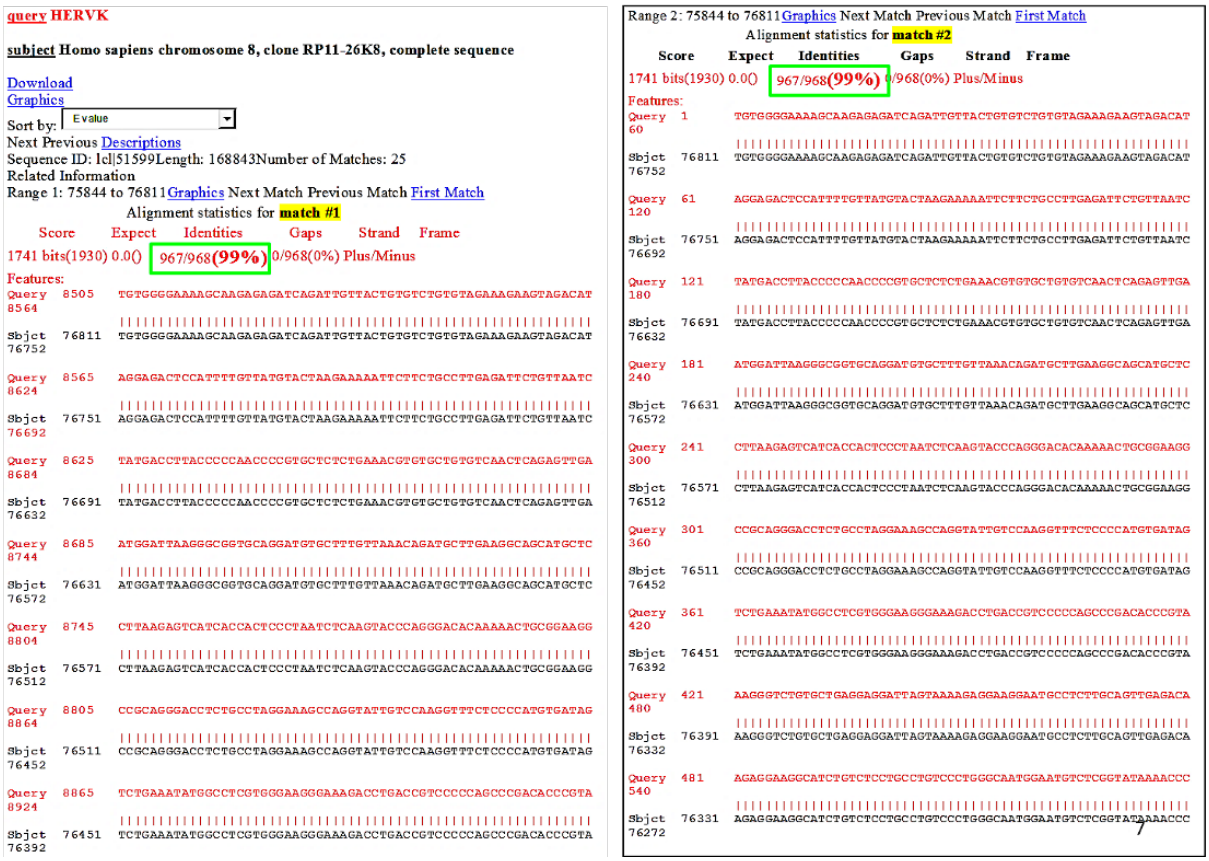

Figure S 1. Homo sapiens chromosome 8, clone RP11-26K8 showed 99% similarity with HERV-K sequence.

Dr Sylwia Ammoun submitted 17 sequences with unknown functions that were previously identified in vestibular schwannoma by Halum *et al*. [304] to BLAST. Consequently, Homo sapiens chromosome 8 Clone RP11-26K8 (1 of the 17 unknown sequences) showed 99% similarity to HERV-K (HML-2).

HERV-K Env		HERV-K Gag	
NMT-NF2+/+	MN-GI-NF2-/-	NMT-NF2+/+	MN-GI-NF2-/-
2	2	1	1
1	2	1	3
2	2	1+	2
1	2	0	2
0	2	1+	2
0	3		3
1	3		2
1	2		
1	2		
2	3		
	2		
	3		

Table S 1. The scoring of immunohistochemistry analysis shown in Figure 13.

Sections of Merlin-deficient grade I meningioma (MN-GI-NF2-/-) and normal meninges (NMT-NF2+/+) were stained with anti-HERV-K Env (n=12, 5 were performed by Dr Sylwia Ammoun) and anti-HERV-K Gag (n=7). Staining intensity (brown) was scored as follows: 0, no staining; 1, equivocal; 1+, weakly positive; 2, moderate; 3, strong.

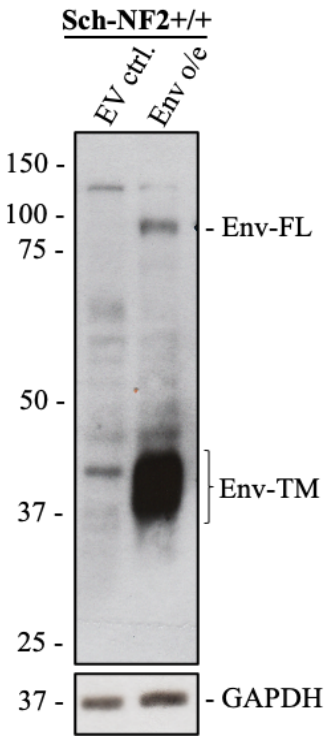

Figure S 2. Specificity of anti-HERV-K Env antibody for HERV-K Env-FL and Env TM was confirmed by overexpressing HERV-K Env in Sch-NF2+/+ cells.

Primary Sch-NF2+/+ cells were infected with empty vector control lentiviral particles (EV ctrl.) and with HERV-K (HML-2) Env expressing lentiviral particles (Env o/e). Following infection, the cells were lysed and processed for protein extraction. Western blotting results confirmed the specificity of anti-HERV-K Env antibody for HERV-K Env-FL and Env-TM. GAPDH was used as the loading control.

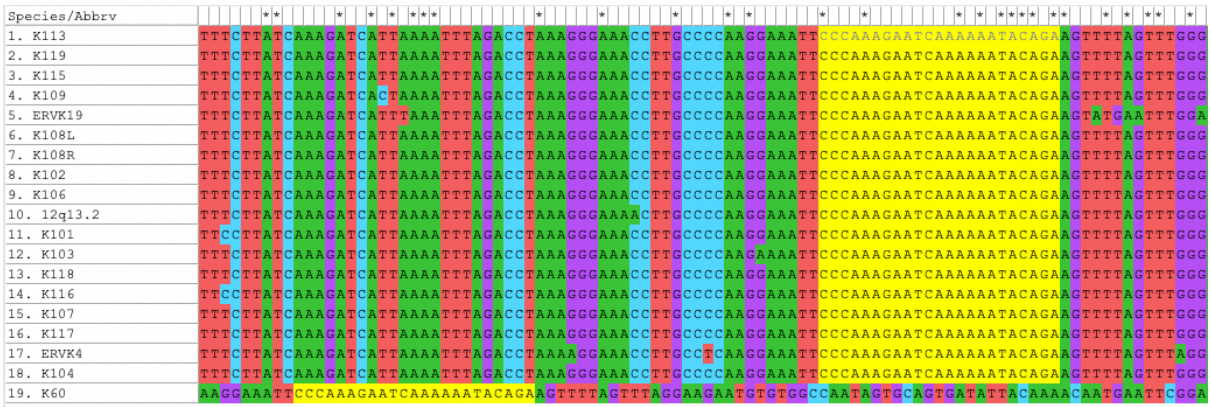

Figure S 3. Alignment of 19 HERV-K (HML-2) proviruses confirms the presence of shRNA target sequence in multiple proviruses.

19 HERV-K (HML-2) proviruses were aligned using MEGAX software. shRNA target sequence 18 (see Table 5, Materials and Methods) was searched in all proviruses. Search results showed the presence of shRNA target sequence 18 in all proviruses (highlighted in yellow), suggesting that the shRNA sequence should target all these proviruses.

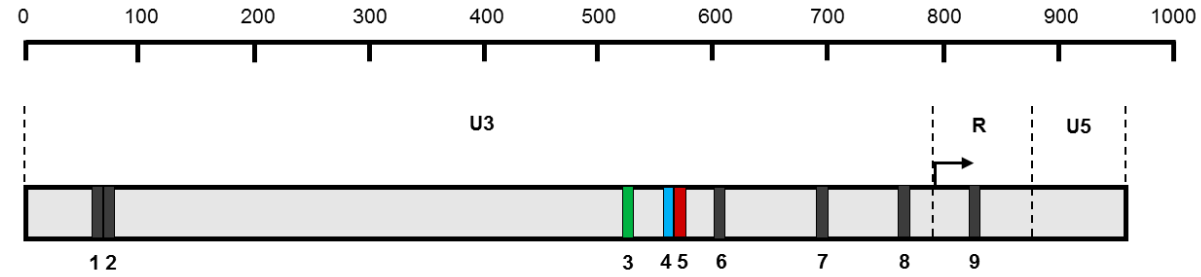

1 NFkB (61-70)
2 YY1 (62-83)
3 TEAD (518-524) / NFkB (519-528)
4 NFAT-1 (568-572) / NFkB (568-579)
5 GC box 1 (575-579)
6 GC box 2 (602-606)
7 Oct4 (691-701)
8 GC box 3 (762-766)
9 GC box 4 (820-824)

		Transcription Factor Binding Motifs								
		1	2	3	4 & 5	6	7	8	9
HERV-K locus	Type	NFkB	YY1	TEAD / **NFkB**	NFAT-1 / **NFkB** / GC box 1	GC box 2	Oct4	GC box 3	GC box 4
K113	2	AGGAGACTCCGGAGACTCCATTTTGTTATGTATGGAATTCTCGAAAAACCGCCTGGGCAGTGATGCCAAGAACCCCCGGCGGG							
K119	2	. . . . .	. . . . .	. . . . .	. . . . .	. . . . .	. . . . . A	. . . . .	. . . . .
K115	2	. . . . .	. . . . .	. . . . .	. . . . .	. . . . .	. . . . . A	. . . . .	. . . . .
K109	2	. . . . .	. . . . .	. . . . .	. . . . .	. . . . .	. . . . .	. . . . .	. . . . .
ERVK19	2	- - - - -	- - - - -	- - - - -	- - - - -	- - - - -	- - - - -	- - - - -	- - - - -
K108L	2	. . . . .	. . . . .	. . . . .	. . . . .	. . . . .	. . . . . A	. . . . .	. . . . .
K108R	2	. . . . .	. . . . .	. . . . .	. . . . .	. . . . .	. . . . . A	. . . . .	. . . . .
K102	1	G	. . . . .	G	. . . . .	. . . . .	. . . . .	. . . . .	. . . . .
K106	1	. . . . .	. . . . .	. . . . .	. . . . .	. . . . .	. . . . . A	. . . . .	. . . . .
12q13.2	1	. . . . .	. . . . .	. . . . .	. . . . .	. . . . .	. . . . .	. . . . .	. . . . .
K101	1	. . . . .	. . . . .	G	. . . . .	. . . . .	. . . . . A	. . . . .	. . . . .
K103	1	. . . . .	. . . . .	. . . . .	. . . . .	. . . . .	. . . . . A	. . . . .	. . . . A .
K118	2	. . . . .	. . . . .	. . . . .	. . . . .	. . . . .	. . . . . A	. . . . .	. . . . A .
K116	1	. . . . .	. . . . .	. . . . .	. . . . . T	. . . . .	. . . . . A	. . . . .	. . . . .
K107	1	. . . . .	. . . . .	G	. . . . .	. . . . .	. . . . .	. . . . .	. . . . .
K117	1	. . . . .	. . . . .	. . . . .	. . . . .	. . . . .	. . . . . A	. . . . .	. . . . .
ERVK4	2	. . . . .	. . . . .	. . . . .	. . . . .	. . . . .	. . . . . A	. . . . .	. . . . . - - - - -
K104	2	. . . . .	. . . . .	. . . . .	. . . . . T	A	. . . . . A	. . . . .	. . . . .
K60	2	. . . . .	. . . . .	. . . . . C	. . . . .	. . . . .	. . . . . A	. . . . .	. . . . . G . . . .

Figure S 4. The presence of TEAD binding site on HERV-K (HML-2) LTR in silico.

LTRs from 19 HERV-K (HML-2) loci sequences were aligned using MEGAX software. Then, the TEAD binding motif TGGAAT from Vassilev *et al*. [377] was manually searched. Search results show that the transcription factor binding site is fully conserved in 17/19 of the sequences aligned. Furthermore, TEAD binding motifs clashes with NFκB on site 3.

A

Ritonavir treated cells	Ki67+ cells (Percentage of DAPI)
Sch-NF2-/- 1	30.6
Sch-NF2-/- 2	30.8
Sch-NF2-/- 3	26.6
Sch-NF2+/+ 1	67.3
Sch-NF2+/+ 2	59.3
Sch-NF2+/+ 3	33.9

B

Lopinavir treated cells	Ki67+ cells (Percentage of DAPI)
Sch-NF2-/- 1	22.2
Sch-NF2-/- 2	6.6
Sch-NF2-/- 3	19.3

C

Atazanavir treated cells	Ki67+ cells (Percentage of DAPI)
Sch-NF2-/- 1	11.8
Sch-NF2-/- 2	8.5
Sch-NF2-/- 3	29.5

Figure S 5. Proliferation index for anti-retroviral drug treatment experiments with primary Sch-NF2-/- and Sch-NF2+/+ cells in basal conditions (media).

Cell proliferation was measured as the number of Ki67+ cells and calculated as the percentage of DAPI. [A] Table shows the proliferation index of cells used in Figure 23. [B, C] Tables show the proliferation index of cells used in Figure 24.